NBSIR 86-3392

Final Report: Technical Contributions to the Development of Incipient Fault Detection/Location Instrumentation

W. E. Anderson, J. D. Ramboz, and A. R. Ondrejka

U.S. DEPARTMENT OF COMMERCE
National Bureau of Standards
National Engineering Laboratory
Center for Electronics and Electrical Engineering
Electrosystems Division
Gaithersburg, MD 20899

April 1986

Sponsored by:
ment of Energy
f Electric Energy Systems
gton, DC 20585

NBSIR 86-3392

FINAL REPORT: TECHNICAL CONTRIBUTIONS TO THE DEVELOPMENT OF INCIPIENT FAULT DETECTION/LOCATION INSTRUMENTATION

W. E. Anderson, J. D. Ramboz, and A. R. Ondrejka

U.S. DEPARTMENT OF COMMERCE
National Bureau of Standards
National Engineering Laboratory
Center for Electronics and Electrical Engineering
Electrosystems Division
Gaithersburg, MD 20899

April 1986

Sponsored by:
Department of Energy
Office of Electric Energy Systems
Washington, DC 20585

U.S. DEPARTMENT OF COMMERCE, Malcolm Baldrige, *Secretary*
NATIONAL BUREAU OF STANDARDS, Ernest Ambler, *Director*

TABLE OF CONTENTS

LIST OF FIGURES

FINAL REPORT: TECHNICAL CONTRIBUTIONS TO THE DEVELOPMENT OF INCIPIENT FAULT DETECTION/LOCATION INSTRUMENTATION

W.E. Anderson, J.D. Ramboz, and A.R. Ondrejka

Abstract

The transmission of electrical energy by use of underground cables is increasing. Fault location techniques have certain limitations; incipient fault detection and location would help reduce the maintenance cost of these lines as well as improve the reliability of service. This report discusses some test results related to RF-probing techniques applied to high-voltage transmission lines. The high frequency losses and attenuation in high voltage cables places certain ultimate limitations on RF-probing techniques for incipient fault detection. Time domain reflectrometry methods were employed to assess the RF-transmission properties of high-voltage cables at frequencies as high as 6 GHz. Fast Fourier transform deconvolution was used to obtain loss measurements as a function of frequency. The loss mechanisms were identified. The measurement hardware and methods are discussed as well as an analysis approach leading to the conclusions.

Keywords: deconvolution techniques; fast Fourier transforms; fault location; high-voltage transmission; incipient faults; RF measurements; RF properties; time domain reflectometry; underground cables.

1. INTRODUCTION

The objective of this NBS program has been to identify and, insofar as practical, remove technical barriers to the development of instrumentation for use in detecting and locating incipient faults in underground power transmission systems. This report will describe the results of the NBS program since its inception in late 1978. Because the work during the period through 1981 has been previously presented [1-3][1], only the major findings of that work will be discussed here.

In recent years, there has been increased interest in the underground transmission of electrical energy. One of the major reasons is economic. In order to transmit ever increasing amounts of energy efficiently, higher and higher voltages are required. These higher voltages require wider rights-of-way which are expensive, and in some cases in congested areas, simply are not available. An alternative to this is to substitute several high-voltage (e.g., 150 kV) underground cables for the required extra-high-voltage (EHV) overhead line. These cables require significantly narrower rights-of-way resulting in greater transmission energy density. The underground cables could be conventional high-pressure oil-filled cables using wrapped Kraft paper for the dielectric or they could make use of more recent technological advancements such as extruded cross-linked polyethylene cables, compressed-gas-insulated systems, superconducting cables, wrapped synthetic cables, etc.

[1]Numbers in brackets refer to the literature references listed at the end of this report.

Besides the increased energy densities underground transmission would allow, aesthetic objections to unsightly transmission towers and environmental problems such as radio and television interference would be eliminated or greatly diminished.

There are disadvantages to underground transmission as well. The cables themselves are, in general, more costly than their overhead counterparts partly because of the more complex dielectric system. Transmission losses due to dielectric heating are a concern for some types of underground transmission systems. Installation costs can be greater than for overhead systems. These disadvantages are known and their effect on the system cost is calculable. This is not the case for the problem of fault location and repair in underground cables. Without accurate knowledge of the precise fault location, considerable resources can be spent locating the fault site and making the repair. The cost to repair the fault can be significant considering the complexities involved with the splices. Because the downtime for underground cables is unpredictable, the additional expense of redundant cables has often proven necessary.

In order to help alleviate the problem of difficult and costly fault locating and repairing, the Office of Electric Energy Systems of the Department of Energy (DOE) issued a Request for Proposal (RFP) entitled "Research and Development of Fault Detection/Location Techniques and/or Equipment for Underground Power Transmission Cable Systems." This RFP solicited proposals for the development of instrumentation to detect and locate incipient faults in various types of underground transmission cables. An "incipient fault" is here defined to be the condition within a cable system in which local insulation degradation is occurring at a significantly higher than normal rate which, if not corrected, will cause the cable system to fail.

If instrumentation which could detect and locate incipient faults did exist, then a major disadvantage of underground power transmission would be lessened. Assuming the incipient fault instrumentation could provide a warning in a useable time frame that a cable was going to fail (i.e., days as compared to microseconds), then the defect site could be repaired during a scheduled outage. Repair would be simplified since the location of the imminent fault site would be known.

As a result of the DOE RFP, contracts were awarded to three different groups: Purdue University, SRI International, and Westinghouse Corporation. The various projects funded were for the development of instrumentation to detect and locate incipient faults using both radio-frequency (RF) probing of the cable dielectric and detection of electrical and acoustical noise emanating from the incipient fault site. A brief description of each of these three programs will follow. For more information refer to the contractors' final reports [4-6].

The Electrical Engineering School of Purdue University proposed to develop instrumentation to detect the electrical noise generated by an incipient fault. They assumed that for most forms of incipient faults partial discharges would be present. Their technique involved using detectors at each end of a length of cable to detect the electrical noise and maximize the time correlation of the two signals by using a variable time delay analysis technique. The amount of time delay necessary would indicate the location of

the incipient fault site relative to the two detectors. Purdue University successfully designed and built the microprocessor-based instrumentation and demonstrated it by accurately locating discharge sites in long lengths of low-voltage coaxial cables. Despite fully meeting their program's objectives, the unavailability of additional funding prevented them from demonstrating their system on an installed power transmission cable.

SRI International had two separate programs to develop instrumentation to detect incipient faults using RF-probing techniques. One of these, proposed by the Remote Measurement Laboratory at SRI, involved using a swept-frequency probing approach whereby the signal reflected from the incipient fault site would be mixed with the transmitted signal. An analysis of the mixer output would, in principle, indicate the location of the incipient fault site. This approach relied on the assumption that the local cable impedance would be different at an incipient fault site (e.g., the dielectric constant would be changed due to impurities, voids, heating, partial discharge, etc.). Instrumentation was developed incorporating this technique. The design included means to mathematically counteract the effects of cable dispersion using data obtained on actual transmission cable systems. SRI International was not able, within the contract period, to demonstrate the success of this approach in detecting incipient faults in either a model or actual transmission cable system.

The second SRI approach was proposed by the Electronics and Radio Sciences Division. This system was predicated on the assumption that an incipient fault site was an area of electrical nonlinearity. If this is the case, introducing two signals of frequencies f and f into the cable will result in the generation of signals of frequencies (f1+ f2) and (f1- f2) at the incipient fault site. The time delay between the introduction of the two signals and the return of the difference- or sum-frequency will yield the incipient fault site location. A complication arises, however, in that an incipient fault site may not only be a locale of nonlinear behavior but also a source of partial discharges resulting in noise signals with frequency components at the sum-and difference-signals. This would make locating the incipient fault site much more difficult. This system was not successfully demonstrated during the contract period.

The R&D Center of the Westinghouse Electric Corporation proposed determining the feasibility of using acoustic waveguides to detect and locate incipient fault sites in compressed gas insulated transmission cables. Similar to Purdue University, the assumption here was that a significant class of incipient fault sites would involve partial discharges. Measurements were made on the acoustic spectra of such discharges to determine the frequency range of high acoustical activity. Next, the propagation properties of various acoustical waveguides were determined over the same frequency range. The Westinghouse conclusion was that an incipient fault detector/locator could be developed for cables up to perhaps one kilometer in length. However, for more representative lengths, the acoustic waveguides suffered too much attenuation. Having successfully determined the feasibility of using acoustic waveguides for incipient fault detection/location, they spent the remaining time of their contract on acoustical-optical techniques (e.g., using the acoustic signals generated by the partial discharges to modulate the light transmission in a fiber optic waveguide). By the conclusion of the project they had successfully demonstrated such a system in their laboratory. Since

the Westinghouse Corporation proposal only called for a feasibility study with no instrumentation development for delivery to the Department of Energy, they fully met their objectives.

The DOE RFP resulted in the development of some instrumentation and the demonstration of both the success and failure (or success of limited degree) of some approaches. Specifically, Purdue University developed instrumentation to detect and locate incipient faults using a noise correlation with variable time delay technique. This instrumentation was demonstrated in the laboratory and was ready for a full-scale test if funding had permitted. Westinghouse Corporation demonstrated the limited feasibility of using acoustic waveguides and the more promising approach of acoustical-optical techniques. SRI International was not able to deliver either of the two instrumentation packages proposed. Large amounts of data were generated in the attempted development of this instrumentation which should be useful in the future. Their lack of success does not imply that those two approaches are necessarily impractical, although some of the measurements made at NBS and discussed below indicate some serious limitations for any RF-probing techniques.

The role of the Electrosystems Divison of the National Bureau of Standards was two-part. First, NBS monitored the efforts of the Department of Energy contractors with regard to technical progress. Second, NBS provided measurementsupport where needed. In the first area, site visits were held, annual progress review meetings were convened, and reports were submitted to the Department of Energy. With the benefit of these site visits and meetings, it was apparent that the general area in which NBS could provide technical support was in determining the RF-transmission characteristics of the various types of underground cables. The previous annual report [1] and quarterly report [3] provide an extensive account of the initial efforts in this area. For completeness, a brief summary of the NBS work is included in the next section, along with subsequent efforts.

2. NBS MEASUREMENT METHODOLOGY AND EARLY RESULTS

The initial measurements involved the use of time-domain-reflectometry (TDR) techniques to determine the RF properties of the various types of cable dielectrics. A block diagram of the measurement system is shown in figure 1. The main components of the system were the digital processing oscilloscope and the "smart" terminal. This enabled waveforms to be digitized and sent to the terminal for processing. A typical TDR waveform is shown in figure 2. It was shown that TDR measurements can be quite sensitive in detecting small changes in the cable impedance. For example, the small deformation effect of placing a mass of 120 grams on a 15-kV extruded dielectric cable was detectable at the ppm level. Unfortunately, no change in the same cable was discernible after 11 high-voltage breakdowns at one site across the cable dielectric. Whereas the TDR input pulse has frequency components to the several gigahertz range, sufficient to allow for detection of the resulting breakdown channel, no change was observed in the TDR response after the breakdowns.

Extensive effort was made to improve the coupling of the high-frequency components into the cable using a tapered transition section. While this measurably improved the high-frequency coupling, the breakdown channel was still not detected. A series of measurements demonstrated conclusively that the problem was high-frequency attenuation in the cable. That is, for the

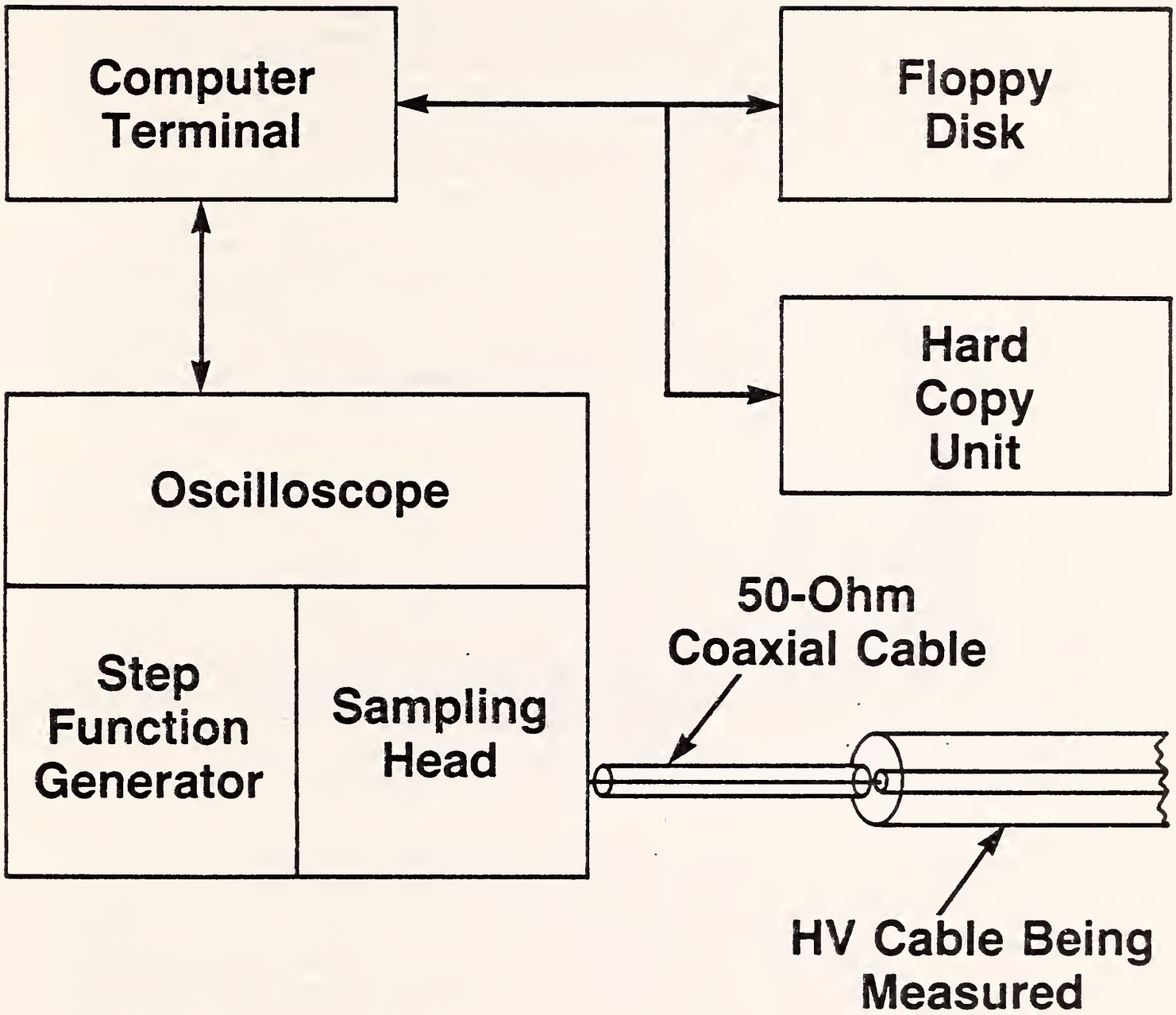

Figure 1. Block diagram of the time domain reflectometer (TDR) and data processing hardware.

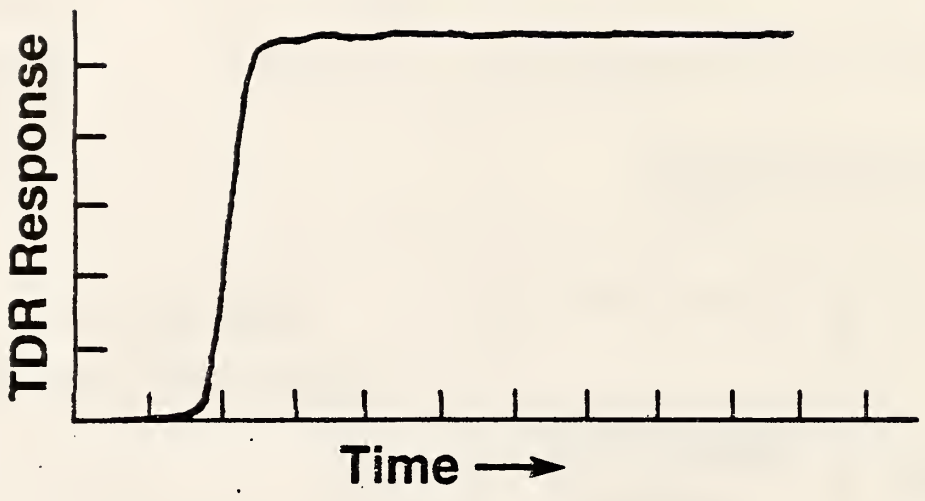

Figure 2. Typical TDR response waveform.

most common type of underground cable dielectric, extruded cross-linked polyethylene with inner and outer layers of semiconducting material, the intrinsic high-frequency attenuation is too large to permit the detection of localized dielectric changes such as breakdown channels, voids, metallic impurities, "water trees," etc. The attenuation prevents RF-probing techniques from being useful in detecting small "incipient" fault sites. At this point in the NBS measurement program, RF-probing techniques were not altogether ruled out for reasons discussed later.

With the above-mentioned equipment, NBS was in a position to provide accurate data on the RF properties of some selected cable samples which would enable system design optimization. The purpose here was twofold: to provide the most accurate design data possible; and to confirm the large high-frequency attenuation that was observed in the earlier measurements. These measurements will be discussed in detail.

2.1 Time Domain Reflectrometry Measurements, Errors, and Corrections

There are two common ways to use the TDR unit, either in a normal reflectometry mode, or in a transmission or substitution mode. Figure 3 shows the configuration for a reflectometry measurement. Here the step function waveform passes through the sampling oscilloscope before leaving the 50-ohm measurement system. At the measurement reference plane, the pulse enters the cable under test, which usually has an impedance other than 50 ohms. The step waveform propagates through the cable, and after being reflected by the short circuit termination, returns to the oscilloscope for viewing. Distortions are produced in the waveform due to undesired reflections at the measurement reference plane and are a major source of error. It will be shown later in the paper that errors introduced when the waveform passes to the right through this plane are not compensated when the waveform returns to the left; hence, corrections are needed.

Figure 4 shows the measurement system being used in the transmission or substitution mode. Here the step function waveform is first measured without the cable (a) to establish a reference which includes information about the actual generated waveform. A second measurement is then made after inserting the high-voltage cable between the generator and the sampling oscilloscope. By measuring the waveform output of the cable, (b), the reference can be deconvolved from it leaving only information unique to the cable. However, six pieces of information are combined in this result and it may be ambiguous. The desired result is the attenuation and total phase shift of the cable. Included are the reflection losses and phase shifts at each of the reference planes in figure 4(b). It has already been alluded to that this distortion produced at the reference plane is not the same entering and leaving the unknown cable. But under some conditions an average effect can be calculated and this artificial average can be used on both reference planes. Still, one average reflection loss and an average phase shift remain which are not part of the desired information about the cable, and for which a correction must be made.

The error caused by a reflection can be measured and corrected to some degree. This could be done in either the time domain or the frequency domain. The problem of multiple reflections can, in most cases, be resolved more easily in the time domain.

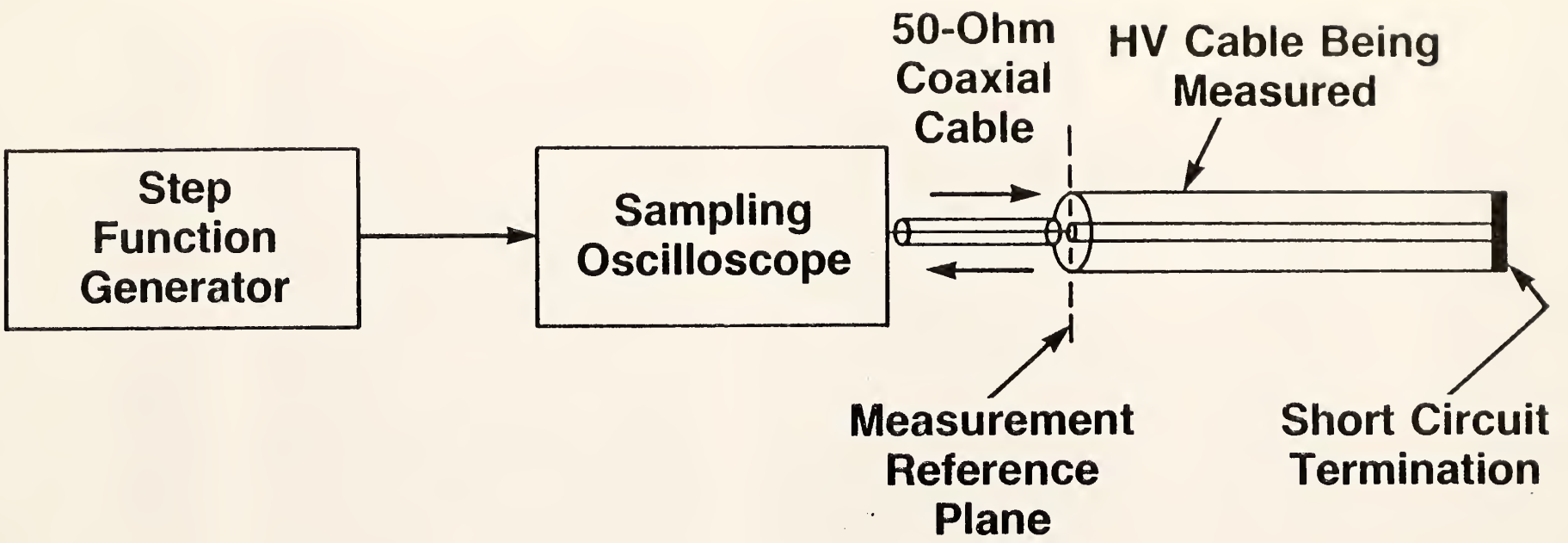

Figure 3. Configuration for a simple reflectometry measurement.

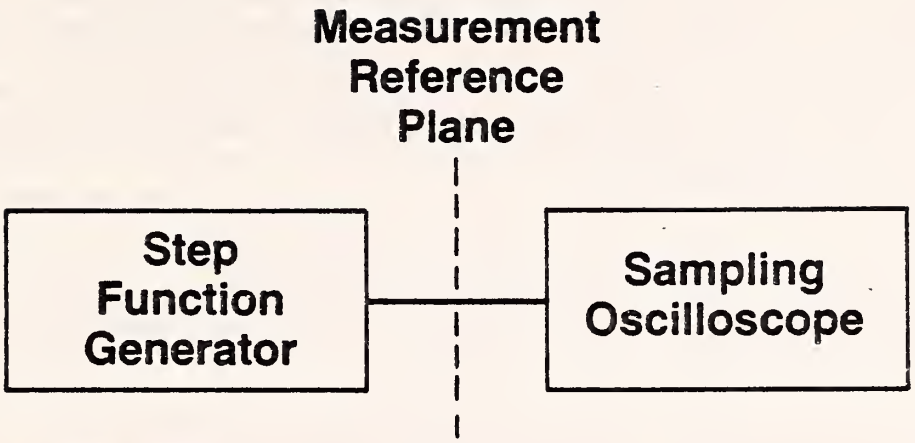

a) Measurement of Reference Waveform.

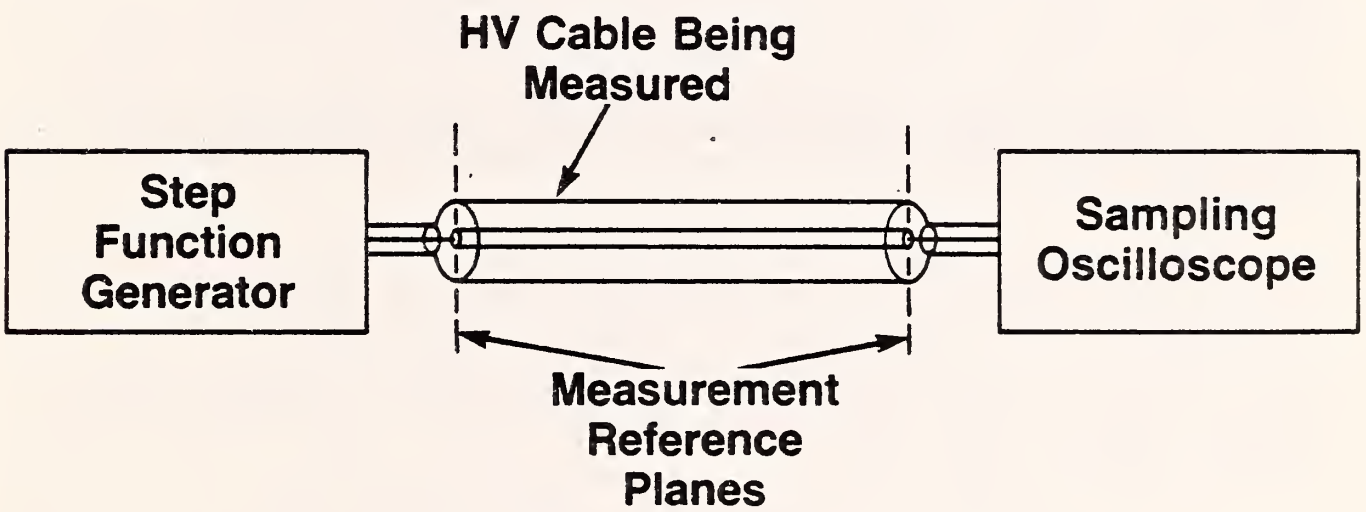

b) Measurement of Cable Output Waveform.

Figure 4. TDR system connections for a two-step transmission (substitution) mode of use. The measurement results from (a) are deconvolved from those resulting from (b).

Consider the arrangement shown by figure 3. As the step waveform returns from the short circuit and intercepts the reference plane, the difference in impedance gives rise to a secondary reflection moving again down the cable toward the short. The process will be repeated many times giving rise to a somewhat repetitive series of step functions. This causes the spectrum of the original step function to be enhanced or suppressed at harmonics of the repetition frequency in a way which is determined mainly by the length of the cable and the severity of end reflections. Again, this is not desired information and contaminates the measurement in a way which is difficult to correct in the frequency domain.

Time domain measurement resolves this problem by "time windowing." The only information that enters the measurement system is that which appears in a viewing time window, e.g., that which appears on an oscilloscope screen. If there is enough time between the occurence of the desired signal and the beginning of multiple reflections, the undesired signal can be delayed beyond the observation window and does not contaminate the measurement. Time windowing becomes difficult when the desired and undesired signals overlap in time. Although some computer processing can be done to separate the signals using techniques such as Prony's algorithm [7] or homomorphic deconvolution, it is usually simpler to change the physical arrangement to allow more time between the desired and undesired signals. For example, if multiple reflections become a problem in the reflectometry mode of figure 3, it might be possible to use a longer cable under test, allowing more time for the reflections to return to the measurement system. On the other hand, consider that a longer cable would have more attenuation and phase shift causing the desired signal to become longer by the same ratio as the increase in time between desired and undesired waveforms so that the two still remain overlapping.

Experiments have shown that in order to correct the effects of either the simple input reflection or the multiple reflections, the additional computations necessary introduce significant noise into the result and therefore increase the uncertainty. So it seems reasonable to try to remove the reflections by using some kind of impedance matching interface at the reference plane. Several approaches have been used and the results will be described later in this report.

2.2 Sampling, Windowing, Time-drift, and Aliasing

It was desirable to measure the attenuation of several power distribution cables as a function of frequency. Time domain analysis was used to take advantage of time windowing to remove reflections. The frequency domain information was computed using a modified Fast Fourier Transform [8,9]. The process of acquiring and digitizing the waveform introduced several errors.

Consider the time viewing window discussed above to be the trace on an oscilloscope screen. The easiest error to visualize is the uncertainty in location of the step-like waveform along the time baseline. There are time delay circuits built into an oscilloscope that an operator can use to position the waveform to some desired location of the screen. Due to changes in temperature or line voltage, this delay may change with time, and actually move the waveform slightly. Some measurements are not sensitive to this time delay drift, while others exhibit undesired errors with as little as

0.2 percent time shift (of full-sweep duration). The amount of drift can be reduced by allowing several hours for the equipment to thermally stabilize. In addition, for those measurements which require high precision delays, software was developed which can measure the delay error in the digitized waveforms and compute new waveforms that are time coincident. Time delays can be corrected to less than 0.01 percent error. The curves in figure 5(a) and (b) are taken from measured results using a method sensitive to time delay drift. The method uses four acquired time domain waveforms, but these were chosen to result in a deconvolved transfer function magnitude of nearly 0 dB. Notice the somewhat cyclic noise in (a) with excursions greater than 1.0 dB. These are due to a time delay shift of only a few tenths of a percent. After computer correction of the delay error, the transfer function is much better behaved as in (b). Curve (c) is the result of an ideal measurement not sensitive to this source of error. How this feature is used is described later in the report.

A second source of error which occurs during waveform acquisition is caused by an inaccurate knowledge of the sweep speed [10]. This has been the subject of two papers (Appendices A and B). The computer receives nominal sweep speed information from the dial settings on the oscilloscope but the actual sweep speed is determined by the electronics and may not agree. Even worse, the sweep speed may not remain constant during the several acquisitions needed for a single measurement. Figure 6 shows computer simulated results of sweep speed drift. Curves (a) and (b) are identical computer generated step waveforms except that the time base for (b) is one percent faster than for (a). Curve (a) was considered the input to a perfect lossless network, (b) was considered the output, and the two were deconvolved. Without the time shift, the two waveforms would have remained identical and the deconvolved waveform should have been unity (0 dB) for all frequencies in the spectrum. The one percent error in time actually produced the sloping spectral response in (c), producing 0.6 dB error at 10 percent of the normalized Nyquist frequency. The usable frequency range for actual measured waveforms usually lies between 10 and 20 percent of Nyquist frequency. So, the one percent sweep time error could produce between 0.5 dB and 1.0 dB error in the deconvolved spectrum. A software package was included which evaluates the slope of (c), and computes and corrects the sweep time error. Figure 7 shows the same effect in real measured waveforms. Curve (a) is the deconvolved spectrum of two time domain waveforms having the same sweep rate. Curve (b) indicates the seriousness of a 1.0 percent error in sweep rate and the corrected waveform appears in (c).

Probably the least obvious source of error in acquiring and digitizing waveforms is aliasing. The waveform being acquired is sampled and stored during the digitizing process. If too few samples are taken along the waveform, the real shape is poorly described by the data and the resulting spectrum will be distorted. This distortion is known as aliasing.

The obvious solution is to increase the sampling rate until aliasing is reduced to an acceptable amount. However, there may be limitations set by the oscilloscope or acquisition system. Some have a fixed number of samples across the screen (e.g., 512 samples) or at least a maximum (e.g., up to 2048 samples) set by the computer. If a waveform has many rapid transitions and there are too few samples residing on these to adequately sample, it may be possible to sweep faster, spreading out these rapid changes, and in this way

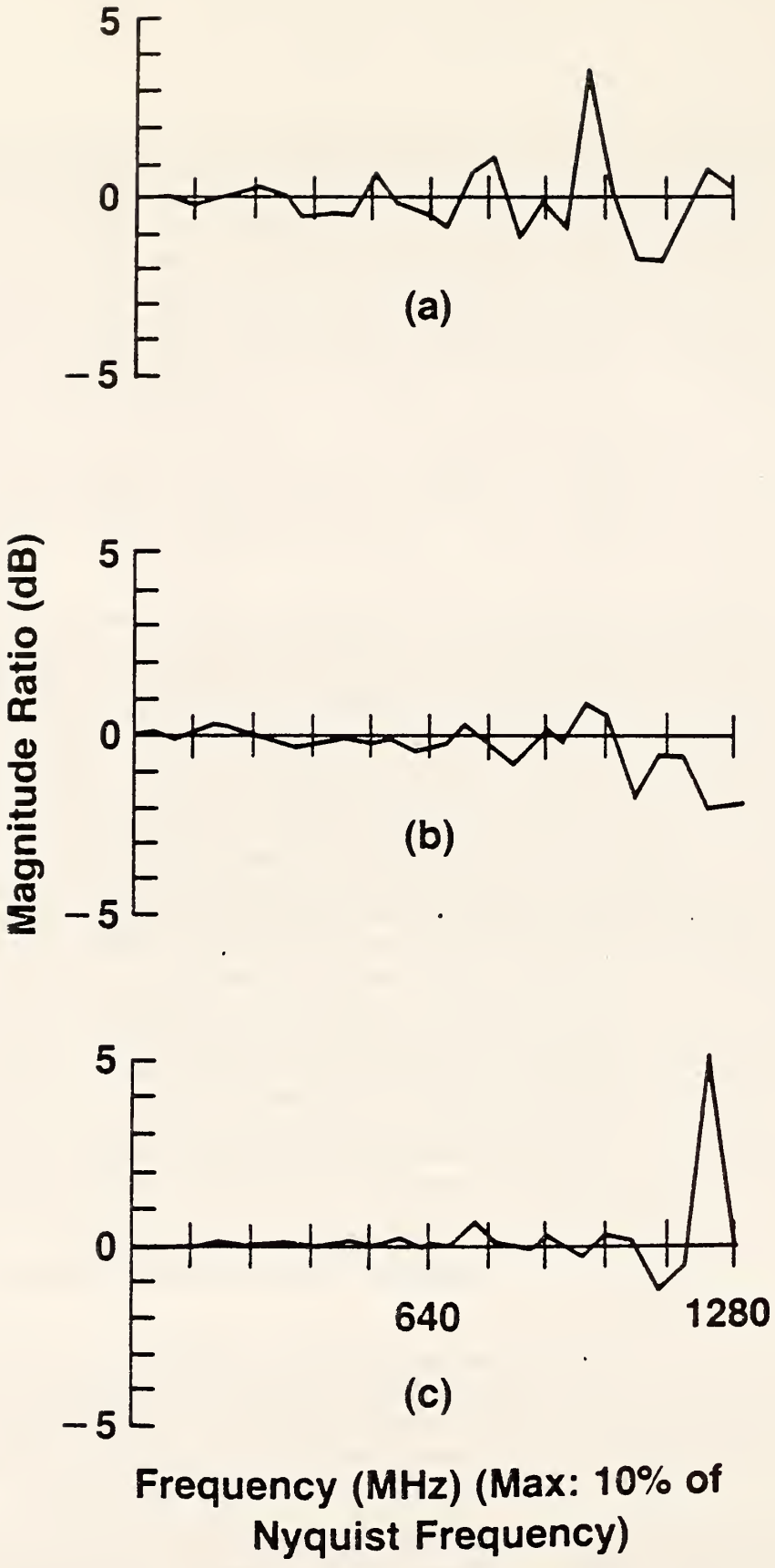

Figure 5. Deconvolved transfer function results showing the effects of delay time drifts. (See text for explanations.)

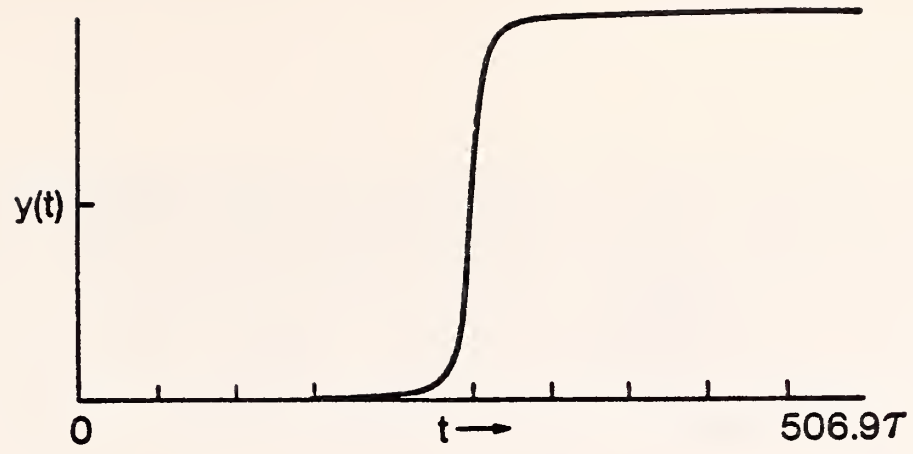

(a)

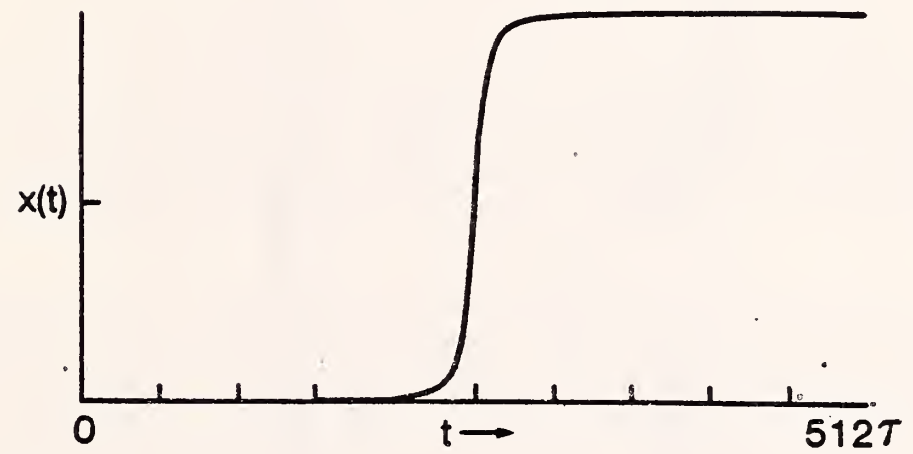

(b)

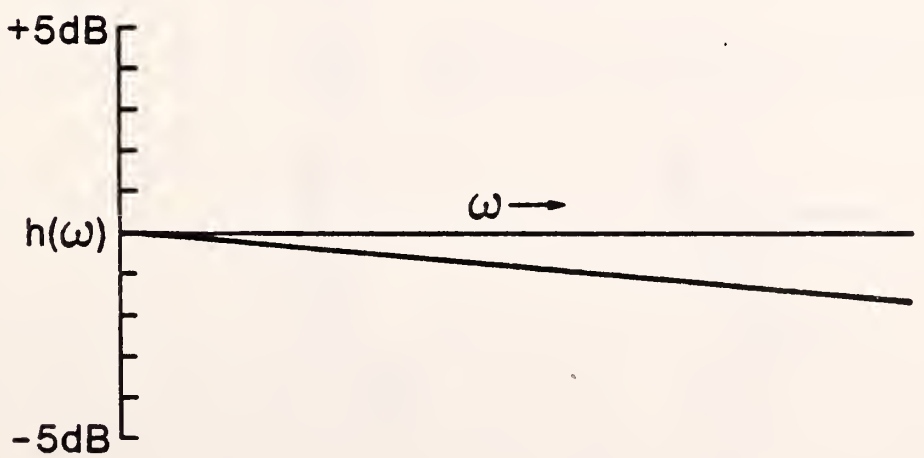

(c)

Figure 6. Error caused by sweep speed changes during the measurement sequence. x(t) is the analytical function sampled at time intervals $T = \tau$ where τ is an arbitrary unit of time. y(t) is the same analytical function sampled at time intervals $T = \tau/1.01$.

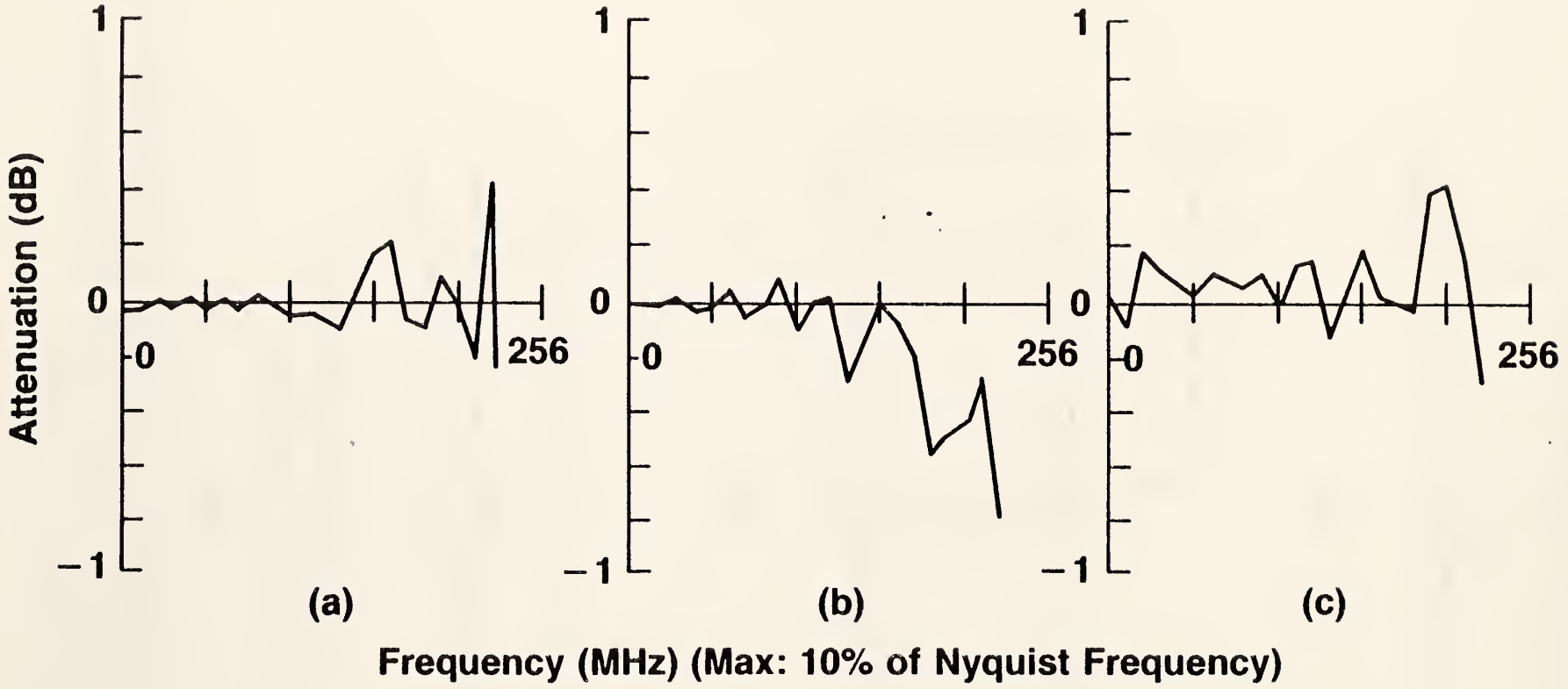

Figure 7. Effect of sweep speed errors and changes on laboratory deconvolved data. Compare to the results of figure 6.

permitting more samples for each transition. On the other hand, if there are some slowly changing portions of the waveform, it may be necessary to slow the sweep speed so that all the important parts of the waveform appear in the time window. The real difficulty becomes apparent in making cable measurements; one portion of the waveform contains a very rapid transition while the other portion is very slowly changing. Both portions contain important information and it is often not possible to select one sweep speed that can present the waveform properly. The rapid transition can be sampled properly by increasing the sampling rate but only if there is no upper limit. Even then, there will be many more samples than necessary on the slowly varying portion. Some sampling oscilloscopes allow a variable sampling rate faster in the portion of the waveform that change rapidly, and slower elsewhere. If the problem is severe, it may not be possible to make the measurement in the time domain.

2.3 Specific Measurement Techniques Used at NBS

2.3.1 Transmission Mode with Matched Resistive Adapters

The simplest measurement configuration is the transmission mode shown in figure 4. As was pointed out, there is a difficulty with reflections if the cable is not the same impedance as the measuring system. It is possible to match these impedances using simple resistive adapters. This was the first approach.

The impedances of several cables were estimated by using time domain reflectometry. A pair of "L" attenuators was built for each of the various impedances using the design criterion that they would minimize reflections with the least amount of attenuation. Figure 8 demonstrates the use of these adapters. As described previously, a reference measurement is taken as in (a) which includes information about the generator, measurement system and both adpaters. This is deconvolved from measurement (b) leaving only the characteristics of the cable. If the cable impedance is Z_c , then the resistors R_1 and R_2 are calculated as follows.

Assuming that $Z_c < 50$ ohms, which was true for all cables tested,

$$R_1 = 50/[1 - Z_c/50]^{1/2}$$

$$R_2 = Z_c/[1 - Z_c/50]^{1/2}$$

As an example, one cable tested has an impedance $Z_c = 37.0$ ohms. This requires that $R_1 = 25.5$ ohms and $R_2 = 72.6$ ohms. Adapters were built using metal film resistors, with a parallel pair of 51-ohm units to approximate the 25.5-ohm resistor. These were connected to the center conductor of a BNC type connector. Three 300-ohm resistors and a 270-ohm resistor were mounted radially to approximate the 72.6-ohm shunt resistor. The physical layout was chosen to be roughly coaxial. Using these resistors, the calculated attenuation of the pair of adapters is an appreciable 9.8 dB.

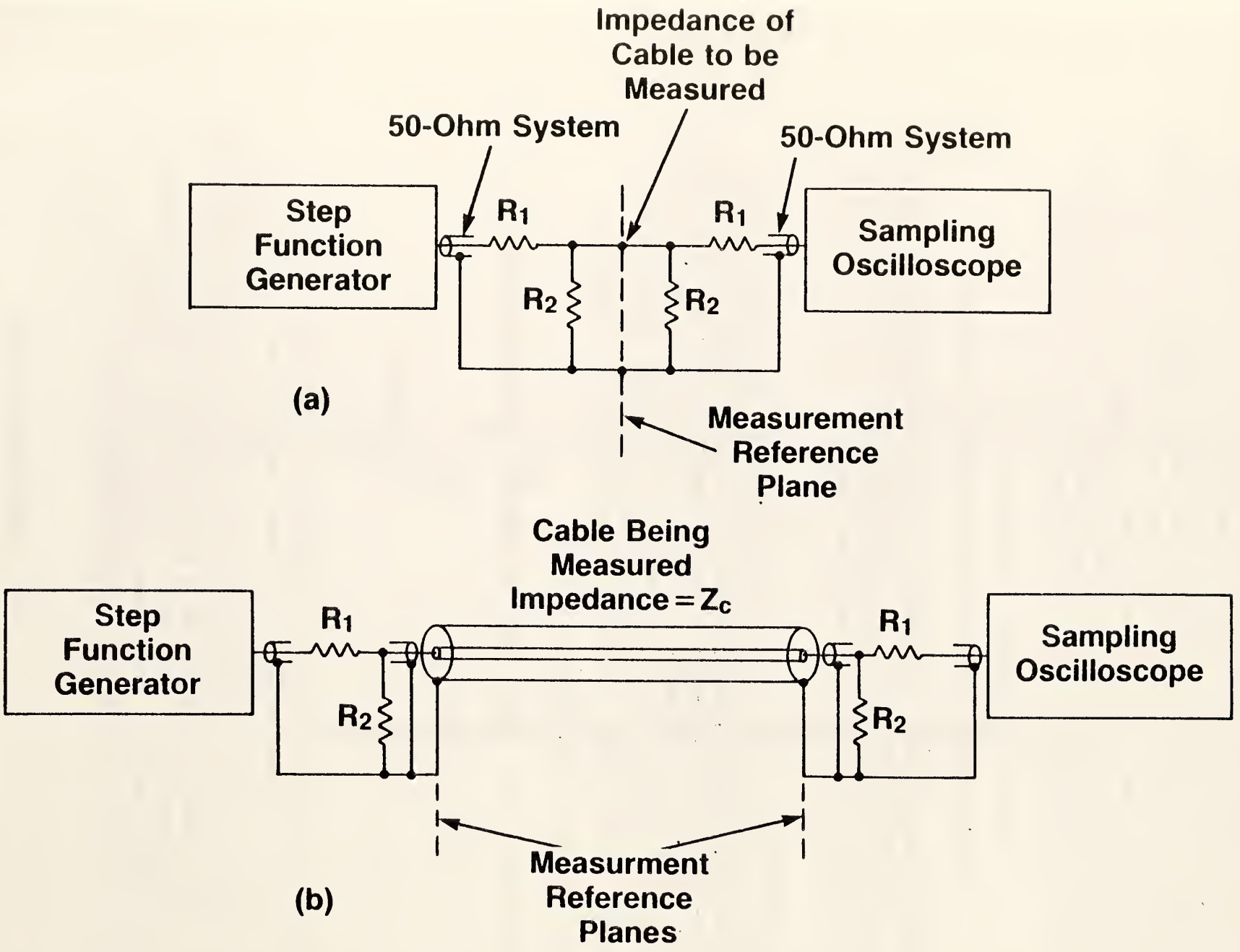

Figure 8. The use of "L" type attenuators for approximate impedance matching and reducing the undesirable reflections at the cable interfaces.

Considering the large loss in the adapters, excessive errors can be predicted when the cable loss is very small. Suppose the cable loss at a certain frequency is only 0.1 dB. If the measurement is made in accordance with figure 8, the loss in the cable would be the difference between the total attenuation in (b) and (a) (i.e., 9.9 - 9.8 dB). Since the desired quantity is only one percent of the measured quantity, an uncertainty of less than one percent is required for the results to be meaningful. Such accuracy is pressing the capabilities of the time domain measurement system, so the method is best used only to measure large attenuations.

To evaluate the useful frequency range of the adapters, a substitution measurement was made using the adapted pair as the unknown. Results shown in figure 9 indicate that they have a constant attenuation of about 9.8 dB for all useful frequencies. Even the variation above 400 MHz can be deconvolved out of a measurement as long as the attenuation does not absorb too much of the useful signal. The adapters have been used in measurements up to 2 GHz.

For large values of attenuation this measurement technique is relatively easy to perform and yields results having low noise and small uncertainties. It can be used on any length cable without concern for multiple reflections. It is the one technique that could work equally well in the frequency domain.

Results of three sets of measurements taken with these adapters on a commonly used distribution cable showed that the attenuation is a linear function of frequency, and this was true for almost all cables tested. It was clear that the smaller values of attenuation deviate more from the straight line than the larger values, supporting the earlier claim that measurements in this lower range are reaching the accuracy limit of the measurement system.

2.3.2 Reflection Mode with Matched Resistive Adapter

Figure 10 is a modified version of figure 3 with the addition of the resistive adapter. The waveform that is viewed on the oscilloscope in (a) is comprised of two parts, as shown in figure 11(a); the output from the step generator passing through the oscilloscope toward the resistive adapter, and the wave reflected from the short returning to the oscilloscope by way of the adapter. The second part contains the information about the original generated step waveform, the oscilloscope transfer function, the round trip transfer function of the adapter and the short circuit termination. The first part of the waveform does not contain this information and is time windowed out as shown. The configuration in figure 10(b) contains all the information of (a) plus a round trip transfer function of the cable as shown in figure 11(b), so that deconvolving (a) from (b) gives the cable characteristics. It is important to recall that this attenuation will be twice as large as the one way-trip measured in the transmission mode.

2.3.3 Reflection Mode Using Abrupt Transition

The reflectometry mode depicted in figure 3 does not make use of matching adapters and avoids the initial expense and time required to construct them. But it should be clear by now that reflections could reduce the accuracy of such a measurement and it is more convenient to use the matching adapters once they are built. On the other hand, it has been shown that the losses in the adapters can cause large errors when measuring cables with small attenuation,

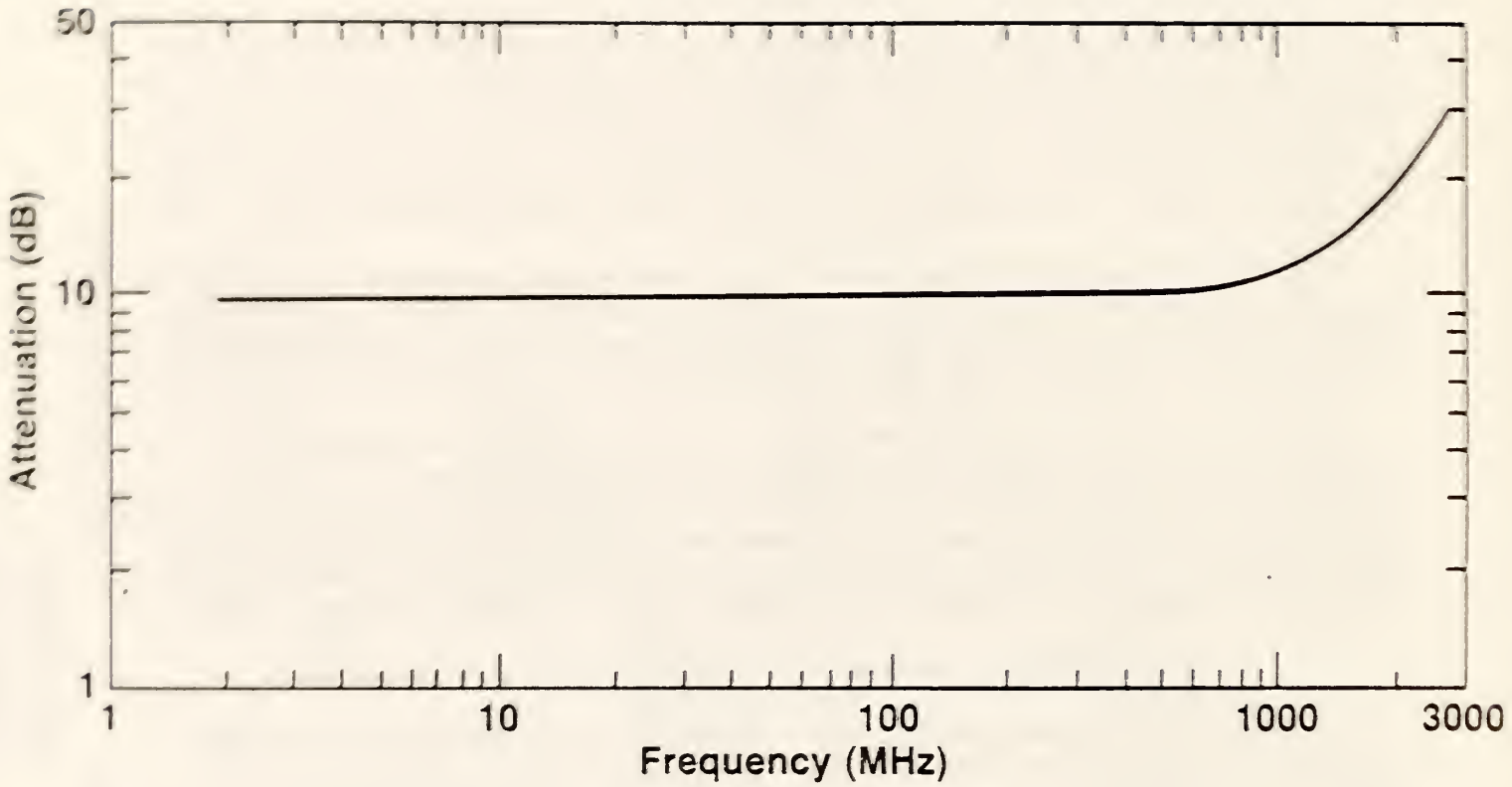

Figure 9. Attenuation as a function of frequency of a pair of "L" type attenuators (adaptors) used in making HV cable measurements.

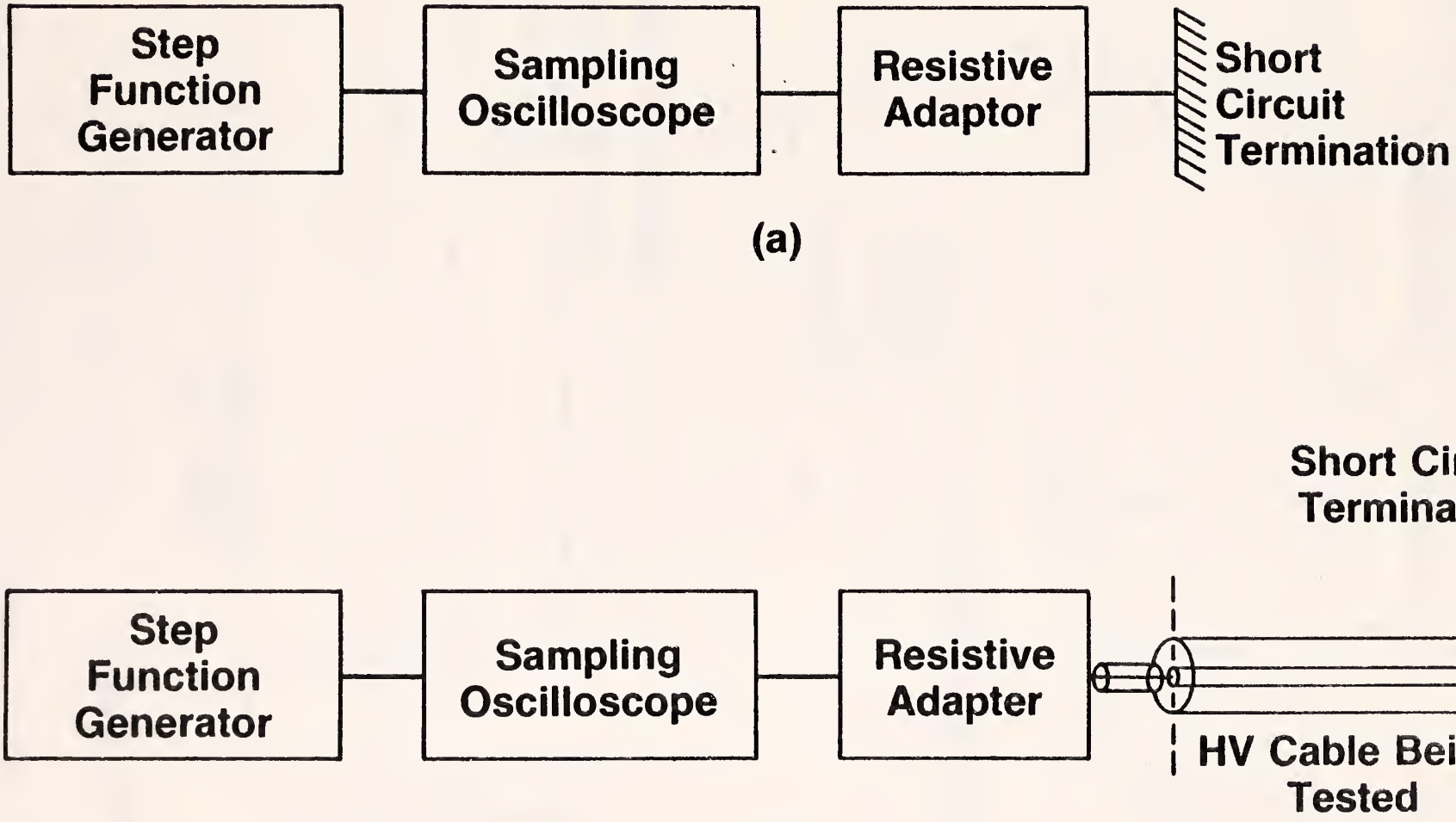

Figure 10. Circuit configuration for making TDR cable measurements incorporating the "L" type resistive adaptors.

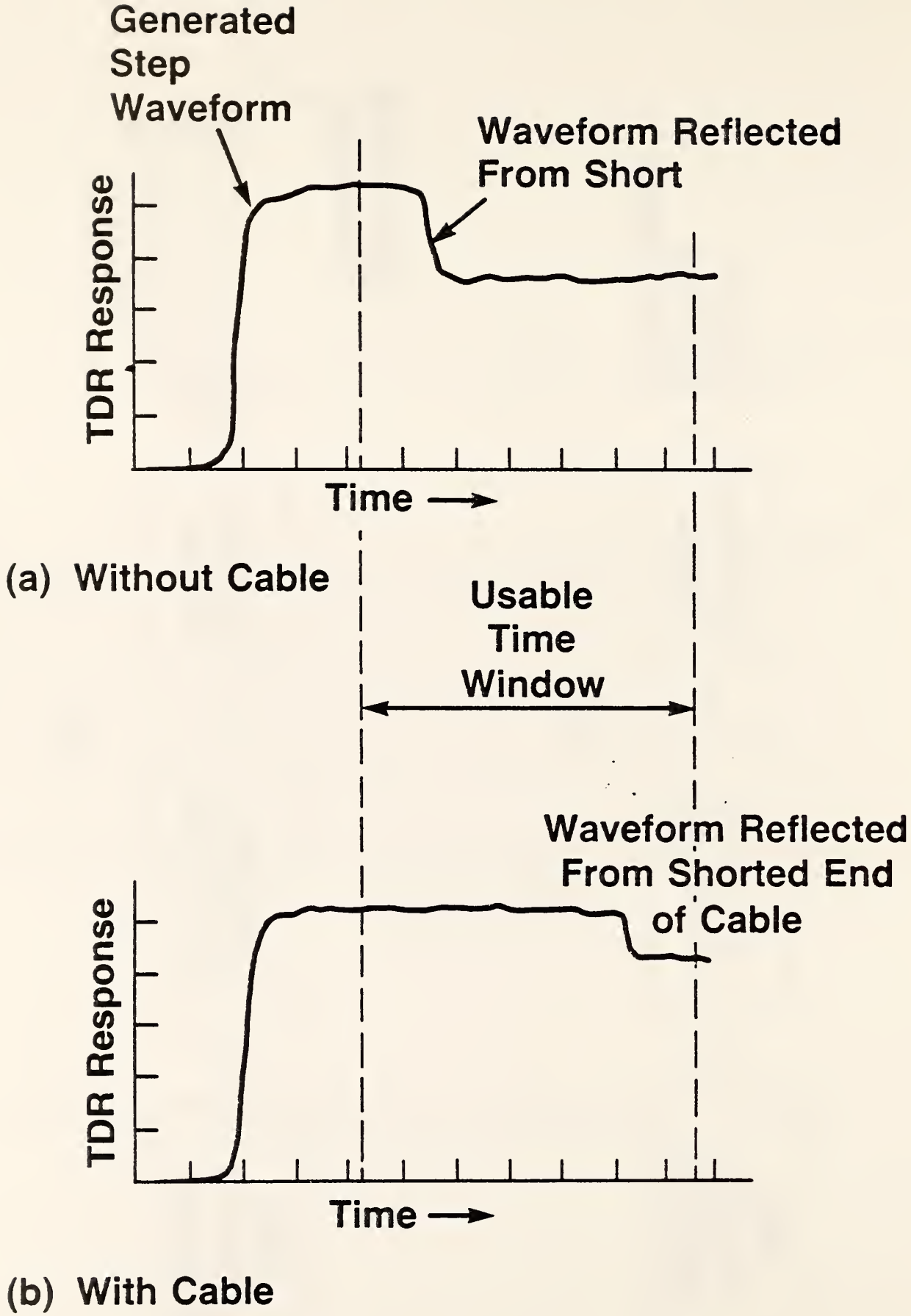

Figure 11. Pulse response with and without a cable when using the resistive-adaptor circuit configuration shown in figure 10.

say less than 1 dB. For these lower attenuations and for quick evaluations, it is useful to make a direct measurement without adapters (referred to as an "abrupt transition" herein) and correct the result for the reflections.

First, consider how large these errors might be. It is straightforward to calculate the reflection error as a step waveform passes across such an abrupt transition. The equivalent circuits are shown in figure 12. In each circuit, the transmission line is considered a Thevenin's equivalent circuit with the source impedance equal to the line surge impedance just prior to the plane defining the location of the equivalent circuit, and the load impedance equal to the line surge impedance just after the plane. The Thevenin's source voltage can be calculated from the load voltage and remains the same as long as the source remains in the same cable. In each case, only the wave travelling in one direction is considered as if it could be time windowed out and separated. Also, only the first reflection from the abrupt junction is considered. Multiple reflections are time windowed out of the problem.

For simplicity, consider both transmission lines to be lossless and their impedances to be resistive (actually nearly resistive). Beginning with circuit (a), assign a source voltage V = e; the actual line voltage must be e/2 because the source and load impedances are equal. At the abrupt junction (b), the source voltage is still that of the 50-ohm line, that is e, but the voltage in the cable is now

$$V_c = \frac{e\ Z_c}{50 + Z_c} ,$$

by simple voltage divider action. Once the wave has propagated into the unknown cable (c), the measured voltage remains the same (V_c) but the new source becomes the unknown cable instead of the 50-ohm transmission line. Therefore a new source voltage must be calculated from the actual load voltage.

Assume that the step wave is reflected from the open circuit termination without attenuation. The same rules apply for the wave moving to the left (d) and (e). To calculate the transfer function of the abrupt transition, consider that the equivalent circuits are resistive and, therefore, the transfer function will be constant with frequency. The magnitude of the transfer function is simply the dividing ratio of the equivalent circuit. It is defined by

$$\text{Transfer Function (TF)} = \frac{\text{Output Voltage}}{\text{Input Voltage}} .$$

For the wave moving to the right,

$$TF_R = \frac{V_c}{V_{50}} = \frac{eZ_c/(50 + Z_c)}{e/2} = \frac{2Z_c}{(50 + Z)}$$

For the wave moving to the left,

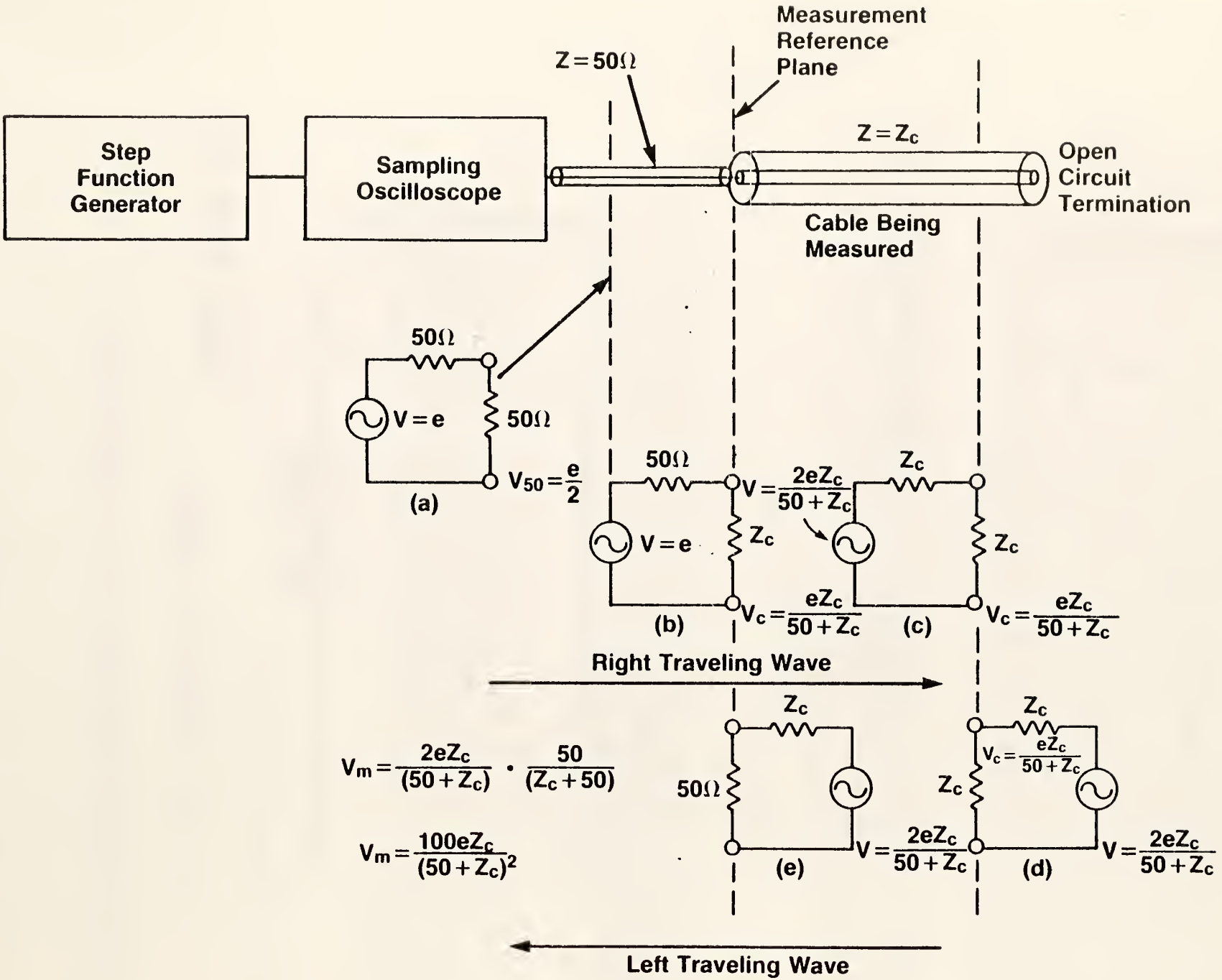

Figure 12. Equivalent circuits of the two-impedance cable system where the interconnecting cable represents an abrupt change of impedance.

$$TF_L = \frac{V_m}{V_c} = \frac{100\ eZ_c/(50 + Z_c)^2}{eZ_c/(50 + Z_c)} = \frac{2(50)}{(50 + Z_c)} \quad .$$

Notice that the transfer function is simply the voltage divider ratio across the transition and is different in the two directions. This will be an important consideration when developing the algorithm to correct the reflection error.

Next consider the transmission loss that a wave suffers while passing through an abrupt transition. (Strictly speaking, this is not an attenuation since the transmission line and cable were assumed to be lossless, but is due to reflection loss.) The important point to consider is that the normal equation for losses cannot be used. That is, loss = 20 log $|V_{out}/V_{in}|$ is not valid because it tacitly assumes that the input and output impedances are equal and have divided out in the ratio. Also, in general, V out and V in are complex so the magnitude of the ratio is needed. The correct approach involves the input and output volt-ampere product, but since our equivalent circuits are resistive, this simplifies to power calculated as V^2/R. So,

$$\text{loss} = 10 \log \left(\frac{V^2_{out}/R_{out}}{V^2_{in}/R_{in}} \right) \quad .$$

If this relationship is used with the voltages on either side of the transition, the one-way loss is

$$\text{loss} = 10 \log \left[\frac{4(50Z_c)}{(50 + Z_c)^2} \right] \quad ,$$

and this is true regardless of the direction the wave propagates.

On the other hand, the round trip transmission loss can be calculated calling V the input and V_m the output and both are in a 50-ohm transmission line. So, using

$$\text{loss} = 20 \log (V_m/V_{50}) \quad ,$$

$$\text{loss} = 20 \log \left[\frac{4(50)Z_c}{(50 + Z_c)^2} \right] \quad , \tag{1}$$

and this is precisely twice the one-way loss as it should be.

Based on this reasoning and understanding that the round trip transfer function for the transition is precisely the voltage ratio,

$$TF = \frac{4(50)Z_c}{(50 + Z_c)^2} \quad ,$$

it is permissible to construct an artificial one-way transfer function, TF, which is simply the square root of the round trip TF, as

$$TF' = \sqrt{TF} = \frac{2\sqrt{50\ Z_c}}{(50 + Z_c)} \quad .$$

This is the geometric mean of the two real TFs and produces the correct value of the one-way transmission loss using

$$\text{loss} = 20 \log|TF'| \quad . \tag{2}$$

This feature makes it simpler to perform the loss calculations if it is used carefully.

As an example, if the cable impedance were 37.50 ohms, the round trip loss calculated using eq (1) amounts to 0.18 dB. One mustseriously question whether the error is large enough to warrant correction. It certainly seems advisable when the attenuation being measured is less than 1 dB, and this is the same range of attenuation for which the resistive adapters produce significant errors.

Finally, let us generate the correct algorithm for the abrupt transition. Now assume that the 50-ohm transmission line is a standard 50-ohm impedance and is lossless, but the unknown cable impedance is not well known and has losses to be measured. The configuration is shown in figure 13. The round trip loss in the cable might be calculated from

$$\text{loss} = 20 \log (V_b / V_a) \quad . \tag{3}$$

However, V_a and V_b are not directly measurable. Instead, a step-like waveform is measured by the sampling oscilloscope as it propagates toward the transition. Two usable reflections return, one from the transition and the second from the open (or short) circuit termination at the far end of the cable. This second reflection contains information about cable attenuation and the round trip transmission loss of the transition. Basically the correction algorithm must take the total measured loss and subtract the abrupt transition loss.

Although the measurement is made in the time domain to take advantage of time windowing to separate the various reflections, the correction algorithm is done in the frequency domain. The voltages shown in figure 13 are the spectral components of the actual waveform at one given frequency. Because of the time windowing, the spectrum can be separated into single frequency components propagating to the right or left as shown. Voltage V_g is the

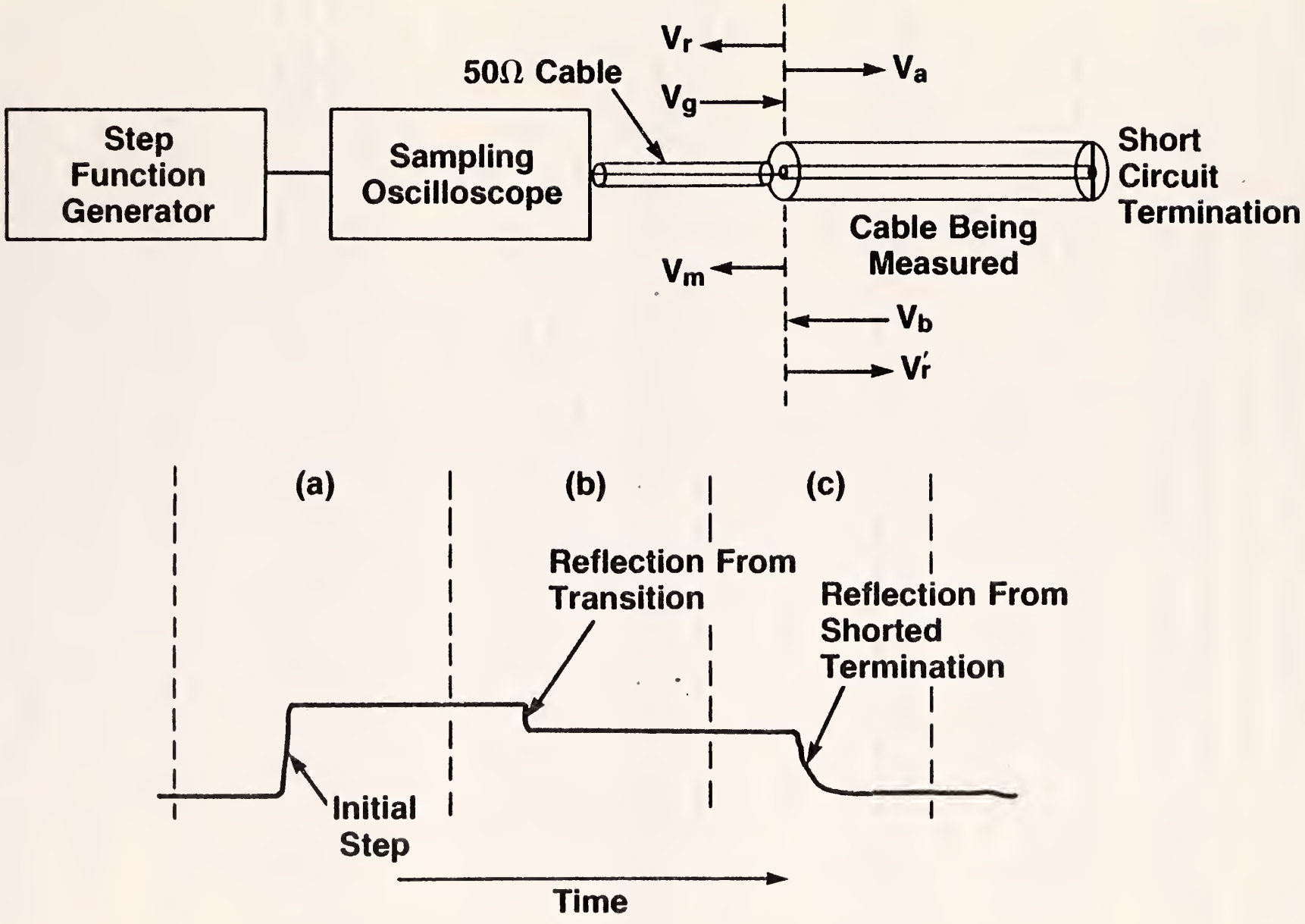

Figure 13. Voltage and pulse response when using an abrupt transition method of measurement.

complex spectral component from the generator as it approaches the reference plane. V_r is the portion of V_g that is reflected back into the 50-ohm system, and V_a is the portion that enters the unknown cable. Voltage V_b has made a round trip through the cable and approaches the reference plane. V'_r and V_m are the reflected and measured portions of V_b, respectively.

To calculate the attenuation of the cable, it is sufficient to consider power flow. The total attenuation and the reflection losses in the cable are given by

$$\text{Total Power Loss} = 20 \log (V_m/V_g) \quad .$$

This is valid since both V_m and V_g are measured in the 50-ohm system. The reflection loss can be calculated as the ratio of the power propagated into the cable divided by the power incident on the transition plane.

$$\text{Reflection loss} = 10 \log \left(\frac{V_a^2/Z_c}{V_g^2/50} \right) \quad .$$

However, the cable impedance Z_c is not well known. It is easier to see that the propagated power is the simple difference between the incident and reflected power, or

$$\text{Reflection loss} = 10 \log \left(\frac{V_g^2/50 - V_r^2/50}{V_g^2/50} \right) \quad ,$$

$$= 10 \log \left((V_g^2 - V_r^2)/V_g^2 \right) \quad .$$

Since this is the loss for a single pass through the transition plane, and it has been shown that the attenuation is the same in either direction, the total reflection loss is simply twice this number. Therefore, the attenuation of the cable is just the difference between the total loss and the reflection loss, or

$$\text{Net Attenuation} = 20 \log (V_m/V_g) - 20 \log \left((V_g^2 - V_r^2)/V_g^2 \right) \quad ,$$

$$= 20 \log \left(V_m V_g / (V_g^2 - V_r^2) \right) \quad . \qquad (4)$$

Because this is based on a power relationship, the magnitude of the appropriate spectral component can be used in the formula rather than the complex voltage. However, it is also possible to calculate the complex

voltages V_a and V_b in terms of V_g, V_r, and V_m and substitute directly into eq (3) with identical results.

This calculation must be repeated for each frequency in the spectrum and the BASIC program that accomplishes this is given in Appendix C. The waveform is shown in figure 13 and is time windowed three times as shown. Portion (a) is V_g, portion (b) is V_r, and portion (c) is V_m.

If the waveform cannot be properly time windowed as shown in figure 13, an alternate method shown in figure 14 can be used. Waveform (a) is taken with a 50-ohm termination on the reference plane. Waveform (b), (c) is taken with the unknown cable on the reference plane but time windowed appropriately. The (a) is V_g, (b) minus (a) is V_r, while (c) produces V_m as before.

When a 50-ohm termination is not available that mates onto the reference plane, the condition can be approximated by measuring a short (d) and open (e) and taking half the sum of the two. This method is available in the software package listed in Appendix D.

2.3.4 Reflection Mode Using a Tapered Transition

The ideal way to measure cable characteristics would be to use a lossless impedance matching device between the measurement system and the unknown cable, for example, a broadband transformer. These tests used a tapered transition, consisting of a section of rigid transmission line with a center conductor whose diameter increased uniformly along its length transforming the impedance from 50 ohms to 37.5 ohms. Figure 15 shows an assembly drawing of the transition section. The right end has a high quality 50-ohm coaxial connector on it, modified to connect to the stepped 50-ohm center conductor and adapter sleeve. The TDR system connects to this coaxial connector. The left end of the 35-cm long tapered section connects to the power transmission line's center conductor. The slit section of the outer conductor clamps over the outside of the power transmission line.

The tapered line is useful as a lossless transformer for frequencies whose wavelengths are less than the length of the transition [11]. For frequencies whose wavelengths are considerably longer, the taper looks like an abrupt transition. This can be seen in an approximate way from the time domain waveform, figure 16. Portion (a) is just the initial step waveform as before. Portion (b) is the reflection from the taper and is a linear ramp joining the voltage of the 50-ohm system to the voltage in the unknown cable (approximately 37.5 ohms). Waveform (c) is the reflection from the unknown cable and its short circuit termination. It is apparent that the transition has a reflection and that its time characteristics are slower than the initial step input. Also, considering that the spectrum for a step decreases inversely with frequency, while for a ramp, it decreases as the inverse squared, the reflected ramp waveform should have much smaller high frequency components than the incident step, or conversely, the taper must be matching the cable to the system better at high frequencies than at low. This conclusion is also expressed in the reference [11].

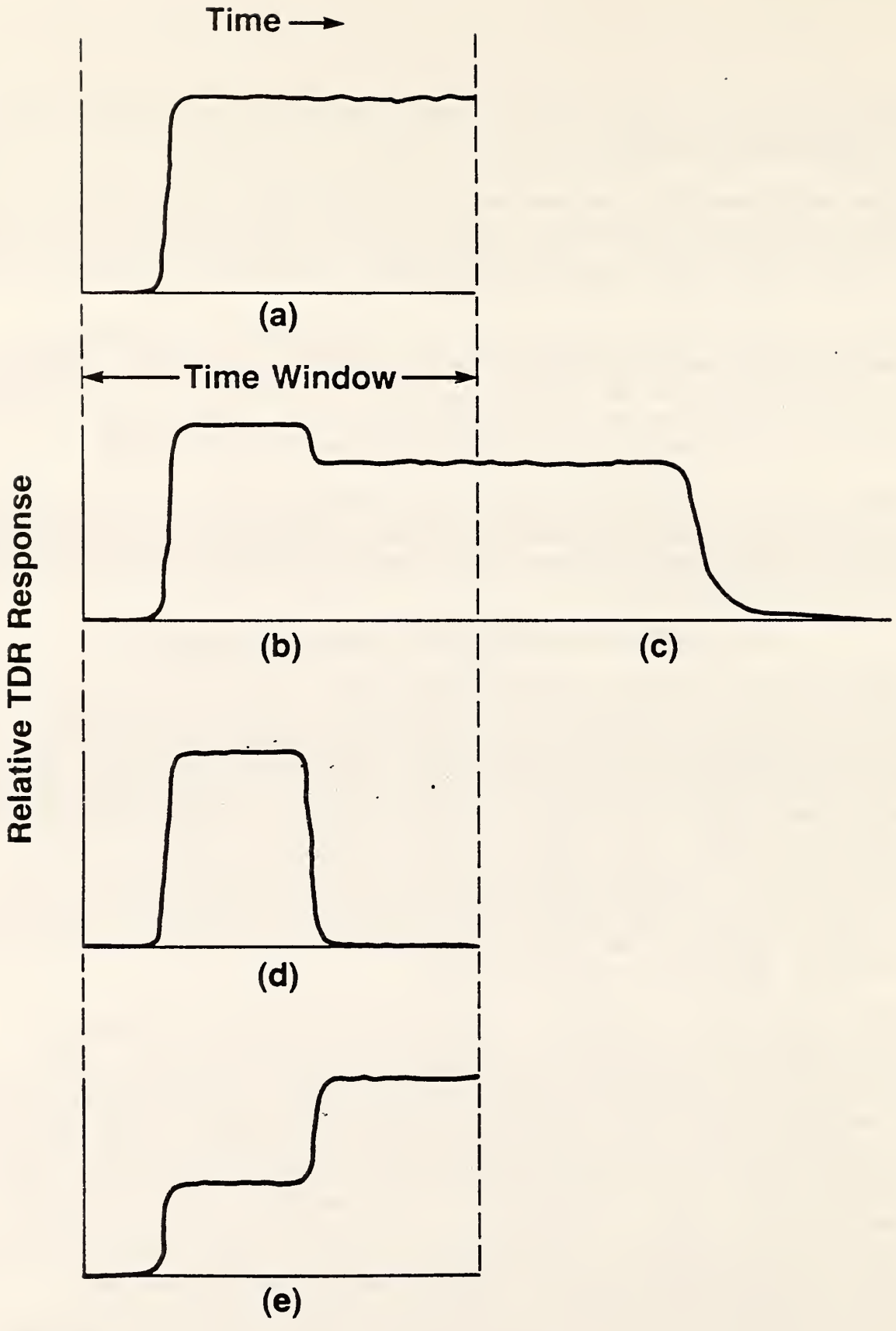

Figure 14. Alternate method for time windowing TDR responses to eliminate the effects of the interconnecting cable.

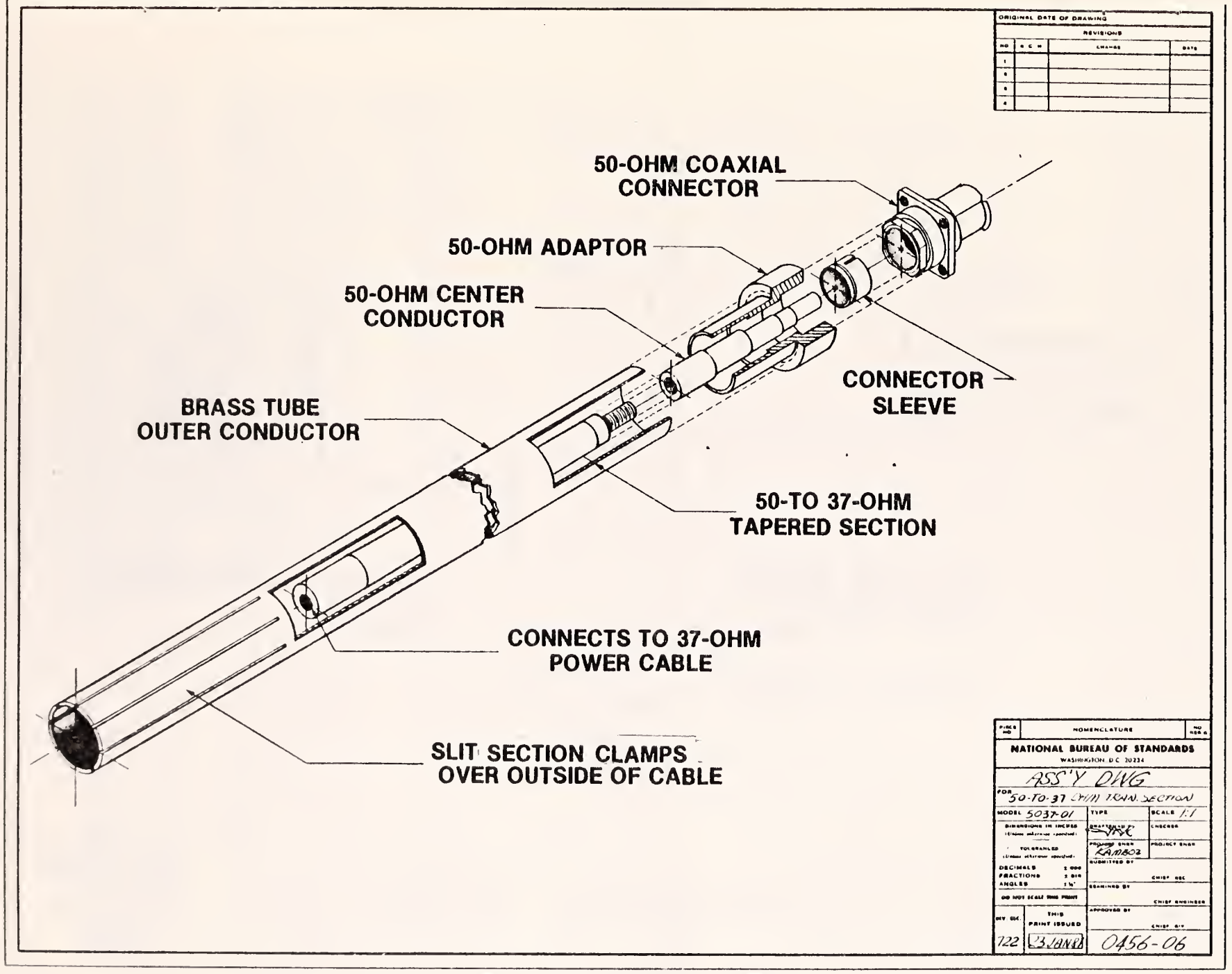

Figure 15. Assembly drawing of the 50 to 37 ohm tapered line transition section.

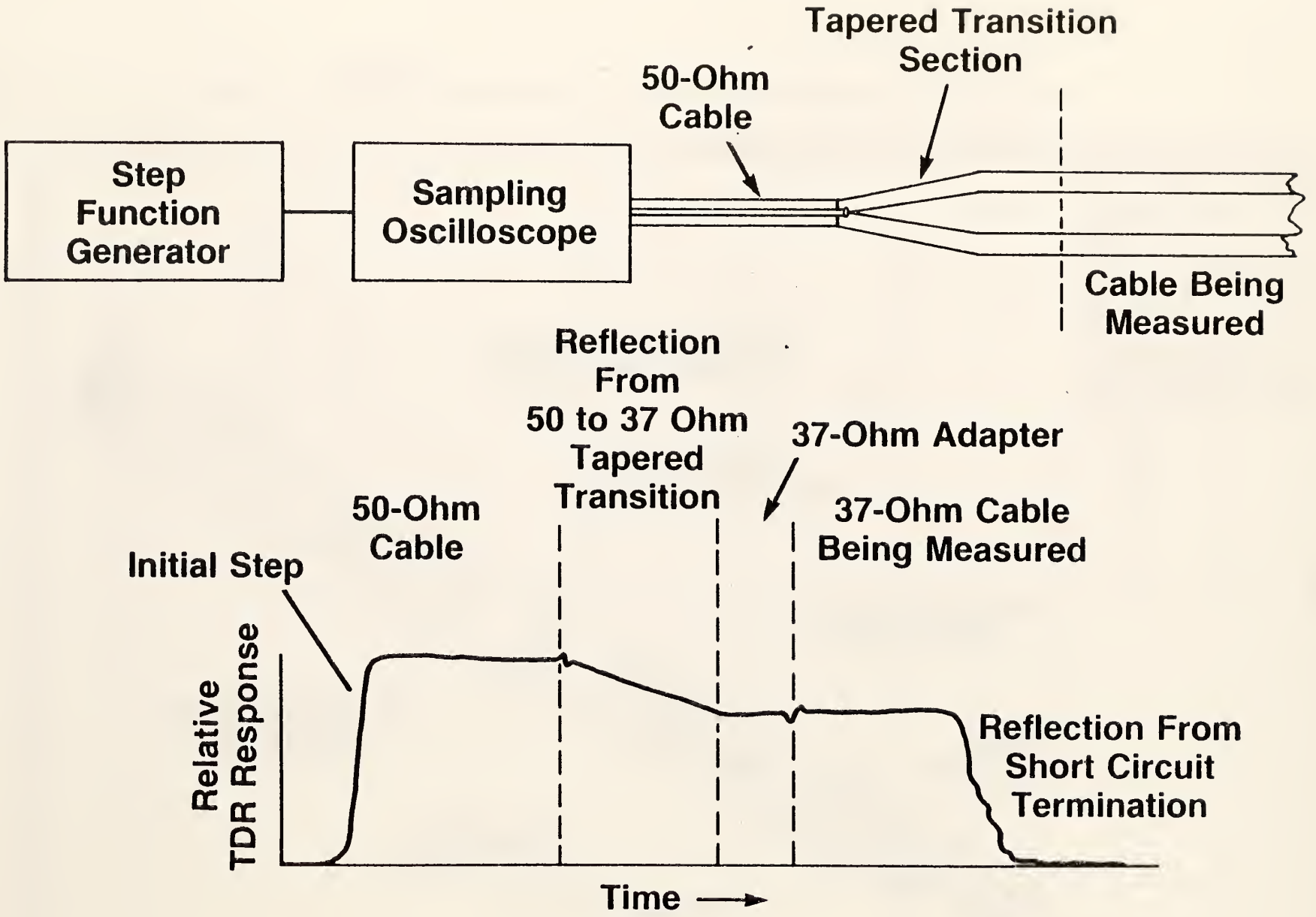

Figure 16. TDR response when using a 50-ohm system and a 50 to 37 ohm tapered transition adaptor.

Over the frequency range that the taper functions well as a matching transformer, the measurement can be made identically as with the transmission and reflection modes using matched resistive adapters (sections 2.3.1 and 2.3.2 of this report). For very low frequencies, the taper can be considered an abrupt transition and can be used as described in the previous section. Frequencies in the range between these two extremes present some unique problems and have not been completely analyzed. The methods described herein will not function as desired for those intermediate frequencies.

2.3.5 Two-Lengths-of-Cable Method

Another method which is conceptually simple depends on measuring two lengths of unknown cable as in figure 17. The "short length" measurement in (a) includes information about the generated step waveform, the oscilloscope response, the transition characteristics, and the attenuation of the shorter length of cable. The measurement in (b) contains all of (a) plus the attenuation of the additional length of cable. Deconvolving (a) from (b) by frequency domain division gives the attenuation of the additional length of cable. All other effects including the transition are removed from the measurement providing that the waveform can be time windowed as in (a) and (b). Only part of the waveform is used and multiple reflections must be excluded. Multiple reflections are characteristic of the length of the cable and therefore different for the two lengths. During deconvolution, only those effects which are identical for the two measurements can cancel, so both sets of multiple reflections would contribute error into the result.

This method works well if the two lengths are not grossly different. The time window must be long enough to capture the entire time response of the longer cable. The same time window must be used for the short length and so it must be short enough so that multiple reflections would not appear in the window. The ratio of two lengths always had to be less than four. Other cables with less loss might permit a larger ratio.

3. MEASUREMENT RESULTS

Several cables were obtained from each of four different manufacturers and selected ones were measured for attenuation using the five methods described above. Some of these results are given here to support general conclusions.

Figures 18 and 19 are plots of the log attenuation versus log frequency for several cables and measurement methods. The log-log plot is used because the attenuation is expected to be a function of some power of the frequency and should plot to a straight line whose slope is that power. In general, the attenuation in dB turned out to be a linear function of frequency so that the straight lines on log-log paper have a slope of approximately one.

Two major loss mechanisms were considered for these cables; the resistive skin-effect loss in the center conductor and the outer braid, and the dielectric loss. Skin effect losses are known to increase as the square root of frequency and plots with slopes of 1/2 would have been expected. Since this was not normally found in the measurements, it was concluded that the attenuation was principally that related to dielectric loss.

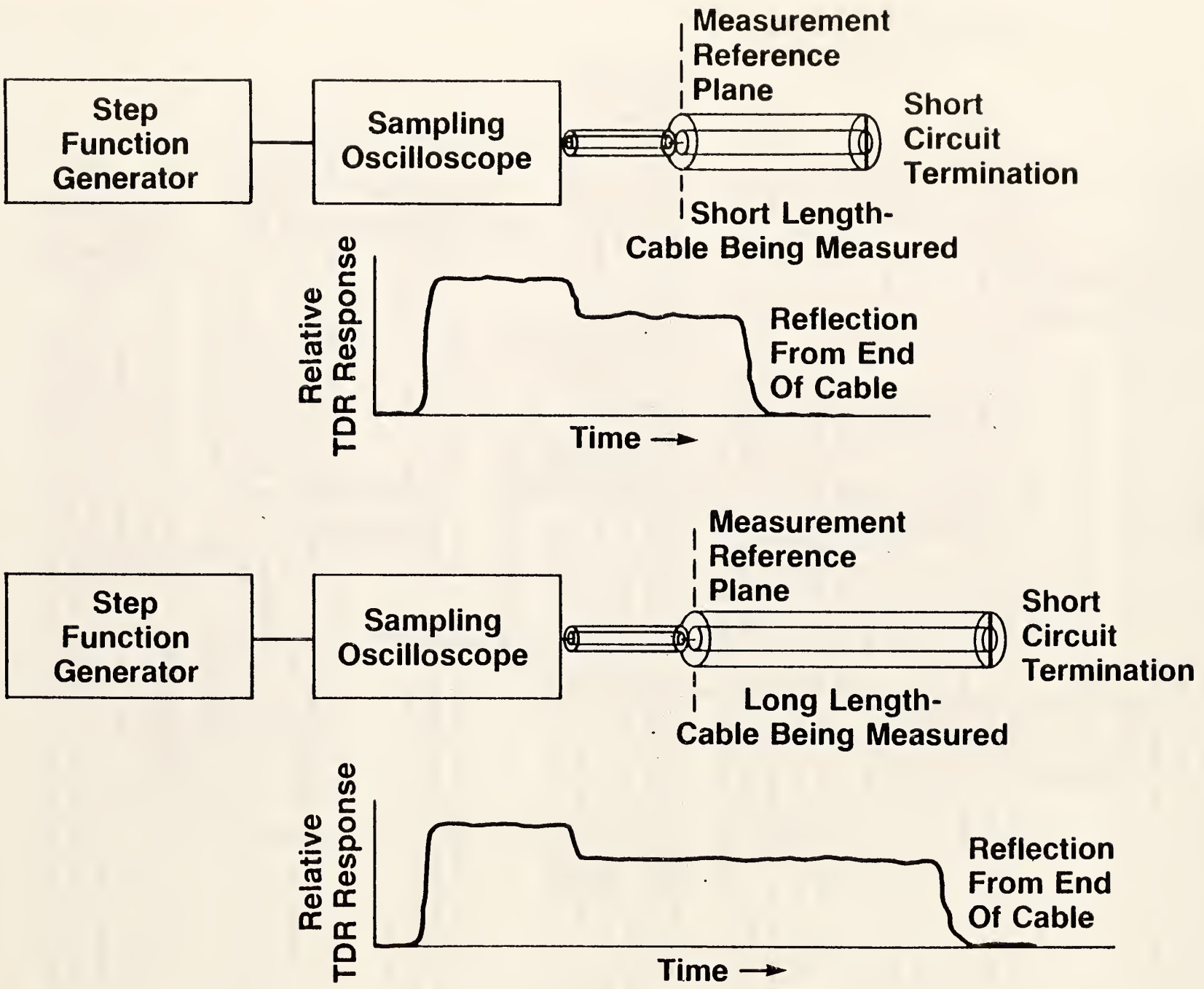

Figure 17. Configuration for measuring cable loss using the two-length method.

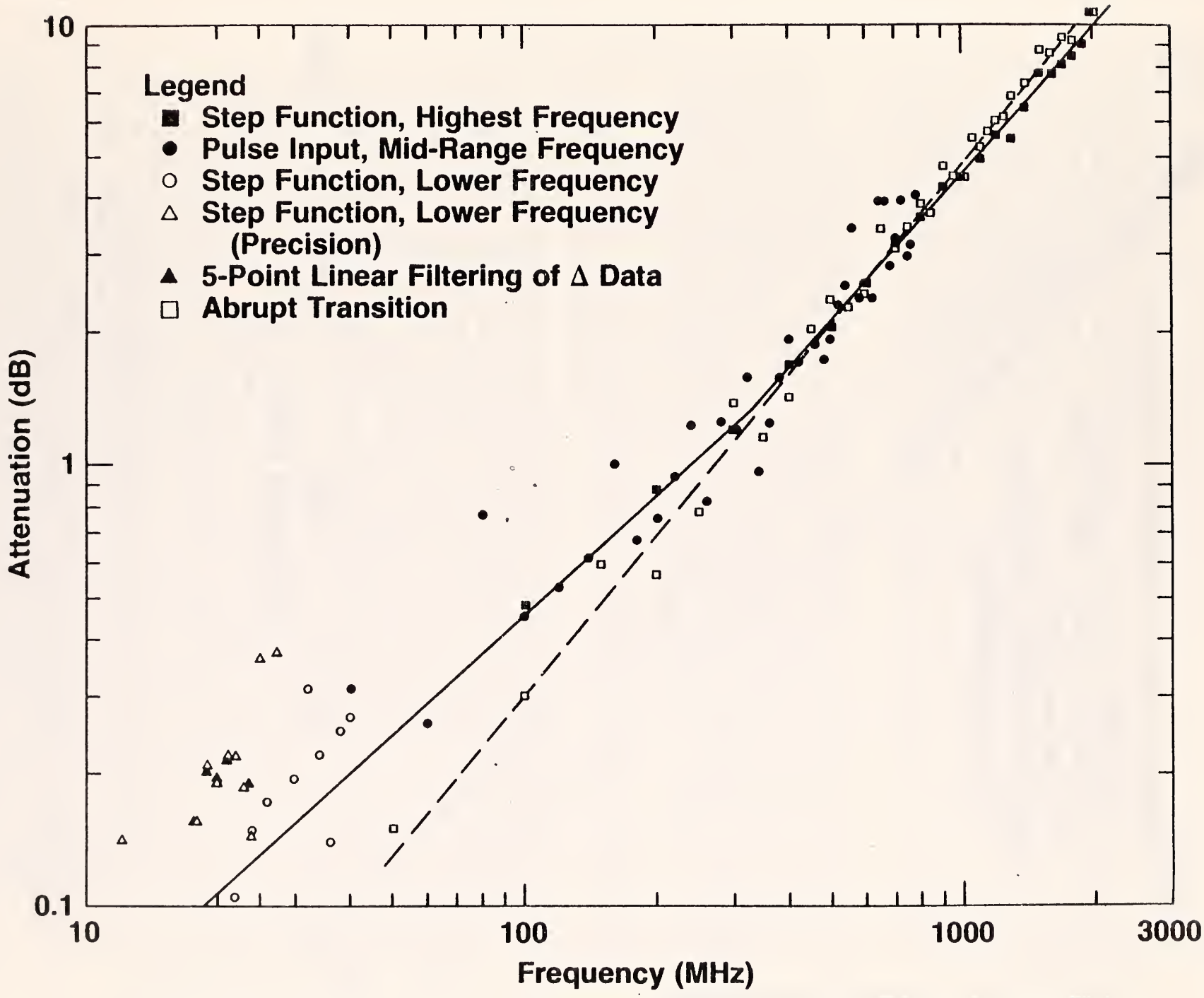

Figure 18. HV-cable loss as a function of frequency using the abrupt-transition and resistive-adaptor techniques. (Cable supplied by manufacturer A.) Losses shown as attenuation in units of dB/meter of cable length.

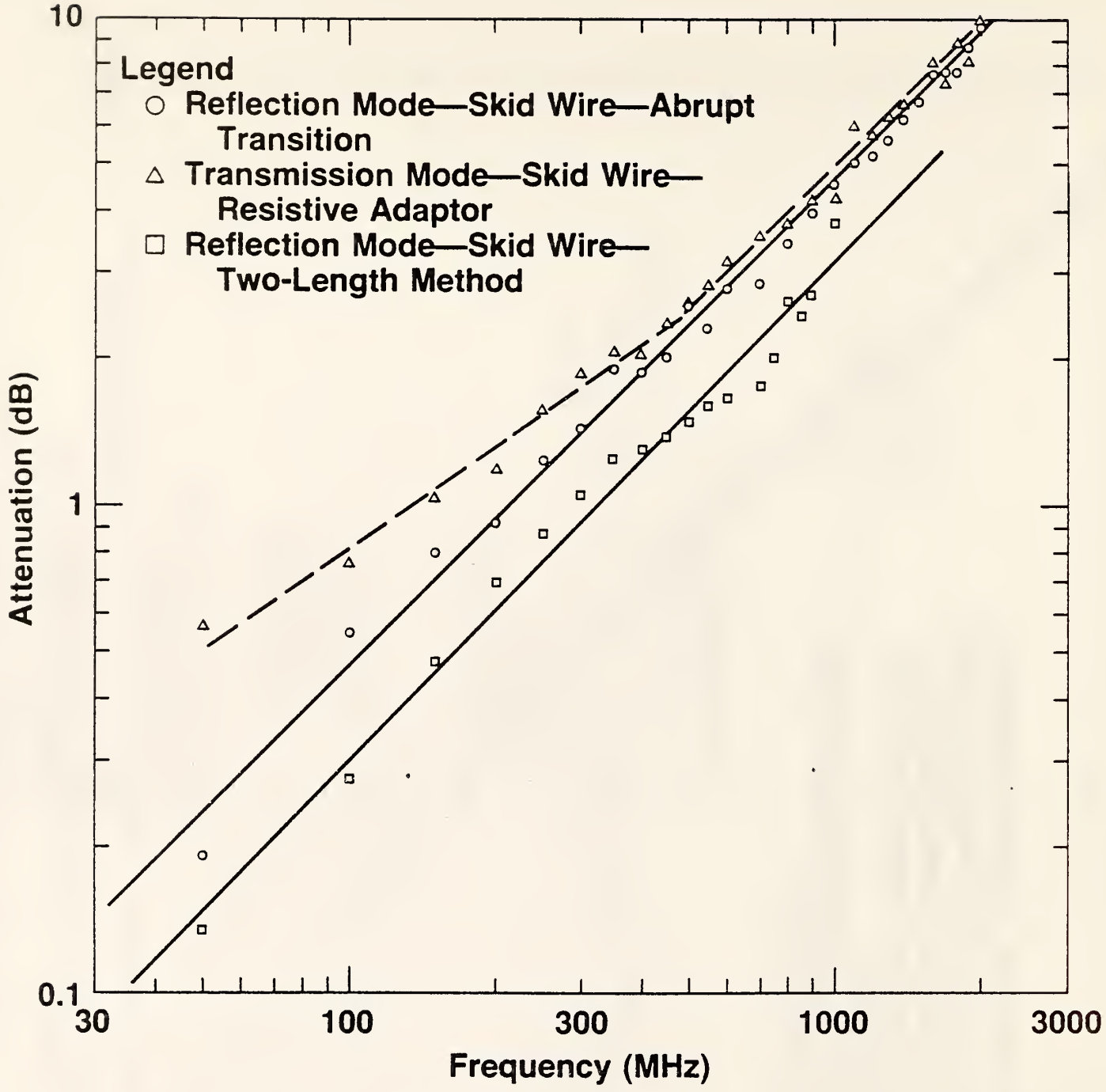

Figure 19. HV-cable loss as a function of frequency using the abrupt-transition, the resistive-adaptor, and two-length measurement methods. (Cable supplied by manufacturer B.) Losses are shown as attenuation in units of dB/meter length of cable.

Figure 18 shows the results taken from a cable of manufacturer A. The skid wires were removed and replaced with copper braid. The data marked with a dashed line was taken using an abrupt transition and it fits a straight line of slope 1.2 quite well. The data taken with the resistive adapters is drawn with a solid line and seems to be composed of at least two straight sections, the higher loss portion which nearly matches the abrupt transition curve and the lower attenuation curve with a slope of about 0.88. This two-slope curve is also evident in figure 19 for a cable from manufacturer B, and seems to be characteristic of measurement made with these particular resistive adapters. (The skid wires were left on this cable and no braid was used.) It appears to be the result of a 0.3 dB constant systematic error added to the normal measurement.

To help determine the source of this error, the adapter characteristics were measured using the time domain system. Two adapters were coupled together forming a 50-ohm attenuator. As can be seen in figure 20, the measured attenuation is 9.8 dB for all frequencies up to 400 MHz. The calculated attenuation is 9.8 dB, showing excellent agreement. This did not provide a clue to the source of the 0.3 dB error which is still unresolved. Figure 19 also shows results of a two-length measurement and is in only fair agreement with the abrupt transition measurements.

Figure 21 shows data taken with the tapered transition compared with abrupt transition data. Note how the two agree well at higher frequencies where the taper matches well.

It was important to decide if the loss was really due to the lossy dielectric, and if so, what part of the cable was producing such large attenuation. The loss of a one-meter length with various portions of the dielectric removed was measured. In each case, a copper braid was pulled over the cable. Figure 22 shows the losses (1) of the original cable, (2) of the same cable with outer semiconductor layer removed, and (3) the same cable with both inner and outer semiconductor removed and a copper rod replacing the original aluminum conductor. Two conclusions are obvious. First, the cable is six times lossier when both semiconductor layers are in place than when they are removed. Second, a meter length of cross-linked polythylene cable still is very lossy (1 dB at 1.5 GHz). All three curves have nearly the same slope at lower frequencies. The slope of the curve for the cable with the inner semiconductor removed has an obvious change of slope at about 1.5 GHz. The steeper slope indicates that a second source of loss is becoming dominant above this frequency. The source of this loss is not known, but it may be a skin effect loss at the surface of the copper raid due to the higher loss of the solder layer plating the copper. It seems likely that it was also present in the other cable configurations but was not so obvious because of their higher dielectric losses.

An idea was proposed to propagate a microwave signal through the cable in such a mode that practically all the energy was confined to the less lossy polyethylene and would not penetrate the semiconductor near the metal conductors. This last experiment indicates that at the frequencies required to propagate for long distances, only the largest diameter cables could be considered. For the small diameter cables (3-6 cm), the frequencies must be above 10 GHz. This compares to ordinary TEM propagation at 1 GHz at similar losses for larger cables. The testing of small diameter cables is not

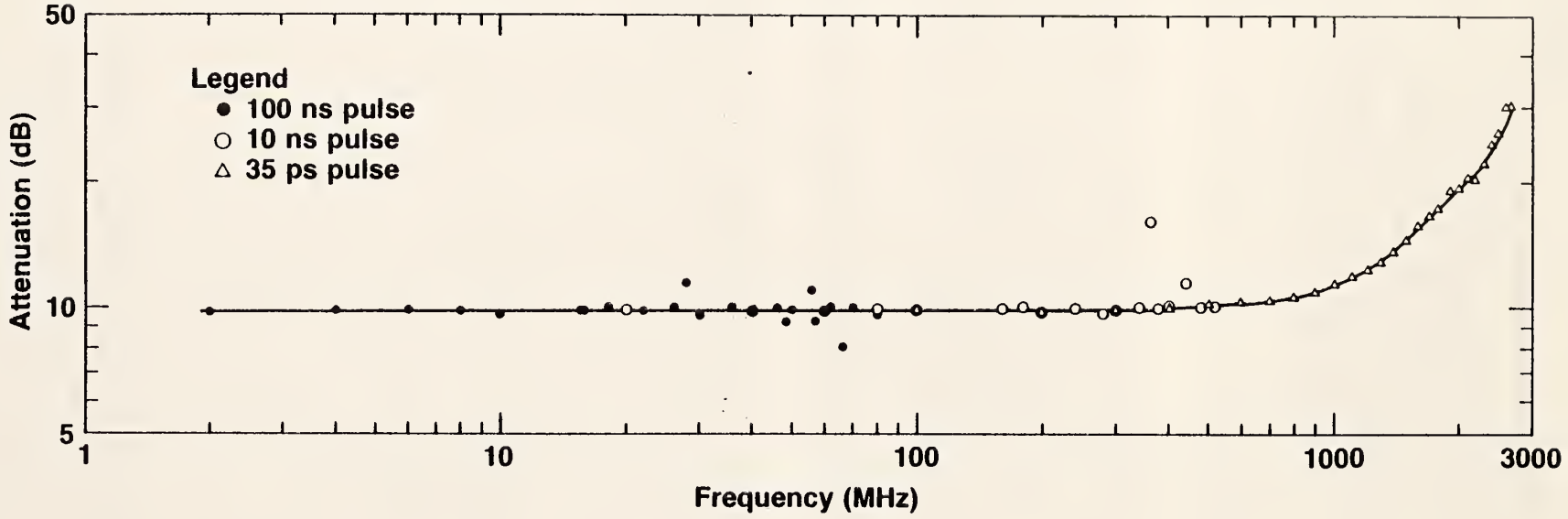

Figure 20. Loss characteristics of the two resistive adaptors as a function of frequency for three different test pulses.

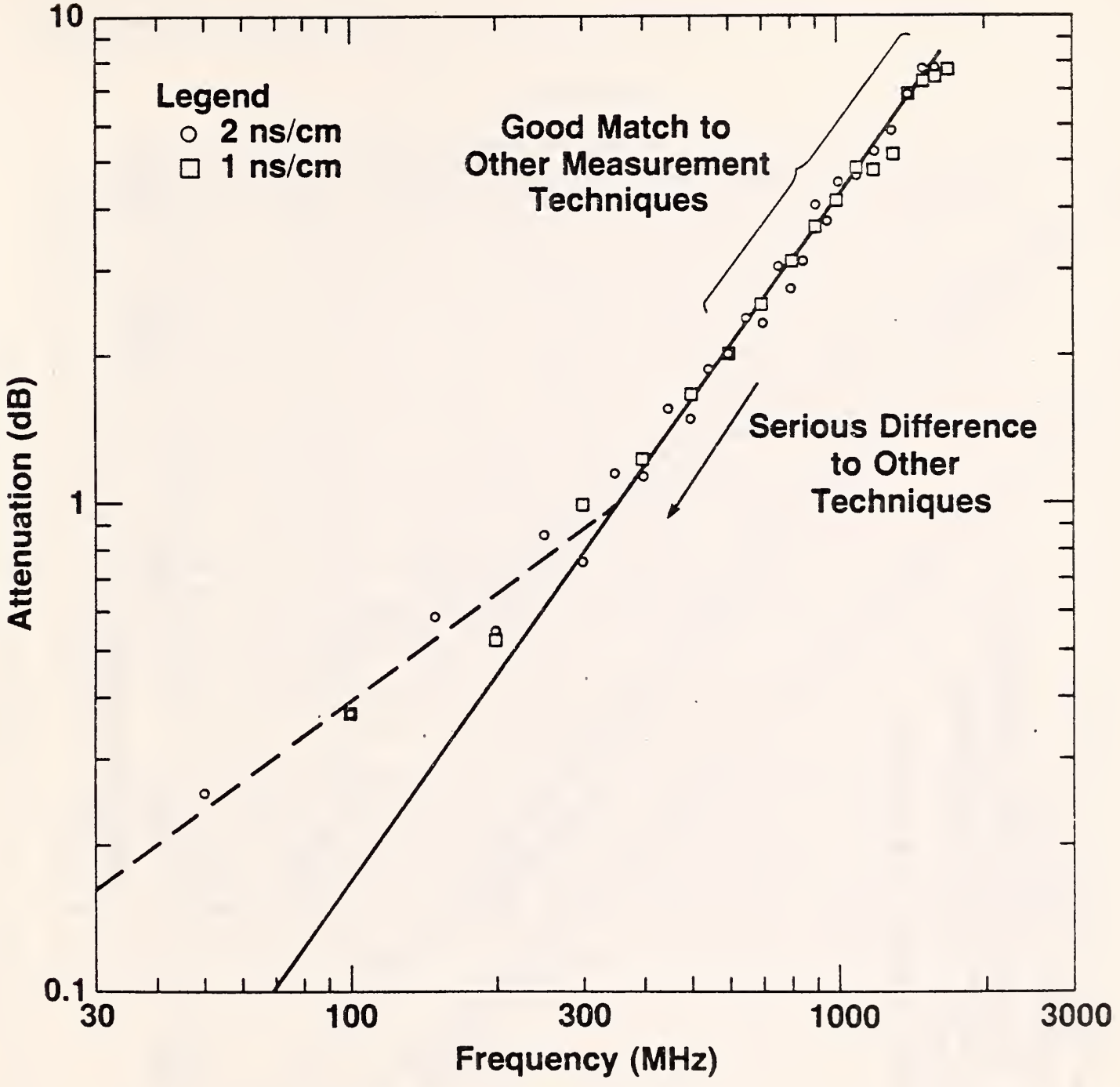

Figure 21. HV-cable loss as a function of frequency using the tapered-transition adaptor and the abrupt-transition methods. Losses shown in units of dB/meter length of cable.

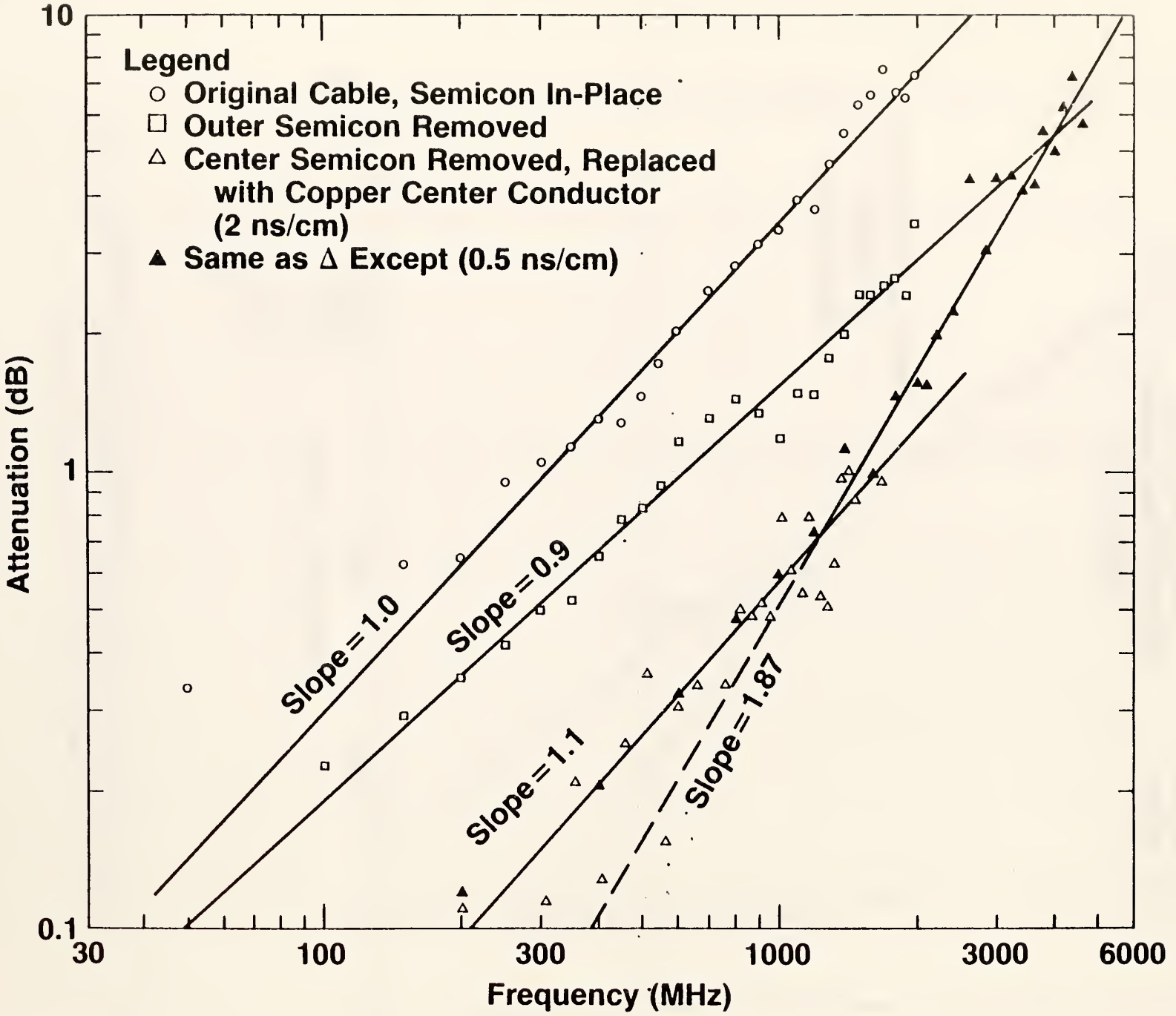

Figure 22. HV-cable loss, with and without semiconductor layers. Losses shown are in units of dB/meter length of cable.

practical for long distances. However, it may become useful for short distance cable evaluation.

4. CONCLUSIONS

The Department of Energy sponsored program on incipient fault detection/location has resulted in significant contributions that should be utilized in the future. Purdue University's time-delay noise correlator passed all laboratory tests and appeared to be fully capable of meeting the DOE objectives. Westinghouse has determined that acoustical-optical techniques appear promising for the detection and location of incipient faults in compressed gas-insulated cables. SRI has obtained vast amounts of data on the propagation properties of several cables under actual field conditions. They have explored the use of two different RF-probing techniques for incipient fault detection/location. NBS has demonstrated some fundamental limitations of using reflectometry approaches in extruded polyethylene cables. In the process, good data on the attenuation of a variety of distribution cables have been obtained. It appears that the largest source of loss in these cables are the two semiconductor layers. Unfortunately, they are required for satisfactory cable performance under high-voltage conditions. The prospect of launching waveguide modes in these cables which would not "see" the inner and outer semiconductor layers was briefly explored. The results looked promising. It may be shown later that the attenuation is still too high for incipient fault detection over appreciable distances, but the waveguide approach might still be beneficial for cable manufacturers as an online defect detector.

5. ACKNOWLEDGMENTS

This work was sponsored by the Office of Electric Energy Systems of the Department of Energy; Mr. Russell Eaton was the technical coordinator. The cooperation of several cable manufacturers is appreciated, namely, Reynolds Metals Company, Electrical Division, of Richmond, Virginia, Phelps-Dodge Company, Yonkers, New York, Piralli Cable Company, Union, New Jersey, and the Okanite Company, Ramsey, New Jersey. The Potomac Edison Company also provided some cable samples which had been taken out of service. The authors would also like to express thanks to Mrs. Barbara L. Frey who prepared this manuscript.

6. REFERENCES

[1] Anderson, W.E., Ramboz, J.D., 1980 Annual Report. Technical Contributions to the Development of Incipient Fault Detection/Location Instrumentation, NBSIR 81-2235, Nat. Bur. Stand., March 1981.

[2] Anderson, W.E., Ramboz, J.D., Ondrejka, R.A., The detection of incipient faults in transmission cables using time domain reflectometry techniques: technical challenges, IEEE Trans. Power Apparatus and Systems, vol. PAS-101, No. 7, July 1982, pp. 928-1934.

[3] Hebner, R.E., Development of Power System Measurements--Quarterly Report January 1981 to March 31, 1981, NBSIR 81-2283, Nat. Bur. Stand., April 1981, pp. 4-7.

[4] Weeks, W.L., Final Report, Detection and Location of Incipient Faults on Power Cables, Contract No. ET 78C013214, Electrical Engineering School, Purdue Research Foundation, February 1981.

[5] SRI International Final Report, not available at this date.

[6] Harrold, R.T., Acoustic Waveguide Technique for Sensing Incipient Faults in Underground Power Transmission Cables, DOE Contract No. ET-78-C-01-2867, Westinghouse R&D Center.

[7] Van Blaricum, M.L., Mittra, R., A technique for extracting the poles and residues of a system directly from its transient response, IEEE Ant. and Prop., vol. AP-32, November 1975.

[8] Samulon, H. A., Spectrum analysis of transient response curves, Proc. IRE, vol. 39, February 1981, pp. 175-186.

[9] Waldmeyer, J., "Fast Fourier transform for step-like functions: The synthesis of three apparently different methods," IEEE Trans., Inst. Meas., vol. IM-29, No. 1, (1980), pp. 36-39.

[10] Ramboz, J.D., Ondrejka, A.R., Anderson, W.E., Sampling-rate drift problems in transfer function analysis of electrical power cables, Proc. of the Waveform Recorder Seminar, Ed. R.A. Lawton, Nat. Bur. Stand. SP-634, June 1982, pp. 47-53.

[11] Skilling, H.H., Electric Transmission Lines, First Ed., McGraw-Hill, (1951) pp. 353-355.

Appendix A

Sampling-Rate Drift Problems in Transfer Function Analysis of Electrical Power Cables

J.D. Ramboz, A.R. Ondrejka, W.E. Anderson

Reprinted from NBS Special Publication 634, Proceedings of the Waveform Recorder Seminar, Edited by R.A. Lawton, June 1982.

SAMPLING-RATE DRIFT PROBLEMS IN TRANSFER FUNCTION ANALYSIS OF ELECTRICAL POWER CABLES

J. D. Ramboz*, A. R. Ondrejka**, W. E. Anderson*
National Bureau of Standards
Washington, D.C. 20234

An examination of measurement problems caused by sampling-rate drift has been initiated at the National Bureau of Standards. This work arose from the study of degradation in underground power distribution and transmission cables, where precise measurements of radio-frequency dispersion characteristics (i.e., attenuation and phase delay as a function of frequency) are necessary. Cable dispersion results are obtained using time-domain-reflectometry and fast Fourier transform methods and spectra obtained from different data sets are compared. But because the data are necessarily taken at different times, drifts in sampling rate can occur and cause erroneous results in the frequency domain. Measurement methods for the detection of sampling rate drifts and computation methods for correcting the data are discussed and illustrated.

Key words: sampling-rate drift; digital sampling; deconvolution; fast Fourier transforms;

1. Introduction

There is an increasing interest in underground electric power transmission and distribution which is growing from environmental and economic concerns. Fault location in buried power cables can present technically challenging problems, especially when it is required that the fault site be located accurately at some great distance from the measuring location. There is an additional interest by the utilities in being able to use the same buried cables for communication purposes. Both of these needs require a knowledge of the rf propogation characteristics of the cable.

An experimental program had been initiated at the National Bureau of Standards to determine the rf characteristics of power cables using time-domain reflectometry (TDR). A thorough examination of the systematic sources of error using TDR techniques revealed the problem of sampling-rate drift and the effects such drift can have on the measured transfer function of the cable.

In the time domain, the effects of sampling-rate drift are readily apparent. Basically, in experiments of this sort, two different time-domain waveforms are acquired. One, for example, would correspond to the pulse response of a known length of cable and the second would correspond to a longer length of the same cable. The parts of the pulse-response waveforms corresponding to the output impedance of the pulse generator, the connection between the pulse generator and the cable, and the response of the shorter length of cable should be identical. If they are not, sampling-rate drift has occurred. If the two waveforms are then transformed to the frequency domain and divided to obtain the transfer function of the extra length of cable, errors will result. Based on the expected behavior of the cable, the transfer function can be corrected to minimize the effects of sampling-rate drift.

Sampling-rate drifts are discussed, along with their effects, and a method to correct this type of error is given. Analytical generation of typical TDR-type waveforms is used in the discussion to aid in the understanding of the problem and to show the effects of the correction process. Real data is then examined before and after corrections are applied.

2. Power Cable RF Attenuation Measurement Process

One method to measure the radio-frequency (rf) attenuation of underground power cables over a wide band of frequencies is to employ time-domain-reflectometry (TDR) techniques in conjunction with Fourier analysis. A method used by the authors requires that a length of cable be pulsed and the TDR response be recorded. A known change then is made in the length of the cable being measured and a second TDR response recorded. The data collection and analysis process are diagrammed in figure 1. The change of measured response between the two recorded waveforms can be related to the change of length and, thus, attenuation per unit length can be calculated. Specific details of the measurement process relating to coupling the cables and other miscellany are the subject of a forthcoming paper. This discussion is aimed more directly to the data analysis and, specifically, the effects of a sampling-rate drift.

---

* Electrosystems Division, NBS, Washington, DC 20234
** Electromagnetic Technology Division, NBS, Boulder, CO 80303

Referring to figure 1, the recorded waveforms are each amplitude shifted in a software process so that the two recorded waveforms, shown by figure 2, begin at zero amplitude, rise through a step-like function, and then continue at some positive amplitude. The data originally began at a non-zero value because of offsets in the measuring instrumentation, some of which were intentionally introduced to improve amplitude resolution. However, the particular fast Fourier transform (FFT)

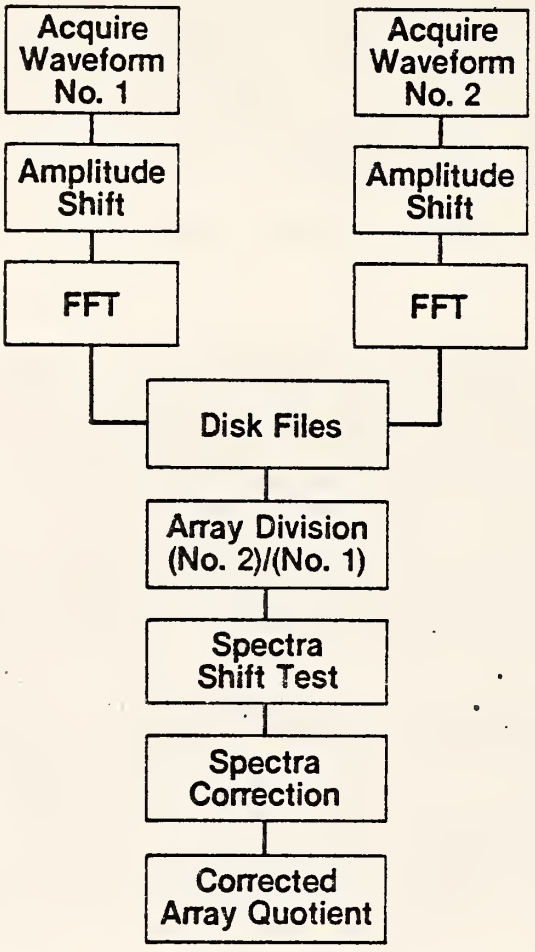

Fig. 1. The data collection and analysis process steps.

algorithm used in this analysis requires that the beginning points of the waveform be made zero. After the amplitude shift, an FFT result is obtained for each of the two waveforms and these results are stored on computer disk files. An array division corresponding to the deconvolution in the time domain is then done. The logarithm of the magnitude of this quotient is scaled to place the results in normalized attenuation units of dB per unit length of cable.

Figure 2 shows two recorded TDR response waveforms (already amplitude shifted) which were obtained from the cable measurement setup. No changes were made in the setup arrangement and, therefore, the two waveforms should be the same. The second waveform was taken 44 minutes after the first. Processing these two waveforms yielded the results shown in figure 3. Attenuation is given over a ±1 dB range and the frequency is shown over a range from 0 to 128 GHz, which results from a time interval between samples of about 2 ps and a total of 512 sample points. It is not expected that useful data can be obtained for frequencies beyond 10 to 20% of the Nyquist frequency because of noise and, in this instance, band limited frequency content of the TDR pulses. The pulse responses shown in figure 2 have rise times of the order of 35 ps, which should contain measurable frequency components up to the 15 to 20 GHz range.

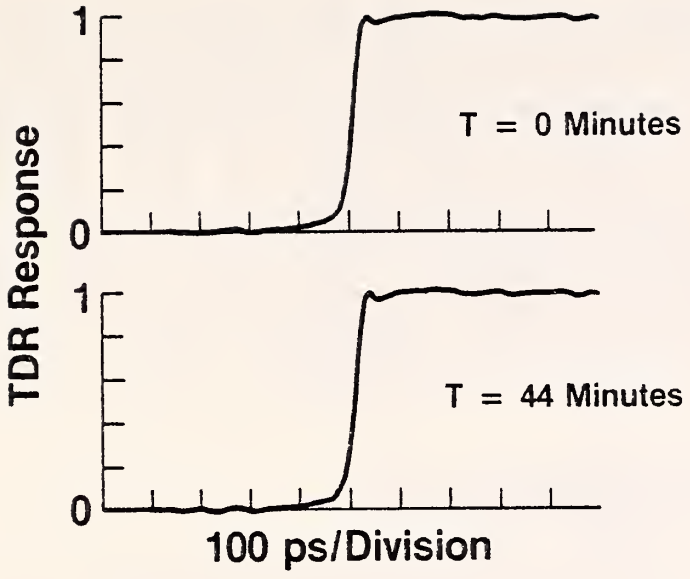

Fig. 2. Typical TDR response waveforms for two collection cycles.

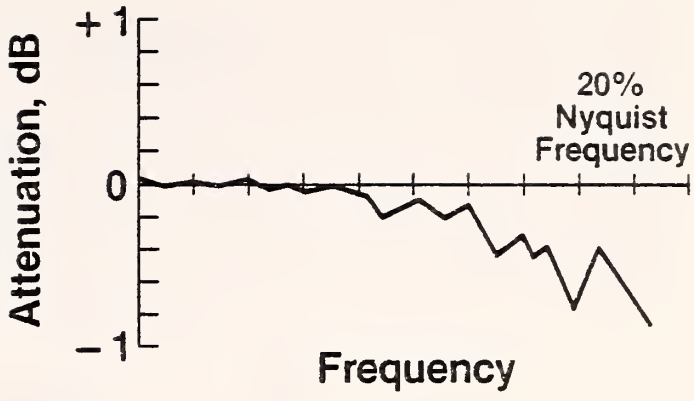

Fig. 3. Erroneous cable attenuation results due to sample-time drift.

If the recorded waveforms as shown in figure 2 were identical, the array division would yield a straight line of 0 dB over the entire frequency range up to the Nyquist frequency (and, indeed, if one uses this technique, the identical data can be analyzed in the two analysis "channels" to verify that the software is functioning correctly). Note, however, in figure 3 that the attenuation as computed shows a value more than -1 dB at a frequency less than 10% of the Nyquist where, in fact, a straight line of 0 dB over the range would be expected. If interpreted literally, a negative attenuation represents a system gain which, for these experiments, is not possible. This result led the authors to examine sampling-rate drift.

3. Sampling-Rate Shifted Data

Electronic sampling devices, such as the TDR equipment, sample a waveform at periodic intervals, either as a function of linear ramp sweep circuits or by some system "clock." In either instance, if the sweep-speed or clock rate changes from one set of measurements to a second set, then the "true" waveform is "time distorted" by this sampling-rate drift. It is assumed for purposes of this discussion that the time interval, or period between each individual sample of one "sweep" or data-gathering cycle, is constant and that for a second cycle, the period is also constant but not necessarily the same as the first. This is illustrated in figure 4. An arbitrary rising waveshape is shown as an "unshifted" waveform with the sampling occurring at times indicated by the solid dots. The time

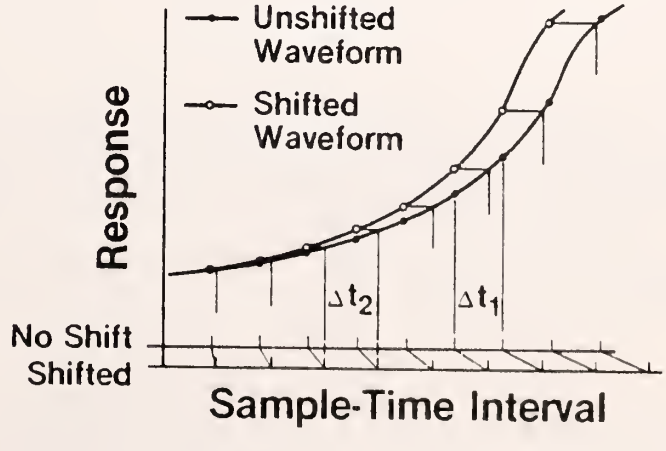

Fig. 4. An arbitrary rising waveform with and without sampling-time drift.

interval between individual samples is shown as Δt_1 on the time scale identified as "no shift." Here each Δt_1 is equal for the entire data collection cycle. If, at some later time, a second data set is collected where a change has occurred in the sampling rate, as shown by figure 4 as Δt_2, time distortion occurs. Bear in mind that it is exactly the same waveform that is being measured but because of the change in sampling rate, the apparent waveshape as shown by the "shifted" waveform results. Any particular sample is made at time $N\Delta t_2$, where N is the Nth sample, on the unshifted waveform as indicated by the vertical line from the "shifted" time axis. It is assumed, however, that the measurement was made at a time $N\Delta t_1$, as indicated by the open dots. For example, for an increase in the sampling period from Δt_1 to Δt_2, an apparent faster rising waveshape results. The same phenomenon occurs on an ordinary oscilloscope if a constant and repetitive waveform is being observed and the horizontal sweep speed is decreased a small amount; the waveshape appears to have a faster rise time to the observer. Figure 5 shows an exaggerated example on a typical TDR response for two different sampling times. One rise time appears faster than the other; however, this was due purely to a change made in the sample-time interval between the time sweeps.

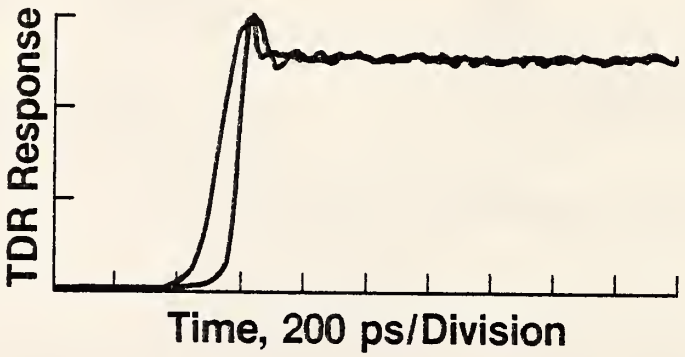

Fig. 5. An exaggerated example of a typical TDR response waveform sampled at two different rates.

When the subsequent data processing occurs, it is assumed that the sampling-time intervals were the same for the two recorded waveforms. However, because of a sampling-rate drift, one waveform appears to be "steeper" than the other. This waveform, in turn, when processed through Fourier analysis, contains more high frequency components than the "slower" (or unshifted) waveform. When the array quotient is obtained from two "apparently" different spectra, erroneous results such as those shown in figure 3 are obtained.

For measurements of cable attenuation, precision of the order a few tenths of one dB are often required. It has been observed that a sampling-rate drift of only a few tenths of 1% can cause results such as shown in figure 3; these are considered unusable.

To characterize the process, an analytically-generated waveform was used. The expression is shown by eq. (1).

$$W(I) = [M/(M^2 + 100)^{1/2}] + C \qquad (1)$$

where $M = I - 256.5$.

The function is generated for an array of 512 points and is symmetrically centered in and around the center point of 256.5. The expression W(I) is in an array notation where I varies from 1 to 512 in steps of 1. The constant, C, is chosen to force the first point to zero amplitude so that it may be operated on by the subsequent FFT computations.

Figure 6 shows two computed waveforms having step-like transitions similar to those of actual TDR responses. The waveforms were generated using eq. (1). The lower waveform has been time-shifted by an amount 1% with respect to the upper waveform. This simulates a typical sampling-rate drift situation.

Figure 7 is the result of the array division process as discussed previously. The ordinate is plotted for a range of ±1 dB and the abscissa is given for a frequency range from 0 Hz to 20% of the Nyquist frequency. The "droop" is clearly present and is entirely the result of the 1% shift in sampling rate.

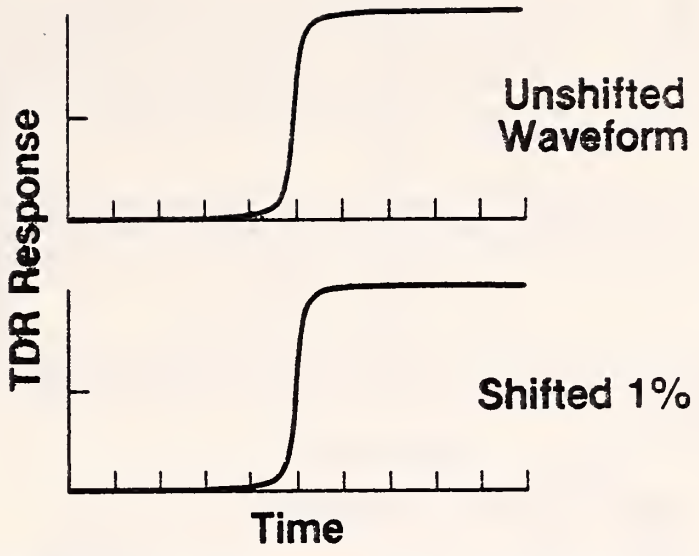

Fig. 6. Analytically-generated wave forms having similar characteristics to typical TDR responses, the lower waveform being time-shifted by 1%.

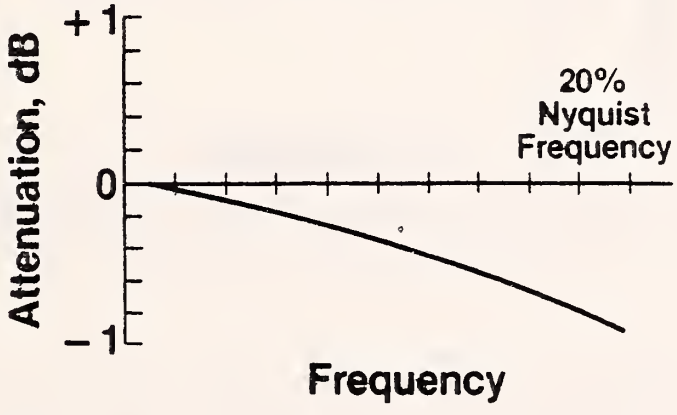

Fig. 7. Attenuation versus frequency from the waveforms shown in fig. 6; erroneous due to sampling-time drift.

The response droops when the second of the two time-domain waveforms is shifted to appear as a slower rising pulse (i.e., sampling rate is faster), and conversely, the attenuation plot would rise when the sampling rate for the second wave form is slower. Had no sampling-rate drift occurred (as in a perfect measuring system), then the attenuation plot would be a straight level line at 0 dB over the entire frequency range. For the set of measurements made by the authors, it was judged more advantageous to correct the "rate-drift" problem in software in the frequency domain rather than to try to eliminate the drift from the sampling hardware, or to correct for it in time-domain software. Because it is known that typical sampling-rate drifts result in attenuation responses such as shown in figure 7, it was predicted that expanding or compressing one of the two frequency spectra would, in effect, compensate for the rate drift and would, in turn, force the attenuation back to zero for some reference condition over the frequency range of interest. An expression shown in eq. (2) operates on an array B(M) such that the array division results in a corrected array D(I) which has the "droop" removed.

$$D(I) = \{(I*A_2-M)*[B(M+1)-B(M)] + B(M)\}*A_2^{-I/32} \qquad (2)$$

where D(I) is the Ith point in the corrected array,
I is an integer, $1<I<512$,
M is the integer part of $(I*A_2)$ for $1<I<512$,
B(M) is the Mth point in the uncorrected array, and
A_2 is a correcting factor derived from the slope.

The correcting term A_2 is derived from the slope of the uncorrected attenuation response (figure 7). A weighted mean slope is calculated from 33 points, starting with the third array point B(3) and continuing to point B(35). The weighting is such that the individual slopes received weighting factors inversely proportional to the order; thus, the lower points influence the results more heavily than do the higher points. This was done because the amount of noise increases as the order becomes higher and this weighting scheme reduces the effect of noise. The term A_2 is equal to 1 + the mean slope.

The process using eq. (2) adds a small positive shift to the process and this can be removed by using the following empirically derived relationship (shown in array notation):

$$D(I) = D(I)-[16*(1-A_2)]. \qquad (3)$$

Figure 8 is the corrected attenuation plot of the uncorrected attenuation shown in figure 7. Here the response has been corrected to be within approximately ±0.05 dB over a frequency range up to 20% of the Nyquist frequency.

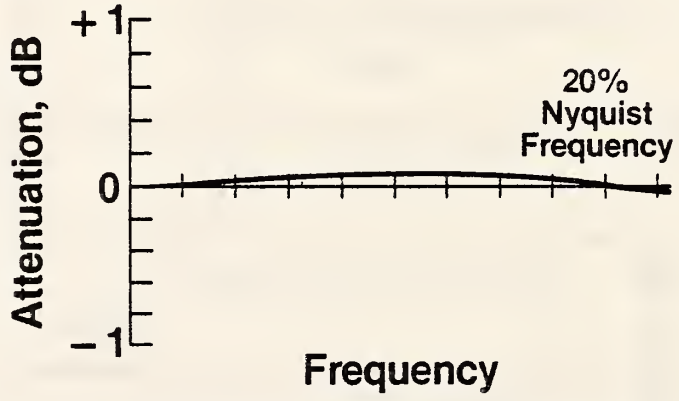

Fig. 8. Corrected attenuation of the data shown in fig. 7.

For real TDR data, a pulse such as shown in figure 9 was obtained from the laboratory. A second response was obtained which had a synthesized sampling-rate shift of 0.1%. Figure 10A shows the attenuation plot that resulted when no rate-shift correction was applied. Figure 10B shows the corrected attenuation which removed the effect of the "droop" in an attempt to improve the results.

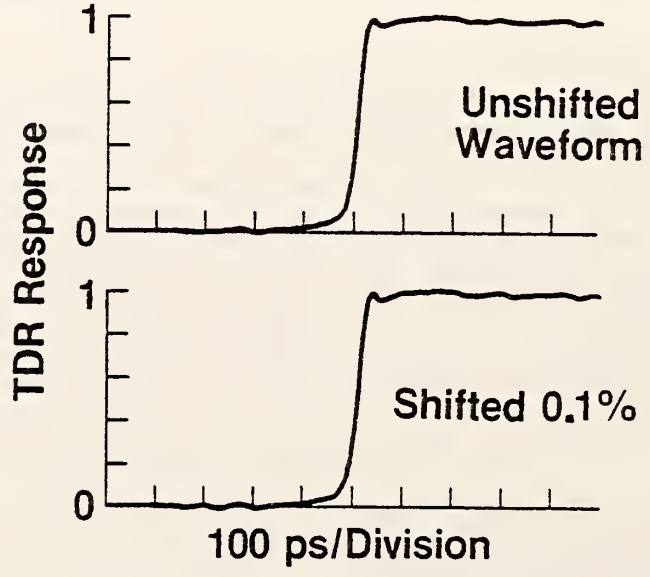

Fig. 9. Two TDR response waveforms, the second having a time shift of 0.1% with respect to the first.

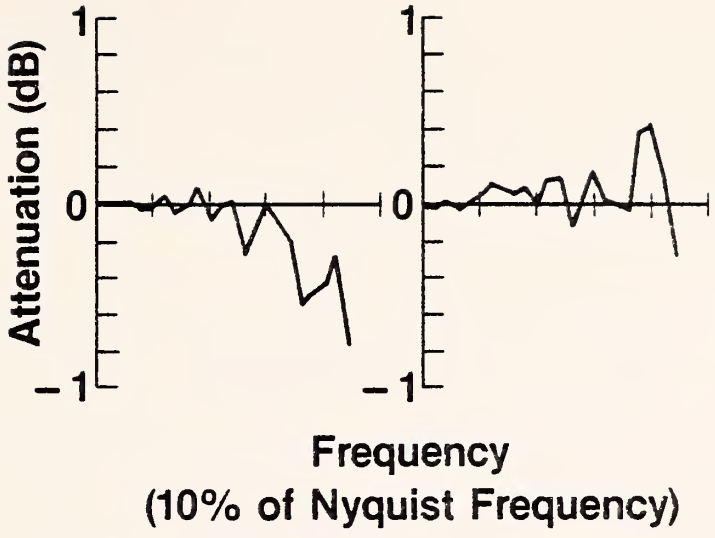

Fig. 10A. (Left) Attenuation results from waveforms shown in fig. 9 containing a sampling-time drift of 0.1%.

Fig. 10B. (Right) Corrected attenuation results using technique discussed.

The techniques discussed above analyzed a TDR response which had been "time-shifted". In practice responses are compared for two different experimental conditions (e.g., two different cable lengths). The overall TDR response for the second test condition can be markedly different from the first because of the increased cable length. The part of the time-domain response representing the impedance transitions between the TDR generator and the cable under study however should be constant for both measurements and the only change in response would be due to a sampling-rate drift. It is from the analysis of this data that sampling-rate drift can be determined and a correction factor estimated.

4. Conclusions

Errors in transfer function analysis, which result from digital techniques where the sampling-rate drifts between sets of measurements, can be minimized by applying a correction factor in the frequency domain. Analytical examples are shown that demonstrate the effect when such drifts occur. Empirically-derived equations are given which, when applied to the array quotient, correct for the effects of the time drift. In analytical examples, errors of several dB can be corrected to the order of 0.1 dB or less.

Most of the relationships given in this paper were derived empirically. Their applicability, therefore, depends on the details of the process studied and the apparatus used. They are intended only to illustrate the errors which can be produced by sampling-rate drift and to suggest an approach to the correction of these errors. It is presumed, however, that more general and more rigorous correction algorithms can be derived. The correction appears to be a direct function of TDR pulse characteristics and this complicates the possible solution. A thorough examination of the sampling-rate drift needs to be completed.

5. Acknowledgments

This work was sponsored by the Office of Electric Energy Systems of the Department of Energy.

6. References

1. W.E. Anderson, J.D. Ramboz, 1980 Annual Report. Technical Contributions to the Development of Incipient Fault Detection/Location Instrumentation, NBSIR 81-2235, Nat. Bur.Stand., March 1981.

Appendix B

The Effects of Sampling-Rate Drift on Transfer Function Measurements

W. E. Anderson and J. Hagler
National Bureau of Standards
Washington, DC

THE EFFECTS OF SAMPLING-RATE DRIFT ON TRANSFER FUNCTION MEASUREMENTS

William E. Anderson, Member IEEE

James Hagler, Non-Member

National Bureau of Standards
Washington, DC 20234

ABSTRACT

Digital sampling using waveform recorders represents a powerful and valuable technique in the field of high voltage measurements. It enables a researcher to study transient behavior by forming a replica of the actual event using the sampled data. This replica may not represent the actual event because of errors caused by the sampling process which may range from quantizing errors in the waveform recorder's analog-to-digital converter to aliasing caused by too few samples.

For precise determination of the transfer function, the stability of the waveform recorder's "clock" poses a limitation. Uncertainties in this "clock" will result in similar uncertainties in the frequency domain response.

The problems associated with the instabilities of this "clock" (called sampling-rate drift) are presented. Examples are shown for both actual data and a sampled analytical waveform. Mathematical techniques for removing the effect of this drift are presented and their limitations discussed.

Introduction

Digital waveform recorders (i.e., waveform recorders which use digital electronics to sample and store waveforms) have seen increased usage in measurement applications in the electric power industry. Traditionally researchers measuring electrical waveforms had to rely on a photograph of an oscilloscope trace to store the waveform for later analysis. This subsequent analysis (e.g., a risetime calculation) required time-consuming and often relatively inaccurate measurements with a ruler. With a digital waveform recorder, all that has changed. The waveform recorder can transfer the sampled waveform to a computer for immediate analysis. Although these recorders are valuable for steady-state measurements, they are particularly useful for high voltage impulse and other transient measurements [1].

While most researchers are familiar with oscilloscopes and can use them without difficulties, the use of a digital waveform recorder can lead to errors, some of them quite subtle. The purpose of this paper is not to list all the problems generic to the use of waveform recorders, which has already been done by others [2]. However, a presentation of a couple of the problems will illustrate the point that waveform recorders should be used with care.

First, in order to avoid a problem called "aliasing," the bandwidth of the measured signal must be less than one half the sampling frequency of the waveform recorder [3]. For example, a 1-MHz waveform recorder sampling a waveform having frequency components through, say 10 MHz, will work in the sense that a waveform will be recorded. But this waveform will be an incorrect representation of the original waveform and the uninitiated researcher may not be aware of the problem at all. Second, uncertainties in the amplitudes of the sample values are a problem. A typical amplitude resolution for a waveform recorder is 1 part in 512. This resolution is limited by the analog-to-digital converter in the waveform recorder. In addition, digitizing errors occur, such as those caused by quantization noise, integral and differential nonlinearity, offset, etc. Also, the calibration of the dynamic performance of the converters poses a challenge. As a result, the amplitude accuracy of waveform recorders is difficult to establish. These problems are subtle in that the researcher may have little knowledge of their occurrence. Sampling-rate drift is a similar problem and can have serious consequences in a particular class of measurements.

The time base or "clock" in a digital waveform recorder determines the sampling rate (number of samples per unit time) of the instrument. This "clock" could be a ramp generator or a quartz oscillator. If the "clock" or time base varies, then the sampling rate will also vary. This variation can lead to serious problems when making transfer function measurements using time domain techniques. In such measurements a voltage step is applied to the system to be measured. Both the input voltage and resulting output response are recorded. Discrete Fourier transforms of the two digitized waveforms are then calculated and the ratio of the magnitude of the frequency components of the output to the frequency components of the input yield the transfer function. If sampling-rate drift has occurred between the measurement of the input and output waveforms, then the resulting transfer function calculation will be compromised.

As an example consider figure 1. The lower waveform $x(t)$ can represent the input to the system to be measured. The upper waveform $y(t)$, instead of being the output of the system, in this case also represents the input. In the time domain they look very much identical. If the two waveforms both represent the same input signal, then the ratio of their Fourier transforms should be unity over the entire frequency spectrum. Figure 2 shows the transfer function $h(\omega)$ for the two waveforms in figure 1 (see (9) below). While the result could be interpreted as high-frequency roll-off, the real culprit is sampling-rate drift. This example will be discussed in more

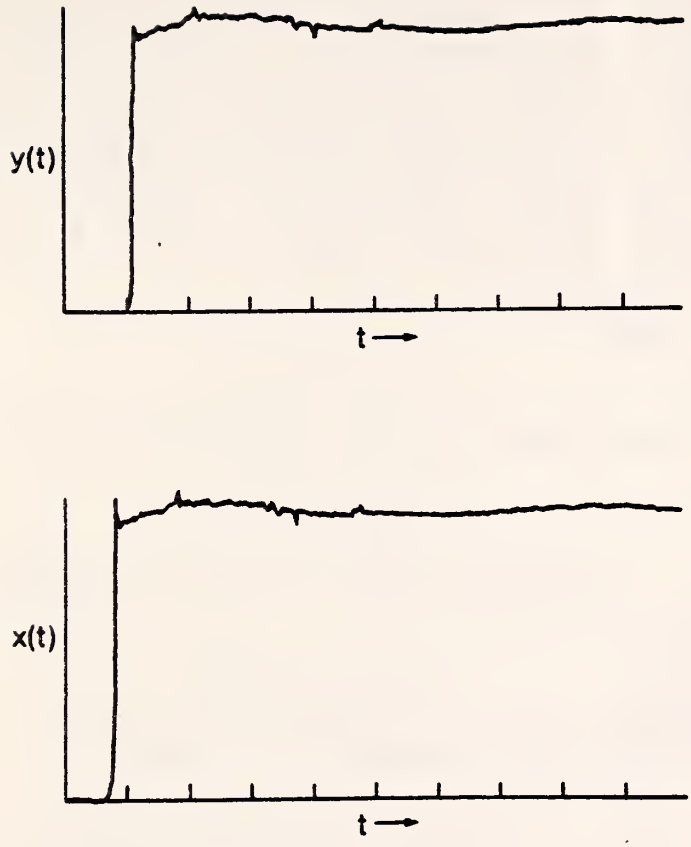

Figure 1. x(t) and y(t) show two actual sampled waveforms taken one minute apart.

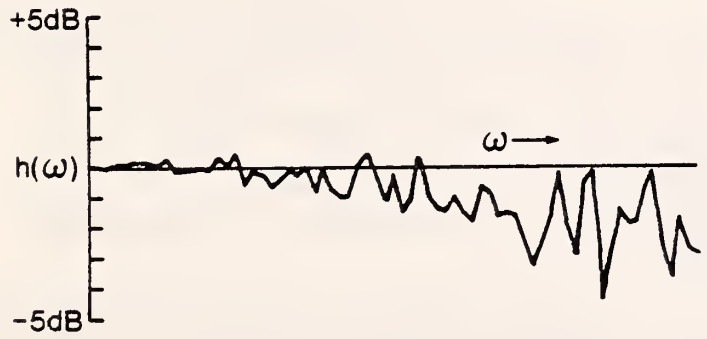

Figure 2. h(ω) shows the effect of sampling-rate drift for the two sampled waveforms in figure 1. Note the roll-off with increasing frequency.

detail later in this paper. For the researcher interested in power spectrum measurements, sampling-rate drift is not much of a problem in that the shapes of the time- and frequency-domain waveforms are only slightly affected. The problem occurs in transfer function-type measurements where ratios of waveforms are calculated.

Besides alerting the power engineering community that this problem can occur, this paper also discusses in some detail what can be done to identify data affected by sampling-rate drift and what corrections can be made to the data to minimize the effect of the drift. Recommendations are then given as to the best ways to deal with this problem.

Experimental Considerations

The effects of sampling-rate drift were first reported by Ramboz, et al. [4]. They were attempting to make high precision measurements (±0.1 dB) of the transfer functions of various power cables using a voltage step generator. In a typical experiment, the response in the time-domain to a voltage step was recorded after transmission through a length of the cable to be measured. The measurement was then repeated but with a longer length of the cable. Fourier transforms of the two time-domain responses were calculated and the ratio of the second to the first yielded the transfer function of the additional length of cable. The resulting transfer functions sometimes showed roll-off or even gain, which were not observed in repeat measurements and were, therefore, a measurement artifact and not indicative of the properties of the power cable being measured. Subsequent work revealed that this measurement artifact was caused by a drift in the time-base or "clock" of the waveform recorder which resulted in a drift in the sampling rate.

The waveform recorder used in this early work and for this paper was a digital processing oscilloscope. The sweepspeed of the oscilloscope controls the sampling rate. To determine the transfer function of the cable under test, the response of the cable to a voltage step is required. A voltage step generator is used to provide the signal to the cable and the oscilloscope digitizes the cable response by taking 512 uniformly spaced (in time) samples across the waveform with an amplitude resolution of 1 part in 1024. The digitized waveform is then transferred to a computer for processing. The experiment consists of acquiring two waveforms. The first waveform is the response of the system consisting of the output impedance of the step generator, the signal cable connecting the generator to the power cable under test, the electrical connector between the signal and power cables, and some length of power cable. The second waveform is the response of the same system as the first but includes a longer length of cable. Therefore, the Fourier transform of the second waveform divided by the Fourier transform of the first waveform will give the transfer function of only the extra length of power cable. The effects of the signal cable, electrical connectors, etc., common to both measurements will cancel. Discrete Fourier transform software based on a modification of the fast-Fourier transform algorithm suitable for step-like waveforms was used to calculate the transfer function [5].

In the original measurements, having anticipated some of the problems associated with instrumental drift, care was taken to leave the digital processing oscilloscope on for several hours before taking data. Despite these precautions, problems caused by sampling-rate drift were apparent in the computed transfer function. Although the sampling-rate drift was small, the precision of the measurement was large (±0.1 dB) so the effects were apparent. (The effects of sampling-rate drift are a function of both the size of the drift and the rate of roll-off of the waveform in the frequency domain -- see next section.)

For the data presented in this paper, the same instrumentation was used. However, to emphasize the sampling-rate drift problem, the measurements were taken immediately after the oscilloscope was turned on. The other difference is that, unlike the initial measurements, both measurements were made on the same length of cable. This was done to focus on errors due to sampling-rate drift without having the additional complexity due to the sample response.

It should also be noted that the fast Fourier transform used gives values for the discrete Fourier transform of x(t) at 256 points. The graphs of Fourier transforms and h(ω) in this paper are drawn in "analog form" although, of course, they are discrete functions. In addition, the graphs of h(ω) are shown only for the first 70 of the 256 computed points (i.e., frequencies up to 70/256 of the Nyquist frequency). The higher frequency portion of the graphs exhibits a large noise component for real data due to the fact that numbers close to zero are being divided by each other. Neither time, frequency, nor amplitude scales are shown on the graphs because they are totally arbitrary for the purposes of this discussion.

Theoretical Considerations

Recall that for a two-terminal pair network, the voltage transfer function H(jω) is defined as:

$$H(j\omega) = V_o(j\omega)/V_i(j\omega), \tag{1}$$

where $V_o(j\omega)$ is the output voltage and $V_i(j\omega)$ is the input voltage in the frequency domain. Measurements of the transfer function are frequently, and conveniently, performed in the time domain by measuring the step response. The unit step response is related to the voltage transfer function through the inverse Laplace transform

$$g(t) = L^{-1}\{(1/j\omega)H_1(j\omega)\}, \tag{2}$$

where $H_1(j\omega)$ is the normalized voltage transfer function. It is therefore recognized that equation (1) is the frequency domain analogue of the convolution equation

$$v_o(t) = \int_o^t v_i(t-\tau)g'(\tau)d\tau, \tag{3}$$

where $g'(\tau)$ is the impulse response function. In general, then, the application of equations (1) or (3) requires the measurement of two quantities (using either two different instruments at the same time or the same instrument at two different times) and thus, if there is a sampling-rate drift, an error can occur.

The consequences of sampling-rate drift can be examined mathematically. Suppose the two waveforms x(t) and y(t) (both zero for $t \leq o$) are sampled at sampling intervals T, yielding digitized values x(T), x(2T), ••• and y(T), y(2T), •••. For convenience the transfer function h(ω) is used in this paper where $h(\omega) = 20 \log (|Y(\omega)|/|X(\omega)|)$ where Y(ω) is the Fourier transform of y(t). If the two waveforms x(t) and y(t) are identical (as would be the ideal case if the waveforms are generated under the same experimental conditions), the two sampled waveforms x(T), X(2T), ••• and y(T), Y(2T), ••• will be identical and h(ω) would equal zero. In practice there is always some noise present in the system but h(ω) would still be expected to be close to zero, and fairly evenly distributed about zero (at least at low frequencies).

Now consider the case where sampling-rate drift has occurred. That is, the second waveform y(t) is identical to the first waveform x(t), but the waveform recorder's "clock" has changed so that when it registers one unit of time, α units of time have actually passed. (Note: It is assumed that the sampling rate is constant during the sampling of each of the two waveforms but has changed between the acquisition of the first and second waveforms.) Thus, in sampling the second waveform, the waveform recorder "thinks" it is sampling at times T, 2T, ••• when it is actually sampling at times αT, 2αT, •••. The relation between the two sampled waveforms is then $y(nT) = x(n\alpha T)$ for n = 1,2,3, •••. In other words, sampling from waveform y(t) with a sampling interval of αT is equivalent to sampling from x(αt) with a sampling interval of T. Recall that the Fourier transform X(ω) of the waveform x(t) is given by

$$X(\omega) = \int_o^\infty x(t)e^{-j\omega t}dt. \tag{4}$$

Likewise the Fourier transform Y(ω) is given by

$$Y(\omega) = \int_o^\infty y(t)e^{-j\omega t}dt. \tag{5}$$

From the preceding discussion, y(t) corresponds to x(αt) thereby

$$Y(\omega) = \int_o^\infty x(\alpha t)e^{-j\omega t}dt. \tag{6}$$

A change of variable $\tau = \alpha t$, results in

$$Y(\omega) = (1/\alpha)\int_o^\infty x(\tau)e^{-j(\omega/\alpha)\tau}d\tau \tag{7}$$

or

$$Y(\omega) = (1/\alpha)X(\omega/\alpha). \tag{8}$$

To simplify the discussion, consider the case where $\alpha < 1$ (i. e., the sampling rate has increased by a factor of α^{-1} or equivalently the sampling interval has decreased by α). Then

$$h(\omega) = 20 \log (|Y(\omega)|/|X(\omega)| \tag{9}$$

or

$$h(\omega) = 20 \log (\alpha^{-1}|X(\omega/\alpha)|/|(X(\omega)|). \tag{10}$$

If $|X(\omega/\alpha)|/|X(\omega)|$ is less than α, then h(ω) will be less than zero. That is, if $|X(\omega)|$ decreases rapidly enough with increasing frequency, then the system will appear to be exhibiting roll-off.

In other words, a sampling-rate drift of $1/\alpha$ (a corresponding sampling interval change from T to αT) where $\alpha < 1$ can result in an apparent roll-off in the frequency domain. This roll-off depends quantitatively on how fast $|X(\omega)|$ is decreasing with increasing frequency and on the sampling-rate drift $1/\alpha$.

To illustrate the effect of one percent sampling-rate drift, consider the analytical function

$$x(t) = \frac{(t-256.5)}{(t-256.5)^2 + 100} + K, \tag{11}$$

where K is chosen so that x(0) = 0. This function was chosen because its shape is similar to the real waveforms to be discussed later. In figure 3, the lower

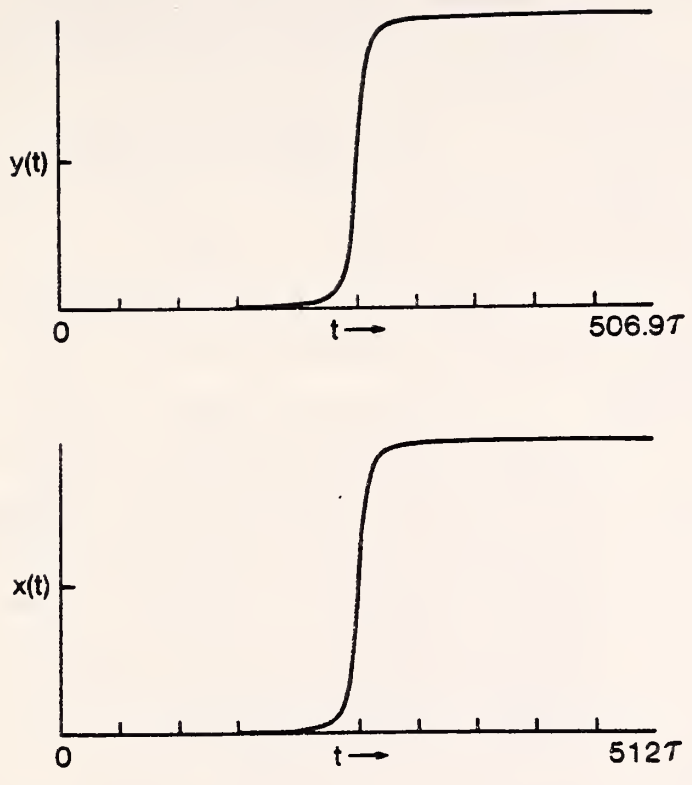

Figure 3. x(t) is the analytical function in (11) sampled at time intervals T = τ where τ is an arbitrary unit of time. y(t) is the same analytical function sampled at time intervals T = τ /1.01.

graph shows (11) sampled at t = 1, 2, ••• 512 (in units of time arbitrarily given as τ). The upper graph shows (11) sampled at t = $(1.01)^{-1}$ x 1, $(1.01)^{-1}$ x 2, ••• $(1.01)^{-1}$ x 512. Note the similarity of the two graphs in figure 3 despite the 1.01 sampling-rate drift. Figures 4 and 5 show, respectively, the transform X(ω) of x(t) sampled at t = 1, 2, ••• 512, and the roll-off exhibited by the function h(ω). This example also illustrates the effect of sampling-rate drift

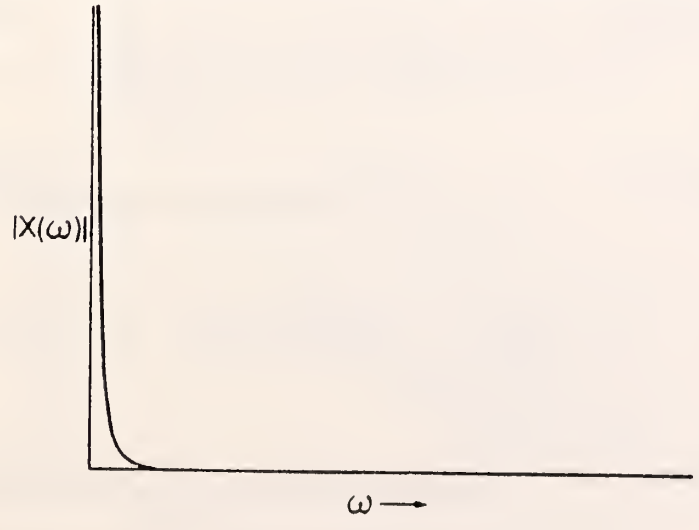

Figure 4. X(ω) is the discrete Fourier transform of the sampled analytical waveform in figure 3.

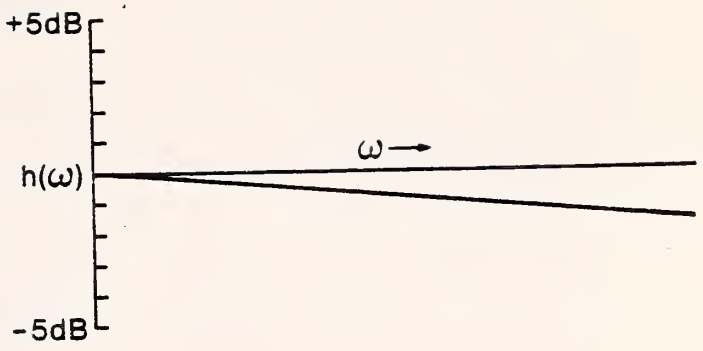

Figure 5. h(ω) shows the effect of sample-rate drift for the analytical waveform in (11).

qualitatively. The second waveform, because of the faster sampling rate, is sampled at smaller time intervals. This will make the steep rise of (11) appear to be less steep for the second waveform y(t) than for the first waveform x(t). The high-frequency components of the second waveform will therefore be less, resulting in h(ω) < 0.

Software Corrections

A researcher performing transfer function or similar types of measurements using digital sampling techniques should immediately suspect sampling-rate drift if results similar to figure 2 are obtained. Once this problem is identified, it should be either eliminated or corrections applied to remove the effect. While it may be straightforward to eliminate the problem (e.g., by using a more stable system clock), correcting data with this problem is a challenge. Several methods have been proposed. These methods, as well as their limitations, will be discussed.

The first correction scheme was proposed by Ramboz, et al. [4]. This is a frequency domain correction, which centers the graph of $h(\omega) = 20 \log(|Y(\omega)|/|X(\omega)|)$ about zero. The approach is to use the average slope of the first few points of h(ω) to obtain a correction factor since, for most systems, one expects h(ω) to be flat at low frequencies. While this approach does force h(ω) to be flat at low frequencies, it does nothing to correct for h(ω) at higher frequencies. From (10) it is apparent that a simple slope change can not completely correct h(ω) for drift.

The approaches taken here are based on the fact that, in these measurements, the first 100 or so points of the sampled time-domain waveforms should be the same for both measured waveforms. These data points represent the measured response between the voltage step generator unit and the cable being measured. If no sampling-rate drift has occurred, these points will be identical. By contracting or expanding the sampling interval of the second waveform with the aid, for example, of linear or cubic interpolation, the first 100 points of the second waveform should align with the first 100 points of the first waveform. There is one major complication, however. The two waveforms are often horizontally displaced with respect to one another (i.e., the "step" does not occur at the same horizontal position on the oscilloscope screen). The approach taken to align the waveforms was to do a least squares fit of the two waveforms by first sliding the second waveform left or right until the correct horizontal displacement was determined, and then doing a least squares fit by expanding or contracting the sampling interval of the second waveform to agree with the first. Unfortunately, these two operations are

not independent, i.e., the best fit sampling-rate drift correction is dependent on the horizontal displacement correction and vice versa.

To illustrate this point graphically, consider the following waveforms x(t) and y(t) shown in figure 6. The second is obtained from the first merely by changing the sampling time interval by a factor $\alpha > 1$, i.e., $y(t) = x(\alpha t)$. One could assume that the point "t = 0" is incorrectly located on the graph of y(t) and "slide" the graph of y(t) to the right to obtain the best least squares fit of x(t) to y(t). The results of the "sliding" are shown in figure 7. Expansion of the y(t) time scale would then yield a correction. But this correction is wrong because for this example, the original zeros are in alignment and only a time-scale expansion of y(t) in figure 6 is required. These two approaches will yield different corrections. The translation and drifting correction cannot be applied independently.

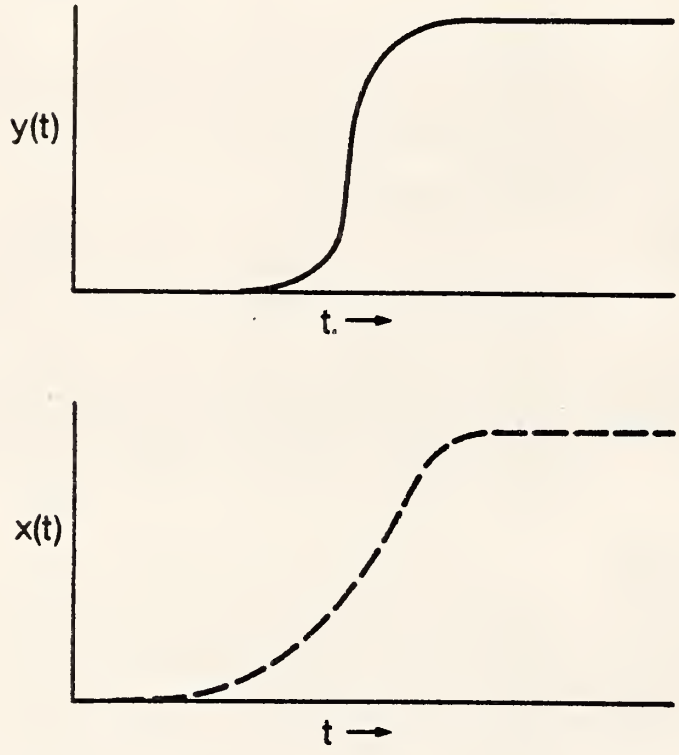

Figure 6. x(t) and y(t) represent waveforms obtained by sampling the same hypothetical waveform at two differing sample rates.

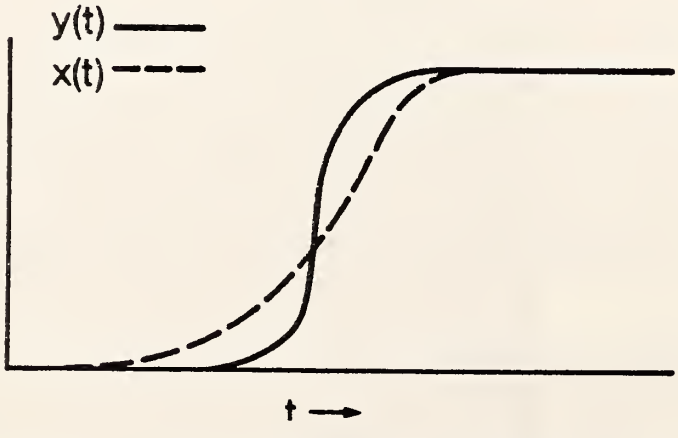

Figure 7. y(t) in figure 6 has been translated to the right to minimize the difference between the two curves.

A more suitable approach to this correction problem may be to consider digitized samples x(T), ···, x(512T) and y(T), ···, y(512T). The problem which needs to be treated mathematically is to minimize (in α and β) the expression

$$\Phi(\alpha,\beta) = \sum_{n=1}^{100} |x(nT)-\tilde{y}(n\alpha T+\beta)|^2, \qquad (12)$$

where $\tilde{y}$ is calculated as follows: find k so that $kT \leq \alpha nT+\beta \leq (k+1)T$. Then $\tilde{y}(\alpha nT+\beta)$ is an appropriately interpolated value between y(kT) and y((k+1)T). It should be noted that if $\beta < 0$, the expression $\Phi(\alpha,\beta)$ is evaluated by interchanging the roles of x(t) and y(t).

To minimize $\Phi(\alpha,\beta)$ in both α and β simultaneously, we used code based on Marquardt's algorithm [6] which is used to minimize a nonlinear sum of squares in a relatively small number of iteration steps. For analytically generated, translated, and shifted waveforms, such as shown in figure 3, this method performed well. The values given by the algorithm for α and β were found to be close to the actual α and β which had been used to generate the analytical waveforms and $h(\omega)$ was nearly zero. However, for real digitized data, this approach was not as successful in giving values which indicated improvement. The criterion for judging improvement was to observe the graph of $h(\omega)$ for the corrected waveforms and to see if this graph was more "centered about 0" than the graph of $h(\omega)$ for the uncorrected waveforms. The reasons why improvement in real data were difficult to obtain are threefold: (1) noise in the data tends to "flatten" the graph of the function $\Phi(\alpha,\beta)$ and the minimum of $\Phi(\alpha,\beta)$ need not give the best correction factors α and β; (2) the interpolation scheme adds error to the comparison; and (3) inputting incorrect initial guesses to the computer program can lead to "spurious" local minima, corresponding to the problems with first "sliding" then "expanding" discussed above.

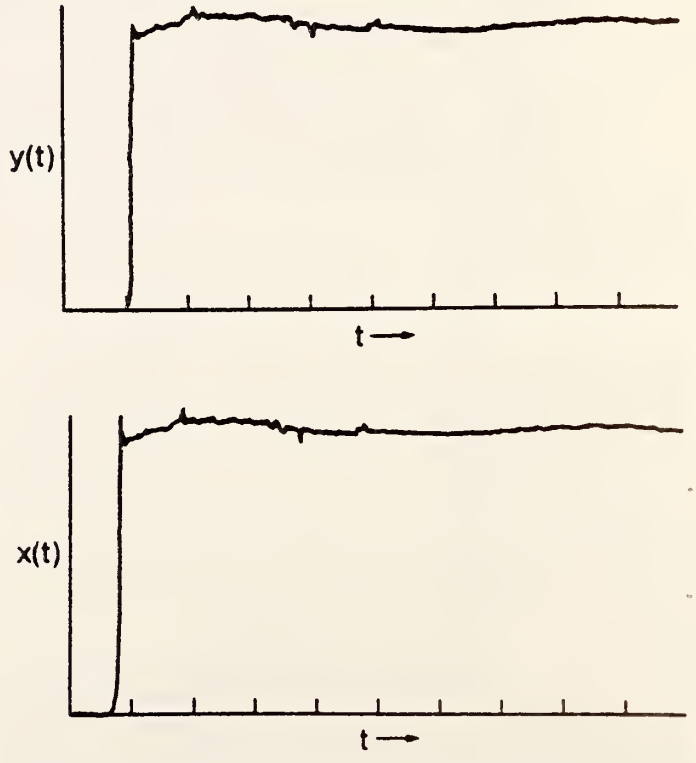

Figure 8. x(t) and y(t) show two real sampled waveforms taken one minute apart.

The difficulty with software correction can be illustrated with the most extreme real data which were gathered. Figure 8 shows two waveform readings taken 1 minute apart shortly after the oscilloscope was turned on. The transform $X(\omega)$ of the first waveform is illustrated in figure 9, and the function $h(\omega)$ for these two waveforms is shown in figure 10. Figure 11 shows the function $h_{td}(\omega)$ for the correction obtained by first finding the best translation, then the best drift. The factors were $\alpha = 0.999$, $\beta = -15.4$. No real improvement is apparent. Figure 12 shows the function $h_m(\omega)$ for the best correction obtained from the code which uses Marquardt's algorithm. Here, $\alpha = 0.73$ and $\beta = 0.37$, approximately. While the function $h_m(\omega)$ exhibits the desired properties, accepting these results means accepting an almost 30% drift in the time scale. This may not be unreasonable for an oscilloscope during the first minute or two after turn on. In some other examples, $h_m(\omega)$ has shown little improvement over $h_{td}(\omega)$.

Figure 9. $X(\omega)$ is the discrete Fourier transform of the sampled waveform $x(t)$ in figure 8.

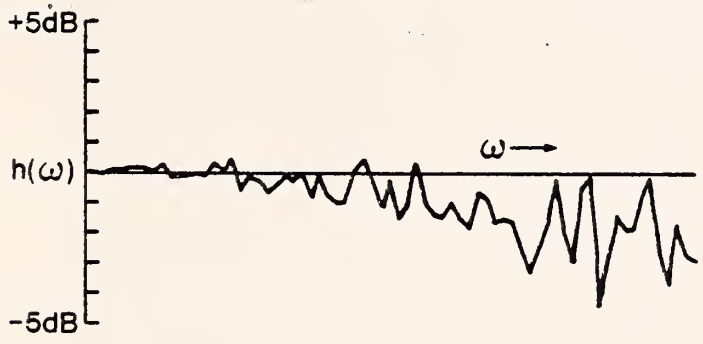

Figure 10. $h(\omega)$ shows the effect of sampling-rate drift for the two waveforms in figure 1. Note the roll-off with increasing frequency.

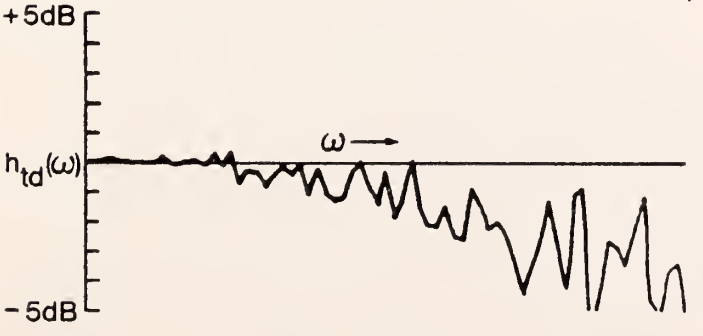

Figure 11. h_{td} was calculated by using corrections obtained by first finding the best horizontal translation of $y(t)$ and then the best drift. No real improvement over figure 10 is apparent.

Figure 12. $h_m(\omega)$ was calculated after using corrections obtained by the Marquardt algorithm. The high-frequency roll-off has vanished.

Conclusion

For precise transfer function measurements, errors caused by sampling-rate drift can pose a problem. Corrections in the frequency domain are straightforward but require a priori knowledge of the transfer functions and are also not complete. Corrections in the time domain do not require this prior knowledge and are theoretically possible. Our results show that time domain corrections work well for analytical waveforms but are less reliable for actual data. The conclusion is that the preferred way to handle the problem of sampling-rate drift is to prevent its occurrence by using a stable external clock instead of the internal time base of the waveform recorder.

Acknowledgments

The authors are indebted to John Ramboz, Arthur Ondrejka, and Robert E. Hebner for their technical contributions to this work, and to Betty Meiselman and Barbara Frey for the manuscript preparation.

References

[1] R. Malewski, "Digital Techniques in High-Voltage Measurements," IEEE Trans. Power App. Syst., Vol. PAS-101 pp. 45084517; 1982.

[2] Proceedings of the Waveform Recorder Seminar, edited by R. Lawton, Nat. Bur. Stand. (U.S.), Spec. Publ. 634; 1981 October.

[3] C. Shannon, "Communication in the Presence of Noise," Proceedings of the IRE, Vol. 37, pp.10-22; 1949.

[4] J. Ramboz, A. Ondrejka, and W. Anderson, "Sampling-Rate Drift Problems in Transfer Function Analysis of Electrical Power Cables," Proceedings of the Waveform Recorder Seminar, Nat. Bur. Stand. (U.S.), Spec. Publ. 634, pp. 47-53; 1981.

[5] W. Anderson and J. Ramboz, 1980 Annual Report: Technical Contributions to the Development of Incipient Fault Detection/Location Instrumentation, Nat. Bur. Stand. (U.S.), NBSIR 81-2235; 1981.

[6] D. Marquardt, " An Algorithm for Least-Squares Estimation of Nonlinear Parameters," J.Soc.Indust. Appl. Math., Vol. II, pp. 431-441; 1963.

Appendix C

BASIC program for transfer function analysis, reflection mode using an abrupt transition, matched termination.

```
1 REM  PROGRAM "@DOE/DPO/ARRAYFFT2"   9-30-80     LAST MOD 19-NOV-80
2 REM  FFT VERSION BY ANDERSON 9-22-80  (DOE TAPE FILE #4;3-4-81)
3 POLL N,M;3
4 DELETE V,W
5 REM DPO DATA COLLECT
6 GO TO 100
8 REM PLOT DPO DATA
9 GO TO 330
12 REM ARRAY SQUASH
13 GO TO 1000
16 REM PLOT SQUASHED ARRAY
17 GO TO 2000
20 REM DFT ROUTINE
21 GO TO 3000
24 REM ATTEN. PLOT
25 GO TO 3380
28 REM DFT MAGNITUDE PLOT
29 GO TO 4000
32 REM TRANSFER DATA TO REFERENCE ARRAY
34 GO TO 7080
36 REM SUBTRACT INPUT WAVEFORM TO CABLE FROM REFERENCE WAVEFORM
38 GO TO 7090
40 REM INTERPOLATE NEW WAVEFORM
42 GO TO 5000
44 REM TRANSFER DATA TO TERMINAL
46 GO TO 150
48 REM DIFFERENCE OF TWO WAVES
50 GO TO 400
52 REM MAKE FIRST N SAMPLES EQUAL ZERO
54 GO TO 1100
56 REM DISC INPUT WRITING ROUTINE
57 GO TO 7013
60 REM DISC OUTPUT WRITING ROUTINE
61 OPEN E$;1,"U",F$
62 GO TO 7050
64 REM READ REFERENCE FROM DISC
66 GO TO 7000
68 REM GENERATE WAVEFORM
69 A9=1
70 GO TO 500
72 REM ADD NOISE TO V ARRAY
74 GO TO 700
100 PAGE
102 GOSUB 9000
104 PRINT "DPO DATA COLLECTION CYCLE"
110 DIM W(512)
115 PRINT "HOW MANY AVERAGES? POWER OF 2 GREATER THAN 2"
120 INPUT A1
125 PRINT "WHAT MEMORY?"
130 INPUT D$
135 PRINT @3:"STO ";D$
140 G$=D$&"/"
142 G$=G$&D$
144 G$=G$&" "
```

```
145 PRINT @3:"HAV ";G$;A1;" S"
149 RETURN
150 REM TRANSFER DATA TO CALCULATOR
151 DELETE W,V
152 DIM W(512),V(512)
155 PAGE
160 PRINT "DATA FROM WHAT MEMORY?"
162 INPUT D$
164 G$="DP"&D$
166 G$=G$&"?"
175 PRINT @3:G$
180 INPUT @3:W
185 W=W-512
187 G$=D$&"1"
190 PRINT @3:"CHL ";G$
195 PRINT @3:"SCL?"
200 INPUT @3:S$
205 DELETE M,V1,X1
210 V1=VAL(S$)
220 M=1
230 V1=V1*10©(-3*M)
240 W=W*(V1/102.3)
247 G$=D$&"2"
250 PRINT @3:"CHL ";"B2"
260 PRINT @3:"SCL?"
270 INPUT @3:S$
280 X1=VAL(S$)
290 M=POS(S$,"S",1)
300 T$=SEG(S$,M-1,1)
310 M=POS("munp",T$,1)
320 X1=X1*10©(-3*M)
321 T=X1*10/512
322 W(1)=W(2)
323 W=W-W(1)
324 HOME
325 RETURN
330 V2=65
332 V3=130
334 V4=50
336 V5=80
340 CALL "MIN",W,M1,I1
346 CALL "MAX",W,M2,I1
350 WINDOW 1,512,M1,M2
354 VIEWPORT V2,V3,V4,V5
356 PAGE
357 PRINT "ENTER TEST CONDITIONS; MAX OF ONE LINE:"
358 INPUT A$
360 PAGE
370 CALL "DISP",W
375 AXIS 512/10,V1
380 HOME
381 GOSUB 9000
382 A$="TEST COND.:"&A$
384 PRINT A$;"J"
```

```
390 PRINT "TIME BASE SETTING: ";X1;" s/DIV"
395 PRINT "VERT. SENS. SETTING: ";V1;" RHO/DIV";"J"
399 RETURN
400 REM DIFFERENCE BETWEEN TWO WAVEFORMS
401 DELETE W,V
402 DIM W(512),V(512)
405 PAGE
407 PRINT "WHAT TWO MEMORIES SHALL I READ FROM? (M,N=M-N)"
408 INPUT D$,J$
410 GOSUB 164
415 V=W
420 D$=J$
425 GOSUB 164
430 V=V-W
435 W=V
499 RETURN
500 REM GENERATE WAVEFORM
505 PAGE
510 DELETE M,V1,X1,T,W,A,B
520 DIM W(512)
530 M=1
532 V1=1
534 X1=1
536 T=1
550 PRINT "WHAT SLOPE FACTOR? (USUALLY >10)"
560 INPUT A
570 PRINT "WHAT LINEARITY FACTOR? (USUALLY >1)"
580 INPUT B
590 A=A©B
600 FOR N=1 TO 512
610 M=N-256.5
620 W(N)=M/(M©2©B+A)©(0.5/B)
630 NEXT N
640 W=W-W(1)
699 RETURN
700 REM ADD NOISE TO V ARRAY
710 PRINT "WHAT AMPLITUDE NOISE? (1=0 dB S/N)"
720 INPUT A8
725 D9=512/A9
728 FOR I=1 TO D9
730 A7=RND(1)
740 A6=RND(1)
750 IF A7=>0.5 THEN 770
760 A6=-A6
770 V(I)=V(I)+A6*A8
780 NEXT I
790 RETURN
999 REM  ARRAY SQUASH SUBROUTNE
1000 HOME
1001 PRINT "JJJJJJJJJJJJJJJJJJ"
1002 PRINT "REDUCTION FACTOR; 1,2,4,8,16,32? ";
1004 INPUT A9
1005 DELETE V
1008 D9=512/A9
```

```
1010 DIM V(D9)
1015 Q2=0
1020 FOR Q1=1 TO 512 STEP A9
1030 Q2=Q2+1
1040 V(Q2)=W(Q1)
1050 NEXT Q1
1052 T1=T*A9
1060 RETURN
1100 REM INITIAL ZEROS
1110 PRINT "MAKE ZERO UP TO WHICH SAMPLE POINT?"
1120 INPUT A7
1130 FOR N=1 TO A7
1140 W(N)=0
1150 NEXT N
1160 A7=A7+1
1170 A8=W(A7)
1180 FOR N=A7 TO 512
1190 W(N)=W(N)-A8
1200 NEXT N
1300 RETURN
2000 V6=V(1)
2001 REM PLOT ARRAY V (SQUASHED ARRAY)
2006 V(1)=0
2010 CALL "MAX",V,M2,I1
2020 CALL "MIN",V,M1,I1
2030 WINDOW 1,Q2,M1,M2
2035 VIEWPORT 65,130,10,40
2040 CALL "DISP",V
2050 AXIS (Q2-1)/10,V1
2052 V(1)=V6
2055 HOME
2056 PRINT
2060 RETURN
3000 DELETE X,Y,M,P,R,C,D
3001 REM BEGIN FFT ROUTINE
3010 PAGE
3012 CALL "TIME",T$
3014 PRINT T$
3016 PRINT A$
3021 F1=1/(2*T1)
3022 PRINT "THE MAXIMUM ANALYSIS FREQUENCY IS ";F1/1000000;" MHz"
3106 D8=D9/2+1
3107 DIM X(D8),Y(D8),M(D8),P(D8),D(D8)
3109 PRINT "A SET OF ";D9/2;" FREQUENCY POINTS WILL BE CALCULATED";"J"
3110 REM *** BEGIN CALCULATION***
3111 M=0
3112 P=0
3113 D=0
3115 F9=F1*2/D9
3120 CALL "FFT",V
3130 CALL "UNLEAV",V,X,Y
3132 PRINT "FREQ.","MAGNITUDE","PHASE,DEG","ATTEN,dB RE M(1)"
3134 PRINT
3135 P9=2*PI/D9
```

```
3136 PRINT @32,26:0
3137 K2=0
3138 K1=8
3140 FOR K=2 TO D8
3150 X(K)=X(K)+W(512)/2
3160 Y(K)=Y(K)-W(512)*SIN(P9*(K-1))/(2-2*COS(P9*(K-1)))
3170 M(K)=SQR(X(K)©2+Y(K)©2)/(2*F1)
3180 P(K)=180/PI*ATN(Y(K)/X(K))
3190 D(K)=20*LGT(M(K)/M(2))
3200 PRINT (K-1)*F9/1000000,M(K),P(K),D(K)
3205 IF K1=34 THEN 3340
3208 K1=K1+1
3210 NEXT K
3330 GO TO 3348
3340 IF K2>0 THEN 3342
3341 COPY
3342 FOR N=1 TO 1000
3343 NEXT N
3344 PAGE
3345 K1=1
3346 K2=1
3347 GO TO 3210
3348 PRINT "GGGGGG"
3350 RETURN
3380 REM BEGIN OF ATTENUATION PLOT; +-45 dB
3385 VIEWPORT 25,120,5,65
3390 WINDOW 2,D8,-45,45
3400 PAGE
3410 AXIS 8,5
3420 MOVE 2,D(2)
3430 FOR I=2 TO D8
3440 DRAW I,D(I)
3450 NEXT I
3460 HOME
3470 RETURN
4000 PAGE
4001 REM BEGIN OF MAGNITUDE PLOT
4012 CALL "MAX",M,M3,I1
4013 PRINT " THE MAXIMUM VALUE IS ";M3;" AT LOCATION ";I1;"J"
4020 PRINT "ENTER THE MIN AND MAX AMPLITUDE LIMITS FOR PLOT: ";
4030 INPUT W3,W4
4040 VIEWPORT 25,120,5,65
4050 WINDOW 2,D8,W3,W4
4060 AXIS (D8-2)/10,W4/10
4070 MOVE 2,M(2)
4080 FOR I=2 TO D8
4090 DRAW I,M(I)
4100 NEXT I
4110 HOME
4120 RETURN
5000 REM INTERPOLATE NEW WAVEFORM
5005 DELETE V,M
5008 DIM V(512)
```

```
5010 HOME
5020 PRINT "JJJJJJJJJJJJJJJJJ"
5030 PRINT "TIME CHANGE FACTOR? (~1)"
5040 INPUT A9
5050 V(1)=0
5060 FOR N=2 TO 512
5070 M=INT(N*A9)
5072 IF M<512 THEN 5080
5074 V(N)=V(N-1)
5076 GO TO 5090
5080 V(N)=(N*A9-M)*(W(M+1)-W(M))+W(M)
5090 NEXT N
5092 V(512)=V(511)
5094 DELETE W
5096 DIM W(512)
5098 W=V
5100 RETURN
6100 DELETE 1,2
6101 DELETE 999
6103 DELETE 2001
6104 DELETE 3001
6105 DELETE 3110
6106 DELETE 4001
6108 DELETE 5
6109 DELETE 6100,6109
7000 REM DISC READING ROUTINE
7001 DELETE M
7004 PRINT "SOURCE OF REFERENCE DATA? UNIT="
7005 INPUT Z
7006 PRINT "WAVEFORM FILE NAME?"
7007 INPUT E$
7008 OPEN E$;1,"R",F$
7009 READ #1:A$,D8,F1
7010 DIM M(D8)
7011 READ #1:M
7012 CLOSE 1
7013 REM DISC WRITING ROUTINE
7014 PRINT "DISC WRITING ROUTINE"
7015 PRINT "UNIT?"
7016 INPUT Z
7017 CALL "UNIT",Z
7020 PRINT "DISC FILE NAME(e.g. DPO/WAVE1)"
7030 INPUT E$
7035 CREATE E$;2500,0
7040 OPEN E$;1,"F",F$
7050 WRITE #1:A$,D8,F1,M
7060 CLOSE 1
7070 RETURN
7080 REM TRANSFER DATA TO REFERENCE ARRAY
7081 PAGE
7082 DIM U(512)
7084 FOR I=1 TO 512
7086 U(I)=W(I)
7088 NEXT I
```

```
7089 RETURN
7090 REM SUBTRACT INPUT WAVEFORM TO CABLE FROM REFERENCE WAVEFORM
7091 PAGE
7092 FOR I=1 TO 512
7094 W(I)=W(I)-U(I)
7096 NEXT I
7098 RETURN
9000 CALL "TIME",B$
9010 PRINT B$
9030 RETURN
9999 END
```

Appendix D

Part I

ASIC program for transfer function analysis, reflection made using an abrupt
ransition, mismatched termination. Main program requires use of program given
n Appendix D, Part II to be appended under program control.

```
1 REM MEASURE TF THROUGH ABRUPT TRANSITION. FILE 6  10 FEB 81
2 REM  FFT VERSION BY ANDERSON 9-22-80 PROGRAM "@DOE/DPO/TFABRUPT2"
3 POLL N,M;3
4 REM BEGIN
6 GO TO 100
8 REM TRANSFER DATA AND CONTINUE
9 GO TO 290
12 REM PLOT SINGLE WAVEFORM
14 GO TO 1600
16 REM CORRECT TIME SHIFT ERROR
17 GO TO 820
20 REM DFT ROUTINE
21 GO TO 4930
24 REM MAKE FIRST N SAMPLES OF ARRAY D ZERO
26 GO TO 1700
56 REM DISC INPUT WRITING ROUTINE
57 GO TO 5810
60 REM DISC OUTPUT WRITING ROUTINE
61 OPEN E$;1,"U",F$
62 GO TO 5900
64 REM READ REFERENCE FROM DISC
66 GO TO 5700
100 REM BEGIN MAIN PROGRAM
110 PAGE
120 REM ACQUIRE DATA
130 PRINT "READY WITH OPEN CIRCUIT WAVEFORM?(Y)"
140 INPUT I$
150 D$="A"
160 GOSUB 4000
170 PRINT "READY WITH SHORT CIRCUIT WAVEFORM?(Y)"
180 INPUT I$
190 D$="B"
200 GOSUB 4000
210 PRINT "READY WITH INPUT WAVEFORM?(Y)"
220 INPUT I$
230 D$="C"
240 GOSUB 4000
250 PRINT "READY WITH OUTPUT WAVEFORM?(Y)"
260 INPUT I$
270 D$="D"
280 GOSUB 4000
290 REM TRANSFER DATA TO CALC.
295 R1=0
300 DIM A(512),B(512),C(512),V(512),W(512)
310 D$="A"
320 GOSUB 4180
330 A=W
340 D$="B"
350 GOSUB 4180
360 B=W
370 D$="C"
380 GOSUB 4180
390 C=W
400 D$="D"
```

```
410 GOSUB 4180
420 V=W
430 REM PLOT WAVEFORMS
440 PAGE
450 PRINT "ENTER TEST CONDITIONS;MAX OF ONE LINE:"
460 INPUT A$
470 PAGE
520 REM PLOT MEM A
530 VIEWPORT 5,60,50,80
540 W=A
550 GOSUB 4460
552 WINDOW 0,130,0,100
555 VIEWPORT 0,130,0,100
560 MOVE 6,83
570 PRINT USING 575:M2
575 IMAGE "ARRAY A;MAX VAL:",FD.4D," mV"
580 REM PLOT MEM B
590 VIEWPORT 5,60,10,40
600 W=B
610 GOSUB 4460
612 WINDOW 0,130,0,100
615 VIEWPORT 0,130,0,100
620 MOVE 6,43
630 PRINT USING 635:M2
635 IMAGE "ARRAY B;MAX VAL:",FD.4D," mV"
640 REM PLOT MEM C
650 VIEWPORT 70,125,50,80
660 W=C
670 GOSUB 4460
672 WINDOW 0,130,0,100
675 VIEWPORT 0,130,0,100
680 MOVE 71,83
690 PRINT USING 695:M2
695 IMAGE "ARRAY C;MAX VAL:",FD.4D," mV"
700 REM PLOT MEM D
710 VIEWPORT 70,125,10,40
720 W=V
730 GOSUB 4460
732 WINDOW 0,130,0,100
735 VIEWPORT 0,130,0,100
740 MOVE 71,43
750 PRINT USING 755:M2
755 IMAGE "ARRAY D;MAX VAL:",FD.4D," mV"
760 HOME
770 GOSUB 5930
780 A$="TEST COND:"&A$
790 PRINT A$
800 PRINT "TIME BASE SETTING: ";X1;" s/DIV"
810 COPY
812 IF R1=0 THEN 820
815 RETURN
820 REM CORRECT TIME ERROR
825 PRINT "DO YOU WANT TIME CORRECTION?(Y,N)"
827 INPUT I$
```

```
828 IF I$="N" THEN 1180
830 R1=1
840 W=A-B
850 GOSUB 6000
860 PRINT "WAVEFORM A-B"
870 CALL "MAX",B,M2,I1
900 W=A
910 V=B
920 GOSUB 6050
930 PRINT "TIME ERROR IN A-B IS ";I7;" SAMPLE POINTS"
940 PRINT "DO YOU WANT TO CORRECT THIS?(Y,N)"
950 INPUT I$
960 IF I$="N" THEN 990
970 GOSUB 6210
975 A=V
980 GO TO 820
990 W=C-B
1000 GOSUB 6000
1010 PRINT "WAVEFORM C-B"
1020 W=C
1030 V=B
1040 GOSUB 6050
1050 PRINT "TIME ERROR IN C-B IS ";I7;" SAMPLE POINTS"
1060 PRINT "DO YOU WANT TO CORRECT THIS?(Y,N)"
1070 INPUT I$
1080 IF I$="N" THEN 1120
1090 GOSUB 6210
1100 C=V
1110 GO TO 990
1120 W=A-C
1130 GOSUB 6000
1140 PRINT "WAVEFORM A-C"
1150 PRINT "ANYMORE CORRECTIONS?(Y,N)"
1160 INPUT I$
1170 IF I$="Y" THEN 820
1180 REM CALCULATE WAVEFORM DIFFERENCES
1190 W=A-C
1200 A=A-B
1210 C=C-B
1220 B=W
1223 D$="D"
1225 GOSUB 4180
1227 V=W
1228 GOSUB 1700
1230 GOSUB 430
1240 PRINT "SHALL I DO DFT?(Y,N)"
1250 INPUT I$
1260 IF I$="Y" THEN 1280
1270 RETURN
1280 DELETE 110,1280
1290 DELETE 4000,4660
1291 DELETE 1600,1820
1295 DELETE 6050,6300
1296 DELETE 1290,1296
```

```
1300 FIND 7
1310 APPEND 100
1315 GO TO 100
1320 END
1600 GO TO 6000
1700 REM WAVEFORM LEADING ZERO ROUTINE
1710 PRINT "DO YOU WANT LEADING ZERO ROUTINE?(Y,N)"
1720 INPUT I$
1730 IF I$="N" THEN 1820
1740 PRINT "MAKE ARRAY D ZERO UP TO WHICH SAMPLE?(MAX 512)"
1750 INPUT I7
1760 FOR I=1 TO I7
1770 V(I)=0
1780 NEXT I
1785 I7=I7+1
1787 V7=V(I7)
1790 FOR I=I7 TO 512
1800 V(I)=V(I)-V7
1810 NEXT I
1820 RETURN
4000 PAGE
4010 GOSUB 5930
4020 PRINT "DPO DATA COLLECTION CYCLE"
4030 DIM W(512)
4040 PRINT "HOW MANY AVERAGES? POWER OF 2 > 2.0"
4050 INPUT A1
4080 PRINT @3:"STO ";D$
4090 G$=D$&"/"
4100 G$=G$&D$
4110 G$=G$&" "
4120 PRINT @3:"HAV ";G$;A1;" S"
4130 RETURN
4140 REM TRANSFER DATA TO CALC.
4180 G$="DP"&D$
4190 G$=G$&"?"
4200 PRINT @3:G$
4210 INPUT @3:W
4220 W=W-512
4230 G$=D$&"1"
4240 PRINT @3:"CHL ";G$
4250 PRINT @3:"SCL?"
4260 INPUT @3:S$
4270 DELETE M,V1,X1
4280 V1=VAL(S$)
4290 M=1
4300 V1=V1*10©(-3*M)
4310 W=W*(V1/102.3)
4320 G$=D$&"2"
4330 PRINT @3:"CHL ";"B2"
4340 PRINT @3:"SCL?"
4350 INPUT @3:S$
4360 X1=VAL(S$)
4370 M=POS(S$,"S",1)
4380 T$=SEG(S$,M-1,1)
```

```
4390 M=POS("munp",T$,1)
4400 X1=X1*10©(-3*M)
4410 T=X1*10/512
4420 W(1)=W(2)
4430 W=W-W(1)
4450 RETURN
4460 REM PLOTTING ROUTINE
4500 CALL "MIN",W,M1,I1
4510 CALL "MAX",W,M2,I1
4520 WINDOW 1,512,M1,M2
4580 CALL "DISP",W
4590 AXIS 512/10,V1
4660 RETURN
5380 PAGE
5810 REM DISC WRITING ROUTINE
5820 PRINT "DISC WRITING ROUTINE"
5830 PRINT "UNIT?"
5840 INPUT Z
5850 CALL "UNIT",Z
5860 PRINT "DISC FILE NAME(e.g. DPO/WAVE1)"
5870 INPUT E$
5880 CREATE E$;2500,0
5890 OPEN E$;1,"F",F$
5900 WRITE #1:A$,D8,F1,M
5910 CLOSE 1
5920 RETURN
5930 CALL "TIME",B$
5940 PRINT B$
5950 RETURN
5960 END
6000 REM PLOT SINGLE WAVEFORM
6005 PAGE
6010 VIEWPORT 5,125,5,95
6020 GOSUB 4460
6030 HOME
6040 RETURN
6050 REM COMPARE TIMES OF TWO WAVEFORMS
6055 I7=0
6057 J1=2
6058 K1=2
6060 FOR I=1 TO 9
6070 I1=I*M2/10
6080 FOR J=J1 TO 512
6090 IF W(J)>I1 THEN 6095
6093 NEXT J
6095 J1=J-1
6100 I5=J-1+(I1-W(J-1))/(W(J)-W(J-1))
6110 FOR K=K1 TO 512
6130 IF V(K)>I1 THEN 6150
6140 NEXT K
6150 K1=K-1
6160 I6=K-1+(I1-V(K-1))/(V(K)-V(K-1))
6170 I7=I7+I5-I6
6180 NEXT I
```

```
6190 I7=I7/9
6200 RETURN
6210 REM CORRECT TIME ERROR
6220 FOR I=1 TO 512
6230 I8=INT(I+I7)
6240 IF I8>0 THEN 6260
6250 V(I)=W(I)
6255 GO TO 6295
6260 IF I8<512 THEN 6290
6270 V(I)=V(I-1)
6280 GO TO 6295
6290 V(I)=W(I8)+(I+I7-I8)*(W(I8+1)-W(I8))
6295 NEXT I
6300 RETURN
```

Appendix D

Part II

BASIC program appends to that given in Appendix D, Part I.

```
100 REM-APPEND PROGRAM-CALC ABRUPT TRANSITION TF (TAPE FILE #6)
101 REM-(PROGRAM "@DOE/DPO/TFABAPPEND"
105 PAGE
110 REM CALC SPECTRA FOUR WAVEFORMS
120 W=A
125 PRINT "SPECTRUM A"
130 GOSUB 2780
140 A=W
150 W=B
155 PRINT "SPECTRUM B"
160 GOSUB 2780
170 B=W
180 W=C
185 PRINT "SPECTRUM C"
190 GOSUB 2780
200 C=W
210 W=V
215 PRINT "SPECTRUM D"
220 GOSUB 2780
230 V=W
240 REM CALC TRANSFER FUNCTION
250 FOR K=1 TO 512
260 W(K)=A(K)+V(K)-B(K)-C(K)
270 NEXT K
272 W(1)=W(3)
273 W(2)=W(4)
280 REM PRINT&GRAPH
282 K2=0
283 K1=8
285 PAGE
286 CALL "TIME",T$
287 PRINT T$
290 PRINT "FREQ.","MAGNITUDE","PHASE,DEG"
295 PRINT
300 PRINT @32,26:0
305 W2=20*LGT(2)
310 FOR K=1 TO 511 STEP 2
320 W1=(K-1)*F9/2000000
330 W(K)=W(K)-W2
340 PRINT W1,W(K)/2,W(K+1)/2
350 IF K1=34 THEN 390
360 K1=K1+1
370 NEXT K
380 GO TO 470
390 IF K2>0 THEN 410
400 COPY
405 GO TO 430
410 FOR N=1 TO 1000
420 NEXT N
430 PAGE
440 K1=1
450 K2=1
460 GO TO 370
470 PRINT "GGGGGG"
```

```
475 FOR N=1 TO 1000
476 NEXT N
480 H$="WAVE RETURNING FROM CABLE END/WAVE INTO CABLE"
500 PAGE
510 GOSUB 1600
520 END
1000 PRINT "WAVEFORM READ ROUTINE"
1010 PRINT "UNIT?"
1020 INPUT F
1030 CALL "UNIT",F
1040 PRINT "WAVEFORM FILE NAME?"
1050 INPUT A$
1060 OPEN A$;2,"R",F$
1070 READ #2:G$,L,F1
1090 READ #2:A
1100 READ #2:H$,L,F1
1120 READ #2:B
1130 READ #2:G$,L,F1
1150 READ #2:C
1160 READ #2:G$,L,F1
1170 READ #2:D
1200 CLOSE 2
1210 RETURN
1600 REM BEGIN RATIO PLOT
1610 PAGE
1615 PRINT "GRAPH ";A$
1517 CALL "TIME",T$
1618 PRINT T$
1620 PRINT "WHAT PERCENT OF POINTS SHOULD BE PLOTTED?";
1630 INPUT L1
1640 L1=INT(512*L1/100)
1650 CALL "MIN",C,M3,I1
1655 PRINT
1660 PRINT "THE MINIMUM VALUE IS ";M3;" AT LOCATION ";I1
1670 CALL "MAX",C,M3,I1
1680 PRINT "THE MAXIMUM VALUE IS ";M3;" AT LOCATION ";I1
1690 PRINT "ENTER THE MIN AND MAX AMPLITUDE LIMITS FOR PLOT: ";
1700 INPUT W3,W4
1710 VIEWPORT 25,120,5,65
1720 WINDOW 1,L1,W3,W4
1730 AXIS (L1-2)/10,(W4-W3)/10
1740 MOVE 1,W(1)
1750 FOR I=3 TO L1 STEP 2
1760 DRAW I,W(I)
1770 NEXT I
1780 HOME
1786 HOME
1787 PRINT "JJJJJJJJ"
1788 PRINT "PLOTTING LOG ";H$
1790 RETURN
1800 REM 5 POINT LINEAR FILTERING ROUTINE
1810 D3=C(1)
1820 D2=C(2)
1830 FOR N=3 TO 40
```

```
1840 D1=(C(N-2)+C(N-1)+C(N)+C(N+1)+C(N+2))/5
1850 C(N-2)=D3
1860 D3=D2
1870 D2=D1
1880 NEXT N
1890 RETURN
1900 REM CALC REFERENCE FROM SIGNAL PLUS HALF THE TRANSFER FUNCTION
1910 FOR I=2 TO L
1920 C(I)=SQR(A(I)*B(I))
1930 NEXT I
1940 C(1)=C(2)
1950 RETURN
1960 REM RECORD RESULTS ON DISC
1970 PRINT "UNIT?"
1980 INPUT Z
1990 CALL "UNIT",Z
2000 PRINT "DISC FILE NAME (eg DPO/REFER1)"
2010 INPUT E$
2020 CREATE E$;2500,0
2030 OPEN E$;1,"F",F$
2040 A$=SEG(E$,5,8)
2050 WRITE #1:A$,L,F1,C
2060 CLOSE 1
2070 RETURN
2080 FOR I=1 TO 1000
2090 NEXT I
2100 RETURN
2110 REM MODIFY SPECTRUM FREQUENCY
2120 PAGE
2130 PRINT "WHAT FREQUENCY CHANGE FACTOR?(=1)"
2140 INPUT A2
2150 C(1)=B(1)
2160 FOR I=2 TO L
2170 M=INT(I*A2)
2180 IF M<L THEN 2210
2190 C(I)=C(I-1)
2200 GO TO 2220
2210 C(I)=((I*A2-M)*(B(M+1)-B(M))+B(M))*A2
2220 NEXT I
2230 RETURN
2370 REM MEASURE TIME DRIFT IN REFERENCE
2380 PAGE
2390 CALL "TIME",T$
2400 PRINT T$
2410 VIEWPORT 25,120,5,65
2420 WINDOW 1,55,-1,1
2430 AXIS 5,0.2
2440 S=0
2450 S1=20*LGT(C(1)/A(1))
2460 MOVE 1,S1
2470 FOR I=1 TO 50
2480 S2=20*LGT(C(I+1)/A(I+1))
2490 IF I>16 THEN 2510
2500 S=S+(S2-S1)*(17-I)
```

```
2510 DRAW I,S1
2520 S1=S2
2530 NEXT I
2540 S=S/136
2550 HOME
2560 PRINT "JJJVERTICAL RANGE IS -1,1 dB"
2570 PRINT "AVERAGE SLOPE IS ";S;" dB PER POINT"
2580 PRINT "TO CORRECT SPECTRUM MULTIPLY BY ";S+1
2590 PRINT "SHALL I TEST THIS CORRECTION? (Y,N)"
2600 INPUT I$
2610 IF I$="N" THEN 2750
2620 PRINT "WHAT FREQUENCY CORRECTION FACTOR?"
2630 INPUT A2
2640 DIM D(L)
2650 D(1)=C(1)
2660 FOR I=2 TO L
2670 M=INT(I*A2)
2680 IF M<L THEN 2710
2690 D(I)=D(I-1)
2700 GO TO 2720
2710 D(I)=((I*A2-M)*(C(M+1)-C(M))+C(M))*A2
2720 NEXT I
2730 C=D
2740 GO TO 2380
2750 RETURN
2760 END
2780 REM BEGIN FFT ROUTINE
2790 DELETE X,Y
2810 CALL "TIME",T$
2820 PRINT T$
2830 PRINT A$
2840 F1=1/(2*T)
2850 PRINT "THE MAXIMUM ANALYSIS FREQUENCY IS ";F1/1000000;" MHz"
2880 PRINT "A SET OF 256 FREQUENCY POINTS WILL BE CALCULATED";"J"
2890 REM *** BEGIN CALCULATION***
2920 W1=W(512)
2930 F9=F1*2/512
2940 CALL "FFT",W
2980 P9=2*PI/512
3000 K2=0
3010 K1=8
3020 FOR K=3 TO 511 STEP 2
3030 X=W(K)+W1/2
3035 K3=(K-1)/2
3040 Y=W(K+1)-W1*SIN(P9*K3)/(2-2*COS(P9*K3))
3050 W(K)=20*LGT(SQR(X©2+Y©2)/(2*F1))
3060 W(K+1)=180/PI*ATN(Y/X)
3070 NEXT K
3080 W(1)=W(3)
3090 W(2)=W(4)
3100 RETURN
3230 PAGE
3240 REM DISC WRITING ROUTINE
3250 PRINT "DISC WRITING ROUTINE"
```

```
3260 PRINT "UNIT?"
3270 INPUT Z
3280 CALL "UNIT",Z
3290 PRINT "DISC FILE NAME(e.g. DP0/WAVE1)"
3300 INPUT E$
3310 CREATE E$;2500,0
3320 OPEN E$;1,"F",F$
3330 WRITE #1:A$,D8,F1,M
3340 CLOSE 1
3350 RETURN
3360 CALL "TIME",B$
3370 PRINT B$
3380 RETURN
3390 END
3400 REM PLOT SINGLE WAVEFORM
3410 PAGE
3420 VIEWPORT 5,125,5,95
3430 GOSUB 4460
3440 HOME
3450 RETURN
6000 GO TO 1600
```

NBS-114A (REV. 2-8C)

U.S. DEPT. OF COMM. BIBLIOGRAPHIC DATA SHEET (See instructions)	1. PUBLICATION OR REPORT NO. NBSIR 86-3392	2. Performing Organ. Report No. 722	3. Publication Date July 1986

4. TITLE AND SUBTITLE

Final Report: Technical Contributions to the Development of Incipient Fault Detection/Location Instrumentation

5. AUTHOR(S)

W. E. Anderson, J. D. Ramboz, and A. R. Ondrejka

6. PERFORMING ORGANIZATION (If joint or other than NBS, see instructions)

NATIONAL BUREAU OF STANDARDS
DEPARTMENT OF COMMERCE
WASHINGTON, D.C. 20234

7. Contract/Grant No.

8. Type of Report & Period Covered

9. SPONSORING ORGANIZATION NAME AND COMPLETE ADDRESS (Street, City, State, ZIP)

Department of Energy
Office of Electric Energy Systems
Washington, DC 20585

10. SUPPLEMENTARY NOTES

☐ Document describes a computer program; SF-185, FIPS Software Summary, is attached.

11. ABSTRACT (A 200-word or less factual summary of most significant information. If document includes a significant bibliography or literature survey, mention it here)

The transmission of electrical energy by use of underground cables is increasing. Fault location techniques have certain limitations; incipient fault detection and location would help reduce the maintenance cost of these lines as well as improve the reliability of service. This report discusses some test results related to RF-probing techniques applied to high-voltage transmission lines. The high frequency losses and attenuation in high voltage cables places certain ultimate limitations on RF-probing techniques for incipient fault detection. Time domain reflectrometry methods were employed to assess the RF-transmission properties of high voltage cables at frequencies as high as 6 GHz. Fast Fourier transform deconvolution were used to obtain loss measurements as a function of frequency. The loss mechanisms were identified. The measurement hardware and methods are discussed as well as analysis approach leading to the conclusions.

12. KEY WORDS (Six to twelve entries; alphabetical order; capitalize only proper names; and separate key words by semicolons)

deconvolution techniques; fast Fourier transformers; fault location; high-voltage transmission; incipient faults; RF measurements; RF properties; time domain reflectometry; underground cables.

13. AVAILABILITY

☒ Unlimited

☐ For Official Distribution. Do Not Release to NTIS

☐ Order From Superintendent of Documents, U.S. Government Printing Office, Washington, D.C. 20402.

☒ Order From National Technical Information Service (NTIS), Springfield, VA. 22161

14. NO. OF PRINTED PAGES 83

15. Price $9.95

USCOMM-DC 6043-P80